

New Craniodental Material of *Pronothodectes gaoi* Fox (Mammalia, “Plesiadapiformes”) and Relationships Among Members of Plesiadapidae

Doug M. Boyer,^{1,2,3,4*} Craig S. Scott,⁵ and Richard C. Fox⁶

¹Department of Anthropology and Archaeology, Brooklyn College, City University of New York, Brooklyn, NY

²New York Consortium of Evolutionary Anthropology, New York, NY

³Department of Anthropology, City University of New York, Graduate Center, New York, NY

⁴Interdepartmental Doctoral Program in Anthropological Sciences, Stony Brook University, Stony Brook, New York

⁵Royal Tyrrell Museum of Palaeontology, Drumheller, Alberta, Canada

⁶Department of Biological Sciences, University of Alberta, Laboratory for Vertebrate Paleontology, Edmonton, Alberta, Canada

KEY WORDS basicranium; Canada; Primates; Paleocene; petrosal; cladistics

ABSTRACT Plesiadapidae are a family of Paleogene mammals thought to have phylogenetic affinities with modern Primates. We describe previously unpublished dentitions and the first skull and isolated petrosals of the plesiadapid *Pronothodectes gaoi*, collected from middle Tiffanian localities of the Paskapoo Formation in Alberta. Other species of *Pronothodectes*, traditionally considered the most basal members of the Plesiadapidae, occur at earlier, Torrejonian horizons in Montana, Wyoming, and Alberta. Classification of *P. gaoi* as a species of *Pronothodectes* has proved controversial; accordingly, we use the newly available samples and the more extensively preserved specimens to re-evaluate the generic affinities of this species. Included in our study are comparisons with craniodental material known for other plesiadapids and plesiadapiforms. Cladistic analysis of craniodental characters is used to assess the hypothesis that *P. gaoi* and

other species in this genus are basal members of the Plesiadapidae. The new dental evidence confirms that *P. gaoi* lacks derived character states of other plesiadapids except for a variably present fissuring of the m3 hypoconulid. Moreover, several aspects of the cranium seem to be more primitive in *P. gaoi* (i.e., more like nonplesiadapid plesiadapiforms) than in later occurring plesiadapids, such as *Plesiadapis tricuspis* and *Plesiadapis cookei*. Cladistic analysis of craniodental morphology supports a basal position of *P. gaoi* among species of Plesiadapidae, with the exception of other species of *Pronothodectes*. The basicranium of *P. gaoi* preserves a laterally placed bony canal for the internal carotid neurovascular system, suggesting that this was the ancestral condition for the family. *Am J Phys Anthropol* 147:511–550, 2012. © 2012 Wiley Periodicals, Inc.

Plesiadapiforms are a paraphyletic or polyphyletic taxon also referred to as “early primates” or “archaic primates” (Simons, 1964, 1967, 1972; Gingerich, 1975b, 1976; Szalay et al., 1987; Bloch et al., 2007). Plesiadapidae is an extinct, diverse family of “plesiadapiforms” that existed mainly in North America and Europe during the Paleogene (Gingerich, 1976). Questionable records of the group also come from Asia (Thewissen et al., 2001; Fu et al., 2002).

Plesiadapids comprise one of the few mammalian taxa from the Paleogene for which species-level evolution has been interpreted from studies of large samples of dental and gnathic remains: from this evidence, plesiadapids seem to have evolved rapidly during their temporal range (Gingerich, 1973, 1975a, 1976). The primary stratigraphic sections through which the patterns of plesiadapid evolution have been established occur in several structural basins in the Western Interior of North America. These basins include the Clarks Fork Basin of northern Wyoming, the Crazy Mountains Basin of south-central Montana, the Wind River Basin of southwestern Wyoming, and the Bison Basin of central Wyoming. The European sequence of plesiadapids is less dense, is mostly comparable with the middle and late occurrences of the family in North America, and includes the youngest plesiadapids so far discovered, from the Paris and London basins (Gingerich, 1976).

The earliest known definitive plesiadapid is *Pronothodectes matthewi* from Gidley Quarry, Montana (but see Van Valen, 1994), which is roughly 63 Megannum (Ma), and the Who Nose? locality in Alberta (Scott, 2003), of similar age; while the latest occurrence is *Platychoerops richardsoni* from Grauves, France, and Herne Bay, UK (~52.4 Ma) [Gingerich (1976); see Gradstein et al. (2004)

Additional Supporting Information may be found in the online version of this article.

Grant sponsor: National Science Foundation; Grant numbers: BCS-0129601, EAR-0308902, and BCS-0622544. Grant sponsors: American Society of Mammalogists, Evolving Earth Foundation, and Natural Sciences and Engineering Research Council of Canada.

*Correspondence to: Doug M. Boyer, Department of Anthropology and Archaeology, Brooklyn College, City University of New York, 2900 Bedford Avenue, Brooklyn, NY 11210, USA.
E-mail: dboyer@brooklyn.cuny.edu

Received 17 February 2011; accepted 22 November 2011

DOI 10.1002/ajpa.22003

Published online 29 February 2012 in Wiley Online Library (wileyonlinelibrary.com).

and Lofgren et al. (2004) for recent age determinations]. The stratigraphic record of plesiadapids has been treated as dense enough to indicate that *Pronothodectes* is an ancestral form, while *Platychoerops* is clearly one of the most derived (Gingerich, 1976). According to this phylogenetic arrangement, earlier occurring, more basal species tend to exhibit: 1) smaller body sizes; 2) retention of a greater number of anterior teeth; 3) more simple molar structure; and 4) less prominently developed m3 hypoconulids (Gingerich, 1976). Since Gingerich (1976) reconstructed plesiadapid phylogeny using the stratigraphic successions of fossils available to him at the time, examples of later occurring specimens with some of the features more characteristic of Gingerich's basal taxa have been discovered (e.g., Watters and Krause, 1986; Fox, 1990b). Naturally, the taxonomic and phylogenetic interpretation of these forms has been difficult.

Specifically, the taxon *Pronothodectes gaoi* described by Fox (1990b) has stimulated such a controversy. Specimens of *P. gaoi* come from middle Tiffanian (*Plesiadapis rex/Plesiadapis churchilli*, or Ti3, biozone of Lofgren et al., 2004) horizons in the Paskapoo Formation of Alberta, Canada. The first evidence of plesiadapids from this region, however, was provided by a small sample of isolated molars from the Red Deer River Valley, Alberta, first described by Simpson (1927) and later the basis for Russell's (1964) *Plesiadapis paskapoensis*; Gingerich (1976) considered *P. paskapoensis* to be a junior synonym of *Plesiadapis rex*. The original sample of *P. gaoi* was also identified by Fox as *P. rex* (Fox, 1990a), based on size and the presence of an expanded, fissured hypoconulid lobe on m3, features that Gingerich (1976) had listed as diagnostic of *Plesiadapis*. Further collecting, however, recovered better preserved specimens of this taxon, ones having articulated anterior lower dentitions that included i2 and the canine. The retention of these teeth led Fox to conclude that the plesiadapid he had originally identified as *P. rex* should instead be referred to *Pronothodectes*, because among the diagnostic features of *Pronothodectes* specified by Gingerich (1976; p.18) is presence of i2 and the lower canine.

At present, two interpretations of the evolutionary significance of *P. gaoi* have been proposed: 1) In the view of Fox (1990b, 1991), *Pronothodectes gaoi* represents persistence of the *Pronothodectes* lineage into the late Paleocene (middle Tiffanian), while paralleling coeval *Plesiadapis* in becoming larger, with expansion of the talonid of m3 and "squaring off" and partial fissuring of its posterior rim. If so, Gingerich's (1976) hypothesis that *Pronothodectes* evolved anagenetically to become *Plesiadapis* and, hence, did not itself survive this transition, is refuted, as is the depiction of early plesiadapid phylogeny in North America as being fully represented by the stratigraphic succession of plesiadapid fossils collected from the local structural basins of Wyoming and Montana listed above. 2) Alternatively, in Gingerich's (1991) view, *P. gaoi* more likely represents *Plesiadapis* that has retained its lower canine and i2, a conclusion based on his stratophenetic phylogenetic hypothesis, which postulates that *Pronothodectes* went extinct at the origin of *Plesiadapis* and *Nannodectes* at roughly the boundary of Torrejonian (To) and Tiffanian (Ti) North American Land Mammal Ages (NALMAs) of the Paleocene (Gingerich, 1976). Gingerich (1991) also suggested that the specimens of *P. gaoi* represent individual variants of *Plesiadapis anceps* and that their source localities are of

uncertain age, points with which other researchers do not concur (Fox, 1991; Webb, 1996; Scott, 2008). Two important implications of Gingerich's (1991) hypothesis are that 1) lack of a lower canine is insufficient for distinguishing early *Plesiadapis* from *Nannodectes*, and 2) the lack of a lower canine and i2 is insufficient for distinguishing early *Plesiadapis* from *Pronothodectes*. Most other generic-level diagnostic characters cited by Gingerich (1976) for *Plesiadapis* are not present in these early species: the refutation of dental formulae as diagnostic features leaves almost no way to discriminate among isolated specimens or samples of the various taxa from the end of the Torrejonian and beginning of the Tiffanian. In fact, under Gingerich's (1991) hypothesis, the only remaining generic-level diagnostic character for *Plesiadapis* separating it from *Pronothodectes* would be size of the central incisors and molars (Gingerich, 1976). *Nannodectes* could still potentially be differentiated from *Pronothodectes* by lack of i2 (but see above), although not by size. Finally, early *Plesiadapis* and *Nannodectes* could potentially be distinguished from one another by size and the shape of the premolars and molars (Gingerich, 1976).

The aim of this study is to provide new, phylogenetically informative data on *Pronothodectes gaoi* from previously undescribed dentitions and the first known cranial material of this species. We examined 228 specimens representing 251 teeth from six correlative localities in the Paskapoo Formation (Fm) of Alberta: Erikson's Landing, DW-1, DW-2, Mel's Place, Joffre Bridge, and Birchwood, all Ti3 in age (Fox, 1990a; Webb, 1996; Scott, 2008; Fig. 1). Included among this material are UALVP 46685, a crushed skull from DW-2; and UALVP 46687 and 49105, isolated basicranial fragments from the DW-2 and Joffre Bridge localities, respectively. The new fossils are described and compared primarily with what is known for other species of plesiadapids. Finally, we evaluate the phylogenetic implications of this new material by undertaking a cladistic analysis of 66 craniodental characters for 28 plesiadapid species and three outgroups.

Background on plesiadapid cranial studies

Before the discovery of the skull described here, cranial material more extensively preserved than maxillary fragments was known for five plesiadapid species, including *Nannodectes gidleyi* (Simpson, 1935; MacPhee et al., 1983), *Plesiadapis tricuspiciens* (Russell, 1959, 1964; Simons, 1960; Gingerich, 1971, 1976; Szalay, 1971, 1972; Szalay and Delson, 1979; MacPhee and Cartmill, 1986; Szalay et al., 1987; Kay et al., 1992; Bloch and Silcox, 2006), *Plesiadapis anceps* (Gingerich, 1976), *Nannodectes intermedius* (Gingerich et al., 1983; MacPhee et al., 1983), and *Plesiadapis cookei* (Gunnell and Gingerich, 1987; Bloch and Silcox, 2001; Gingerich and Gunnell, 2005; Boyer et al., 2010). Plesiadapid cranial material has been previously described as sharing a number of features with crania of the Carpolestidae, the apparent sister taxon of the Plesiadapidae (Bloch and Silcox, 2006; Bloch et al., 2007). However, these taxa also exhibit a number of cranial morphological differences.

Shared derived features currently thought to reflect a close relationship among plesiadapids, carpolestids, and in some cases (features 1–2 below) anatomically modern primates [= Euprimates: Hoffstetter (1977)], include the

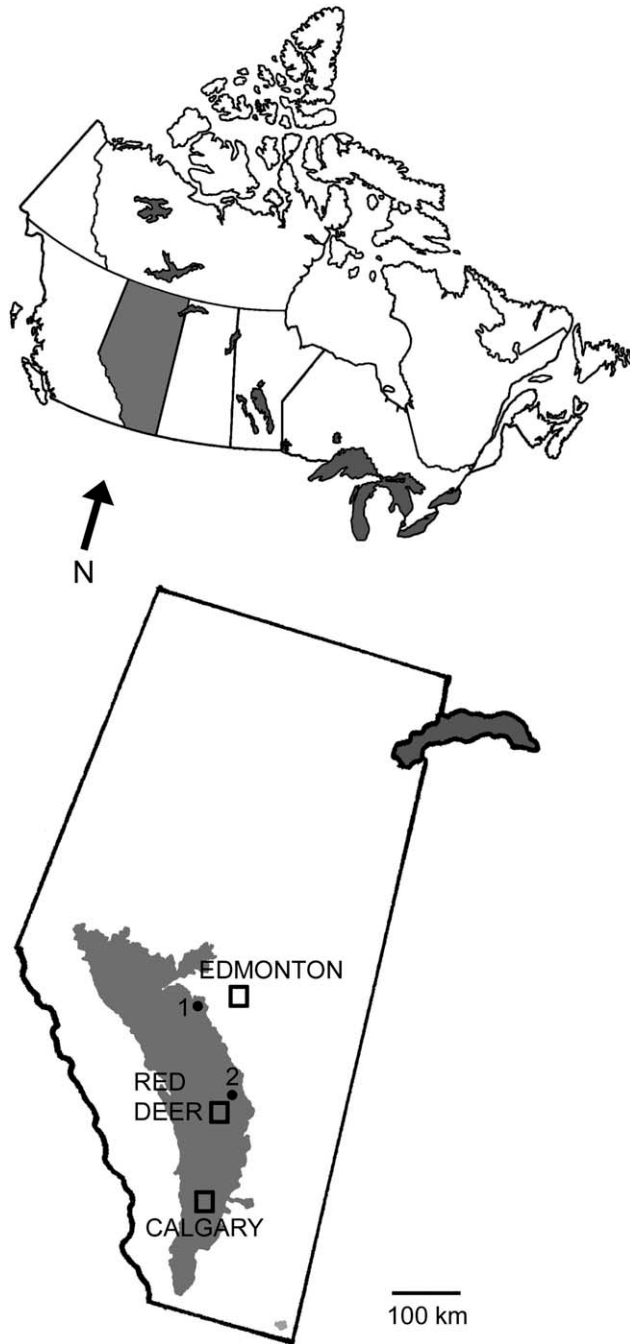


Fig. 1. Map of Alberta, Canada. Numbers indicate localities in the Paskapoo Formation (dark gray inset) as cited in the text. 1, Birchwood locality; 2, Blindman River localities (DW-1, DW-2, Mel's Place), Joffre Bridge Roadcut lower level.

following (Bloch and Silcox, 2006; Bloch et al., 2007): 1) a petrosally derived tympanic bulla; 2) a posterior carotid foramen in a posteromedial position; 3) a separate foramen rotundum and superior orbital fissure; 4) contact between the maxilla and frontal within the orbital cavity; and 5) a nasal that becomes mediolaterally narrow at its posterior extremity, where it contacts the frontal. On the other hand, major cranial features of plesiadapids that currently seem to separate this taxon from the Carpolestidae include the following: 1) premax-

TABLE 1. Numerical list of referenced anatomical features in *Pronothodectes gaoi*

1	Nasal/premaxilla suture (Fig. 8)
2	Nasal/frontal suture (Fig. 8)
3	Premaxilla/maxillary suture (Figs. 8–10)
4	Premaxilla/frontal suture (Fig. 8)
5	Lacrimal/frontal suture (Fig. 8)
6	Lacrimal/maxillary suture (Fig. 8)
7	Lacrimal orbital process (Fig. 8)
8	Lacrimal foramen (Fig. 8)
9	Maxilla/frontal suture (Fig. 8)
10	Infraorbital foramen (Figs. 9, 11, and 12)
11	Point on jugal where anteroposterior width was measured (Fig. 8)
12	Metopic suture (Fig. 8)
13	Frontal/parietal suture (Fig. 8)
14	Frontal temporal ridge (Fig. 8)
15	Zygomatic process of squamosal (Figs. 8 and 9)
16	Glenoid of squamosal (Figs. 8 and 9)
17	Postglenoid foramen (Fig. 9D)
18	Entoglenoid process (Fig. 9E)
19	Point on zygomatic process of squamosal where width was measured (Fig. 9D)
20	Medial and rostral tympanic processes of petrosal (Figs. 11 and 12)
21	Tympanic nerve foramen (Figs. 11, 13, and 14)
22	Tympanic nerve groove (Figs. 11 and 13)
23	Broken facial canal (Figs. 11–13)
24	Remnants of bulla (Figs. 8–10, 12)
25	Dorsal (petrosal?) layer of bone on rostral process of petrosal (Figs. 11–13)
26	Ventral (nonpetrosal?) layer of bone on rostral process of petrosal (Figs. 11–13)
27	Anterior end of basioccipital (Figs. 9 and 10)
28	Occipital condyle (Figs. 9 and 10)
29	Hypoglossal foramen (Figs. 9 and 10)
30	Foramen magnum (Figs. 9 and 10)
31	Nuchal crest (Figs. 9 and 10)

illae that contact the frontals; 2) an external auditory meatus that is expanded into a tube-like structure; 3) absence of expression of stapedia and promontorial branches of internal carotid artery on the promontorium, and 4) a small posterior carotid foramen that suggests the internal carotid artery did not contribute a significant amount of blood to the brain (Gingerich, 1976; Kay et al., 1992).

Here, we reassess morphology of the plesiadapid cranium with respect to some of the features aforementioned using new fossil and comparative data. We focus particularly on those features for which the interpretation has been controversial including the position of the posterior carotid foramen, the presence of an intratympanic route for the internal carotid plexus, and the bony composition of the auditory bulla.

Having new material of a potentially basal plesiadapid clearly represents an advantage over previous studies of the plesiadapid cranium; however, another advantage of this study is the relatively large sample of petrosals of *Pronothodectes gaoi* ($n = 4$). Controversies in the literature concerning the composition of the plesiadapid auditory bulla and evidence for intrabullar neurovascular patterns (e.g., Russell, 1964; MacPhee et al., 1983; MacPhee and Cartmill, 1986; Szalay et al., 1987; Bloch and Silcox, 2001) punctuate the importance of documenting morphological features of the bones of the basicranium and establishing limits on their intraspecific variability.

TABLE 2. Abbreviations for cranial bones and osteological features

<i>Cranial bones</i>	
As	Alisphenoid
Bas	Basisphenoid
Boc	Basioccipital
Bul	Bulla forming bone
De	Dentary
Ect	Ectotympanic
Ent	Entotympanic
Eoc	Exoccipital
Fr	Frontal
Jg	Jugal
Lc	Lacrimal
Mx	Maxilla
Ns	Nasal
Pa	Parietal
Pal	Palatine
Pmx	Premaxilla
Ptr	Petrosal
Os	Orbitosphenoid
Soc	Supraoccipital
Sq	Squamosal
<i>Osteological features</i> (some features are only labeled in Supporting Information figures)	
Aa	Anterior ampulla of vestibular system
Ascc	Anterior semicircular canal
Bs	Bullar suture (?)
Cc	Cochlear canaliculus (visible as the most posterior "septum" on medial aspect of promontorium. Houses a canal that connects the scala tympani to subarachnoid space and transmits the perilymphatic duct [see MacPhee, 1981]. HRxCT data were used in most cases to evaluate the presence of this feature— Supporting Information Figures 1–6)
ccA	Broken open aperture of cochlear canaliculus
Ccr	Common crus of anterior and posterior semicircular canal
Cf	Carotid foramen
ch	Cochlea
CN	Cranial nerve
cs	Cavum supracochleare (for geniculate ganglion of facial nerve)
eam	External auditory meatus
ec	Epitympanic crest
egp	Entoglenoid process
fc	Facial nerve (CN VII) canal
fco	Fenestra cochleae
fo	Foramen/ina
fov	Foramen ovale
fv	Fenestra vestibuli
g1	A groove with a lateral route that likely holds the internal carotid plexus and possibly a remnant of the ica
g2	A groove with a slightly more medial route that may hold internal carotid plexus fibers that approach the s1
g3	A groove that leads to the s2, which likely contains contributions from the tympanic plexus, but primarily contains a small vein as in lemurs and treeshrews
g4	A frequently present alternative or additional groove for tympanic plexus fibers to reach routes 1–3
g5	A Frequently present groove that leads from a point ventral to the vestibular fenestra dorsolaterally, toward the epitympanic crest
gpc	Greater petrosal nerve canal (leads to hiatus Fallopii)
hF	Hiatus Fallopii for greater petrosal nerve of CN VII
iam	Internal acoustic meatus
ips	Inferior petrosal sinus
iof	Infraorbital foramen
jf	Jugular foramen for CN IX-XI
jp	Jugular process of exoccipital
la	Lateral ampulla of vestibular system
lf	Lacrimal foramen

TABLE 2. (Continued)

lsc	Lateral semicircular canal
of	Optic foramen
pa	Posterior ampulla of vestibular system
pn	Pneumatic space (sinus)
pcf	Posterior carotid foramen
pgf	Postglenoid foramen
pgp	Postglenoid process
ppc	Postpalatine canal
ppp	Paroccipital process of petrosal. Also referred to as mastoid process. Serves as attachment point for posterior belly of digastric muscle.
ps	Posterior septum (and internal carotid canal): laterally curving septum of bone that shields the fenestra cochleae dorsally and holds a canal that leads to the posterior carotid foramen ventrally.
rtp	Rostral tympanic process of petrosal bone
s1	First (anterior) septum: Most lateral septum extending anteriorly from promontorium. Tubal canal forms between s1 and epitympanic crest.
s2	Second septum: Medial to s1, projects anteromedially from promontorium. g3 typically leads to the top ventral or medial aspect of this septum. In one case of a <i>Plesiadapis tricuspidens</i> specimen, the septum was not actually preserved, but surrounding morphology indicated to the authors that it had originally been present.
s3	Third septum: projects medially between s2 and raised ridge of cochlear canaliculus, more posteriorly.
scc	Semicircular canal
smf	Stylomastoid foramen
st	Stapes
tc	Tubal canal
tca	Tympanic canaliculus: Foramen and groove on or near ridge of cochlear canaliculus in tympanic cavity marking the entrance of the tympanic nerve from extracranial space, and the re-entrance of the nerve into the promontorium as it moves laterally to contribute to the tympanic plexus. Associated canals do not communicate with cochlea.
tnc	Tympanic nerve canal—destination of tng on promontorium in some specimens
tng	Tympanic nerve groove—extending laterally from tca
vcc	Vestibulocochlear nerve (CN VIII) canal

Anatomical terminology

The anatomical terminology used in this study follows that of MacPhee (1981) with respect to anatomy of the tympanic region. Miller's *Anatomy of the Dog* (Evans, 1993), *Nomina Anatomica Veterinaria* (2005), and *Nomina Anatomica* (1983) have normally been followed with respect to anatomical terminology for the remainder of the cranium. Wible and Gaudin (2004) and Wible (2008, 2009, 2011) provide useful glossaries of terms, as well as lists of terms and synonyms. Table 1 presents numerical codes for anatomical structures. Table 2 is a list of abbreviations for cranial bones and anatomical structures.

MATERIALS AND METHODS

Material examined

In addition to *Pronothodectes* specimens mentioned in the first section, we examined all known plesiadapid specimens that preserve a major portion of the cranium except for one specimen of *Plesiadapis tricuspidens* that

TABLE 3. Material examined

Specimen	Taxon	Description
UALVP (221 specimens)	<i>Pronothodectes gaoi</i>	Dental and gnathic material ^a
AMNH (3 specimens)	<i>Pronothodectes gaoi</i>	Dental and gnathic material from Eriksons Landing ^a
UALVP 46685	<i>Pronothodectes gaoi</i>	Skull from DW-2
UALVP 46687	<i>Pronothodectes gaoi</i>	Basicranial fragment from DW-2
UALVP 49105	<i>Pronothodectes gaoi</i>	Basicranial fragments from Joffre Bridge
MNHN CR 125	<i>Plesiadapis tricuspis</i>	Skull from Berru
MNHN CR 126, 965	<i>P. tricuspis</i>	Cranial fragments from Berru
“Pellouin skull”	<i>P. tricuspis</i>	Skull in private collection
MNHN BR 17414–19, 1371	<i>P. tricuspis</i>	Isolated petrosals from Berru
YPM-PU 19642	<i>Plesiadapis anceps</i>	Edentulous rostrum from 7-Up Butte
USNM 309902	<i>Nannodectes intermedius</i>	Skull from the Bangtail locality (Ti1)
AMNH 17388	<i>Nannodectes gidleyi</i>	Skull from Mason Pocket
UM 101963, USNM 482354	<i>Carpolestes simpsoni</i>	Skull from Clark's Fork Basin
UM 82616	<i>Ignacius clarksforkensis</i>	Skull from Clark's Fork Basin
USNM 421608, 482353	<i>Ignacius graybullianus</i>	Skulls from Clark's Fork Basin
MHNM MaPhQ 334	<i>Adapis parisiensis</i>	Skull from Quercy
YPM-PU 11481	<i>Leptadapis leenhardtii</i>	Skull
YPM 4999	<i>Ptilocercus lowii</i>	Skull
UMMZ 589983, SBU coll.	<i>Tupaia glis</i>	Skulls
AMNH 41527, 41522	<i>Lagostomus maximus</i>	Skulls
AMNH 124181, 39836, 121077	<i>Dipodomys heermanni</i>	Skulls
SBU MRd-12	<i>Sciurus carolinensis</i>	Skull

^a See supplementary information file 1 for a complete list of specimens examined.

TABLE 4. Institutional/specimen abbreviations

AMNH	American Museum of Natural History, New York
MaPhQ	Montauban Phosphorites du Quercy;
MNHN	Muséum Nationale d'Histoire Naturelle, Paris
MHNM	Muséum d'Histoire Naturelle, Montauban
SBU	Stony Brook University, Stony Brook;
SMM	Science Museum of Minnesota, Minneapolis
UALVP	University of Alberta Laboratory for Vertebrate Paleontology, Edmonton
UM	University of Michigan Museum of Paleontology, Ann Arbor
UMMZ	University of Michigan, Museum of Zoology, Ann Arbor
USNM	United States National Museum of Natural History, Smithsonian Institution, Washington, D.C.
YM	Yorkshire Museum, London
YPM-PU	Yale Peabody Museum, New Haven

could not be located—MNHN CR 7377 (Szalay, 1972; Szalay et al., 1987). We additionally examined various other plesiadapiform and euarchontogliroid taxa, both extinct and extant (Table 3 and Supporting Information Document #1). Institutional abbreviations for specimens are given in Table 4.

Methods of examination and documentation

Specimens were studied with the aid of a binocular light microscope. Anatomical features were photo-documented using a Nikon Coolpix 4500 camera mounted on a copy stand or tripod. For more detailed morphology, we used a continuously calibrated (for pixel scale) digital camera mounted on a SteREO Discovery V12 Zeiss microscope. Measurements were taken from the resulting photographs (on structures such as cranial foramina) to the nearest hundredth of a millimeter using the measurement software Axiovision 4.4. For specimens that could not be imaged with the Zeiss microscope, minute morphological features were drawn with the aid of a camera lucida and measured. Before photography, speci-

mens were whitened with ammonium chloride or magnesium oxide to remove tonal contrasts or surface glare. All externally visible morphological structures pertinent to description are labeled in the figures. Most features are labeled with numbers (Table 1); bones are identified with abbreviations (Table 2). Numbers following figure citations in the description section correspond to labels on structures depicted in the cited figures.

High resolution x-ray computed tomography (HRxCT) data were acquired from the Center for Quantitative Imaging of Pennsylvania State University, the High-Resolution X-ray Computed Tomography Facility of the University of Texas at Austin, and the Center for Biotechnology of Stony Brook University (Table A9; data available on request). These data were visualized with the software Amira 4.1.2-1 and Image J and used in our descriptions of internal morphology. HRxCT data were particularly important for verifying identifications of various foramina.

Measurements

Measurements of cheek teeth were taken following Clemens (1966) (Table 5); measurements of I1 follow Gingerich (1976) and Boyer et al. (2010). Four measurements were taken on the petrosal (Tables A1 and A2), and 61 measurements were taken on aspects of the cranium (Tables A3 and A4) using digital calipers, digital photographs, camera lucida drawings, and skeletal reconstructions from scan imagery (e.g., Tables A3 and A5).

Osteology of the tympanic cavity and reconstruction of its soft anatomy

To identify osteological features and to reconstruct the soft anatomical correlates of grooves and foramina within the tympanic cavity of plesiadapids, we use an extant phylogenetic bracket approach (Witmer, 1995). MacPhee (1981) provides descriptions of tympanic cavity osteology and its soft anatomical correlates in a comprehensive and comparable style for both scandentians and

TABLE 5. Tooth dimensions of *Pronothodectes gaoi* from Blindman River localities and Birchwood (Fox, 1990a, b)

Tooth	Dim	N	X	Min	Max	sd	cv
I1	L	24	4.2	3.5	5.1	0.41	9.8
	W	24	2.4	2.0	2.6	0.18	7.8
	P	14	5.9	5.2	6.5	0.45	7.6
I2	L	1	1.9	—	—	—	—
	W	1	1.5	—	—	—	—
C	L	1	1.2	—	—	—	—
	W	1	0.9	—	—	—	—
P2	L	1	1.4	—	—	—	—
	W	1	1.2	—	—	—	—
P3	L	6	1.8	1.6	1.9	0.12	6.6
	W	6	2.4	2.2	2.8	0.23	9.7
P4	L	14	2.1	1.8	2.3	0.15	7.2
	W	14	3.2	3.0	3.5	0.17	5.2
M1	L	17	2.6	2.2	2.8	0.16	6.1
	W	17	3.8	3.2	4.3	0.27	6.9
M2	L	25	2.8	2.5	3.1	0.17	6.1
	W	25	4.2	3.6	4.6	0.24	5.7
M3	L	18	2.8	2.5	3.1	0.18	6.4
	W	17	4.1	3.5	4.5	0.22	5.4
i1	L	28	3.7	3.0	4.3	0.30	8.2
	W	19	2.3	2.1	3.1	0.22	9.6
	P	11	7.5	7.0	8.0	0.43	5.7
i2	L	1	0.9	—	—	—	—
	W	1	0.6	—	—	—	—
C	L	1	0.9	—	—	—	—
	W	1	0.6	—	—	—	—
p2	L	1	1.0	—	—	—	—
	W	1	0.7	—	—	—	—
p3	L	14	2.0	1.8	2.2	0.11	5.6
	W	14	1.7	1.5	1.9	0.14	8.3
p4	L	24	2.1	2.0	2.4	0.12	5.8
	W	24	2.0	1.8	2.2	0.11	5.4
m1	L	26	2.7	2.5	3.0	0.13	4.8
	TrW	24	2.3	1.9	2.5	0.18	7.7
	TaW	25	2.5	2.1	3.1	0.22	8.8
m2	L	30	2.9	2.6	3.2	0.15	5.1
	TrW	30	2.8	2.5	3.3	0.20	7.3
	TaW	30	2.9	2.6	3.3	0.18	6.2
m3	L	21	4.4	4.0	5.1	0.26	5.9
	W	21	2.8	2.4	3.2	0.19	6.6

Abbreviations: dim, dimension; N, sample size; X, sample arithmetic mean; min, minimum value; max, maximum value; sd, standard deviation; cv, coefficient of variation; L, mesiodistal length; TaW, talonid buccolingual width; TrW, trigonid buccolingual width; W, maximum buccolingual width. Units = mm, P, occlusal projection [dental measurement 5 from Boyer et al. (2010) for I1, distance between distal border of margoconid to mesial tip of crown for i1].

euprimates (as well as other taxa). When there is consistency in osteology and soft anatomy between these two groups, that correlation can be used to infer soft anatomical features in extinct, “phylogenetically intermediate” (Bloch et al., 2007) plesiadapiform specimens that exhibit osteology comparable to that of scandentians and/or euprimates.

Phylogenetic analysis of Plesiadapidae

A species level topology was generated using parsimony analyses of a matrix consisting of 32 dental characters, 34 cranial characters, and 31 taxa (Tables A6–A8), including three outgroups (*Purgatorius janisae*, *Elphidotarsius*, and *Carpolestes simpsoni*). Outgroup taxa were scored from the literature, including Bloch et al. (2001), Clemens (2004), and Silcox and Gunnell (2008) for *P. janisae*; Bloch et al. (2001) and Silcox et al.

(2001) for *Elphidotarsius*; and Bloch and Gingerich (1998), Bloch and Silcox (2006), and Bloch et al. (2007) for *Carpolestes simpsoni*. Because species of *Elphidotarsius* are generally poorly known, we used a composite of *Elphidotarsius florencae* and *Elphidotarsius wightoni*, the two most basal species of the Carpolestidae (Fox, 1984; Bloch et al., 2001; Silcox et al., 2001) in the analysis. The 28 plesiadapid species included were scored based on Gingerich (1976), Fox (1990b), Secord (2008), and Boyer et al. (2010), plus newly available data from *Pronothodectes gaoi*, previously undescribed specimens of *Plesiadapis praecursor* (UM 84388) from Douglass Quarry, Montana, *Plesiadapis anceps* (field catalogue # 840313 from UM) (showing the presence of a canine: see Watters and Krause, 1986) from Scarritt Quarry, Montana, and undescribed upper central incisors of *Nannodectes gazini* (CM 76922, CM 76938) from the Saddle locality, Wyoming.

Gingerich (1976) inferred dental formulae for several poorly known plesiadapid species. We follow these inferences in our character coding, unless evidence documented by Gingerich (1976) or elsewhere (i.e., in newly available specimens) contradicts his reconstructions. For instance, Gingerich (1976) inferred that *Plesiadapis cookei*, *Plesiadapis russelli*, and *Platychoerops* species lack upper canines but retain upper second premolars, based on the well-known morphology of *Plesiadapis tricuspidens*. However, as can be seen in a skull (UM 87990) figured by Boyer et al. (2010), *P. cookei* in fact lacks the upper canine and P2. Furthermore, it seems to us that the holotype of *Platychoerops richardsoni* (YM 550) also lacks these teeth. Therefore, it cannot be assumed that *P. russelli* and *Platychoerops daubrei* retained P2.

The character matrix was analyzed with the program NONA (Goloboff, 1999) in WinClada (Nixon, 1999–2002) using a heuristic search of 3,000 replicates.

RESULTS

Systematic paleontology

Class Mammalia Linnaeus, 1758
 Order Primates Linnaeus, 1758
 Family Plesiadapidae Trouessart, 1897
Pronothodectes Gidley, 1923
Pronothodectes gaoi Fox, 1990b
 Figures 2–14; Table 5; Tables A1–A5.

Holotype

UALVP 31238, incomplete left dentary with p3–4, m1–2, and alveoli for i1–2, c1, p2 (Fox, 1990b; p. 639). DW-2 locality; Paskapoo Formation, Alberta, Canada, late Paleocene [middle Tiffanian, Ti3 (Fox, 1990a; Scott, 2008), *Plesiadapis rex*/*P. churchilli* Lineage Zone of Lofgren et al. (2004)].

Material examined

A complete listing of specimens examined for this study can be found in Supporting Information File 1. Table 5 gives sample sizes for each measureable tooth position available.

Age and occurrence

Middle Tiffanian (*Plesiadapis rex*/*P. churchilli* Lineage Zone, Ti3, late Paleocene) of Alberta (Fox, 1990a, b).



Fig. 2. *Pronothodectes gaoi* Fox from the early middle Tiffanian (Ti3) DW-2 (DW2) and Birchwood (BW) localities, Paskapoo Formation, Alberta. UALVP 49292 (BW), right I1 in (A) lateral, (B) medial, and (C) occlusal view; UALVP 46694 (DW2), left I1 in (D) lateral, (E) medial, and (F) occlusal view; UALVP 46695 (DW2), right I1 in (G) lateral, (H) medial, and (I) occlusal view; UALVP 46696 (DW2), left I1 in (J) lateral, (K) medial, and (L) occlusal view; UALVP 46687 (DW2), incomplete skull with right I1 (displaced), P2 (roots), P3–4, M1–3, and alveolus for upper canine (associated petrosal not figured); cheek teeth in (M) labial and (N) occlusal (P3) and posterolingual (molars) view. Scale bars = 2 mm.

Description of dentition of *Pronothodectes gaoi*

Parts of the dentition of *Pronothodectes gaoi* have been described in detail by Fox (1990b). We focus our efforts here on teeth from the new sample that were either unknown or very poorly known from the hypodigm, as well as the anterior parts of the dentition and m3. These latter features have previously been considered important in plesiadapid systematics (see, e.g., Gingerich, 1976). New descriptions of the remaining teeth can be found in Supporting Information File 2.

I1. I1 closely resembles that of other plesiadapids in being elongate and moderately curved, with a broadly concave occlusal surface (Figs. 2A–L and 9A). The robust crown bears two prominent apical cusps, the anterocone and laterocone, and a slightly smaller basal cusp, the posterocone. A small mediocone is developed dorsal and slightly distal to the level of the anterocone. The anterocone is the largest of the apical cusps, being taller and wider at its base than the laterocone, and having its apex directed slightly laterally. Two well-developed crests originate at the apex of the anterocone: the first

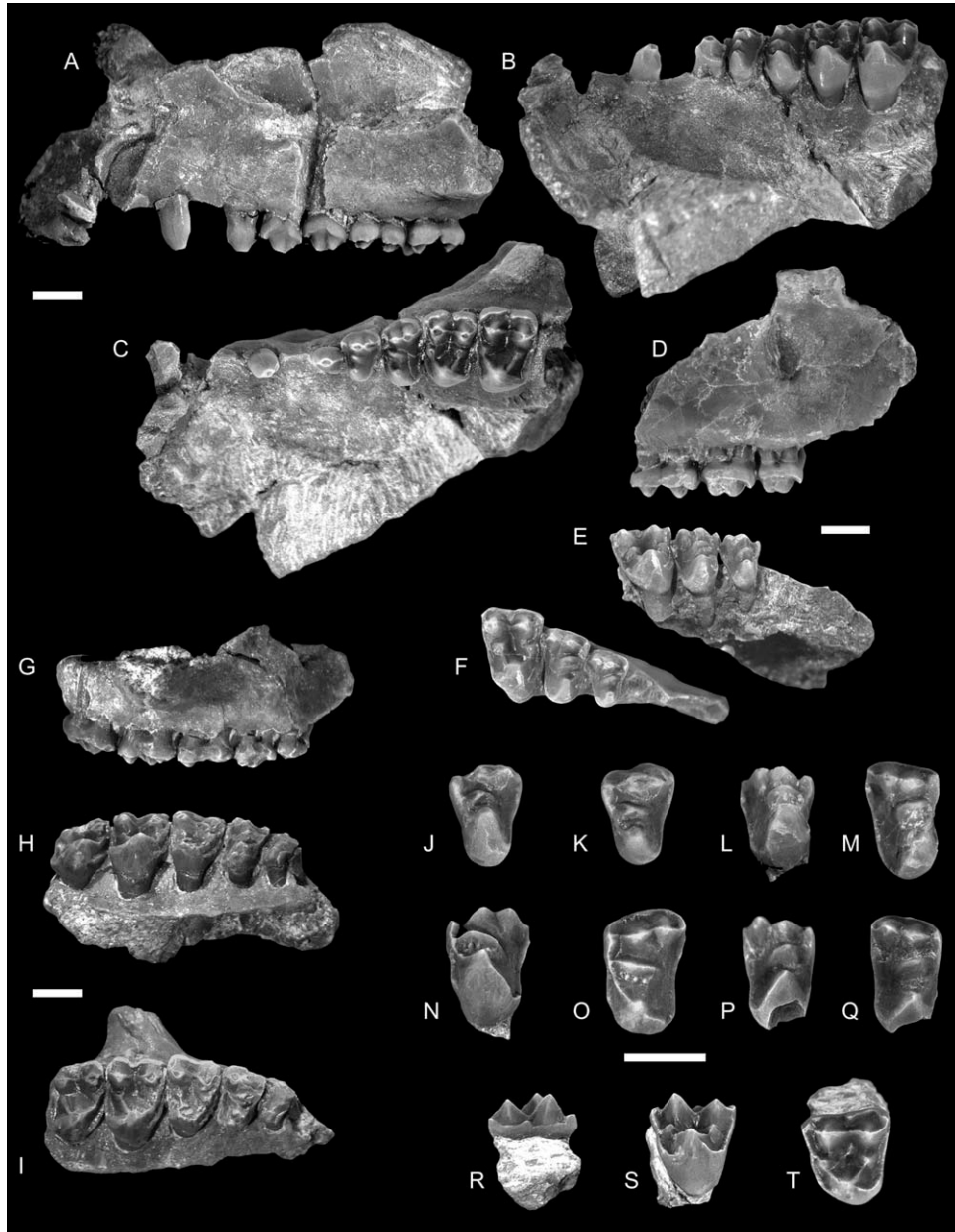


Fig. 3. *Pronothodectes gaoi* Fox from the early middle Tiffanian (Ti3) DW-1 (DW1), DW-2 (DW2), and Birchwood (BW) localities, Paskapoo Formation, Alberta. UALVP 46688 (DW2), incomplete left maxilla with C, P2–4, M1–2, and associated I1 root in (A) labial, (B) oblique lingual, and (C) occlusal view; UALVP 31396 (DW1), incomplete right maxilla with P3–4, M1 in (D) labial, (E) oblique lingual, and (F) occlusal view; UALVP 39359 (BW), incomplete right maxilla with P3–4, M1–3 in (G) labial, (H) oblique lingual, and (I) occlusal view; UALVP 46816 (BW), left P3 in (J) oblique lingual and (K) occlusal view; UALVP 39342 (BW), right P4 in (L) oblique lingual and (M) occlusal view; UALVP 46719 (DW2), left P4 in (N) oblique lingual and (O) occlusal view; UALVP 46720 (DW2), right P4 in (P) oblique lingual and (Q) occlusal view; UALVP 46715 (DW2), left DP4 in (R) labial, (S) oblique lingual, and (T) occlusal view. Scale bars = 2 mm.

extends distolaterally, forming a deep notch between the anterocone and laterocone, whereas the second is shorter and curves distomedially to the mediocone. A raised ridge of enamel on the medial side of the anterocone marks the surface of articulation with the opposing I1; this surface usually bears a flattened, subovoid wear facet as a consequence (e.g., UALVP 46695, Fig. 2H). The apex of the laterocone is directed more distally than that of the anterocone, and a long crest extends from its apex distally and dorsally, defining the lateral margin of the occlusal surface of the crown. A centroconule is not

developed on any of the specimens in the collection in contrast to I1 of *Plesiadapis rex*, in which a centroconule is present (Gingerich, 1976); instead, the enamel is between and slightly dorsal to the anterocone and laterocone is smooth (e.g., Fig. 2I). The mediocone is poorly developed on each of the I1s at hand, appearing most often as a small, nipple-like protuberance (e.g., UALVP 46695, Fig. 2I); a weak crest extends a short distance distodorsally from the mediocone, defining part of the medial margin of the occlusal surface before fading away. The posterocone is conical, and its apex is sharp

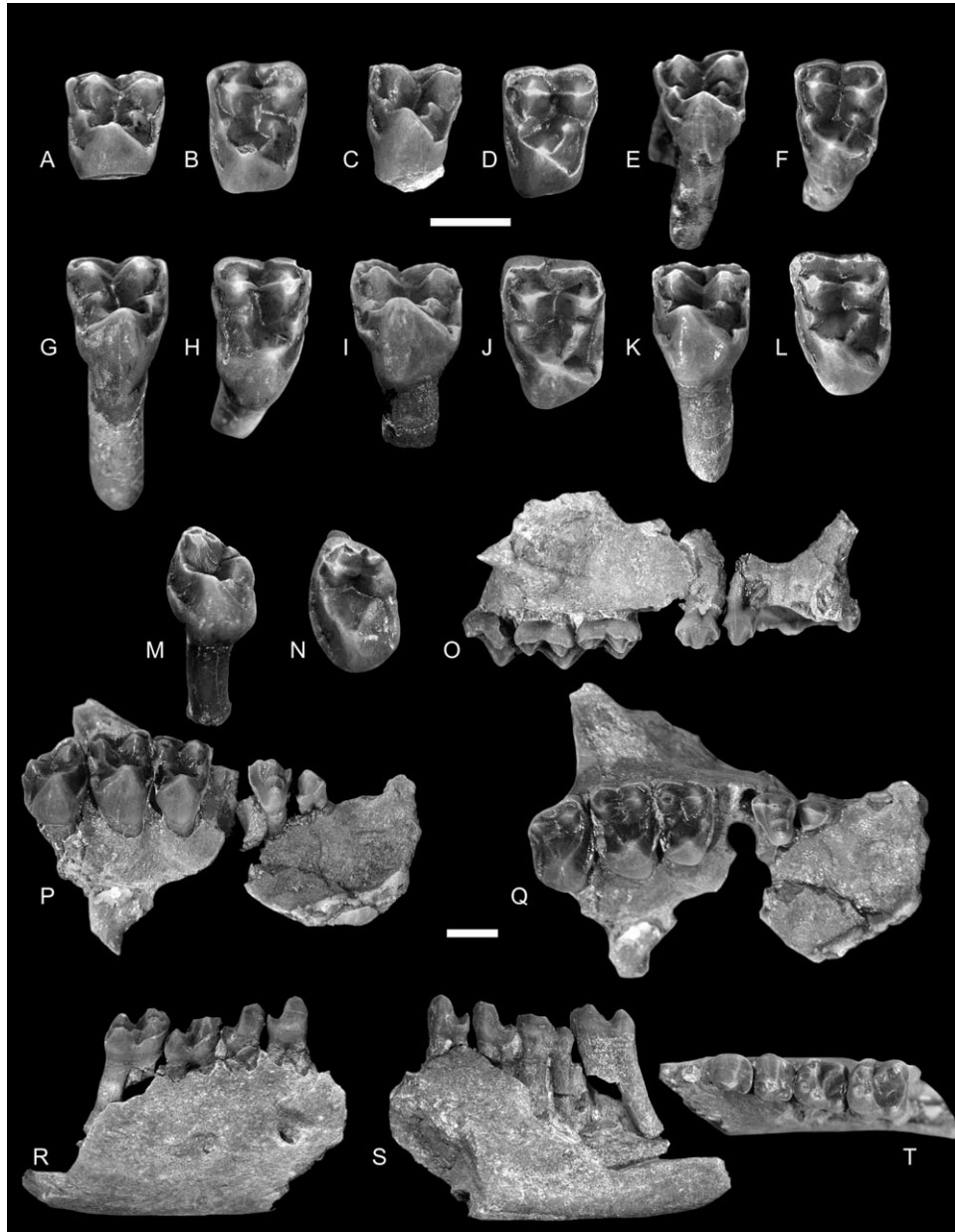


Fig. 4. *Pronothodectes gaoi* Fox from the early middle Tiffanian (Ti3) DW-2 (DW2) and Birchwood (BW) localities, Paskapoo Formation, Alberta. UALVP 46724 (DW2), left M1 in (A) oblique lingual and (B) occlusal view; UALVP 46725 (DW2), left M1 in (C) oblique lingual and (D) occlusal view; UALVP 46726 (DW2), left M1 in (E) oblique lingual and (F) occlusal view; UALVP 39301 (BW), right M2 in (G) oblique lingual and (H) occlusal view; UALVP 49287 (DW2), left M2 in (I) oblique lingual and (J) occlusal view; UALVP 46732 (DW2), left M2 in (K) oblique lingual and (L) occlusal view; UALVP 46818 (BW), left M3 in (M) oblique lingual and (N) occlusal view; UALVP 46686 (DW2), incomplete right maxilla with P2–3, M1–3, alveoli for upper canine and P4, and associated incomplete right dentary with p3–4, m1–2; maxilla in (O) labial, (P) oblique lingual, and (Q) occlusal view; dentary in (R) labial, (S) lingual, and (T) occlusal view. Scale bars = 2 mm.

and directed nearly ventrally; although the posterocrista is conspicuous on UALVP 39332, it is otherwise undeveloped on each of the other specimens at hand. All I1s lack cuspules on the lateral side of the crown between the laterocone and posterocone as occur, e.g., in *Plesiadapis churchilli*.

I2. I2 of *P. gaoi* is preserved in articulation with the crushed but otherwise extensively preserved skull (UALVP 46685, seen best in Fig. 9A) and is the first discovered I2 for the genus. The crown is considerably smaller than that of I1 but is larger than that of the

upper canine. The tooth is single-rooted, and the crown supports a large, somewhat swollen major cusp; a short crest runs distally from the apex of this cusp to near the base of the crown, where it then turns medially and forms a short, weak cingulum.

Upper canine. The upper canine of *P. gaoi* was previously unknown (Figs. 3A–C, 4O–Q, and 9A). The tooth is single-rooted, and the crown closely resembles that of I2. The crown is faintly compressed labiolingually, and a short crest runs distally from its apex, forming a weak distolingual cingulum.

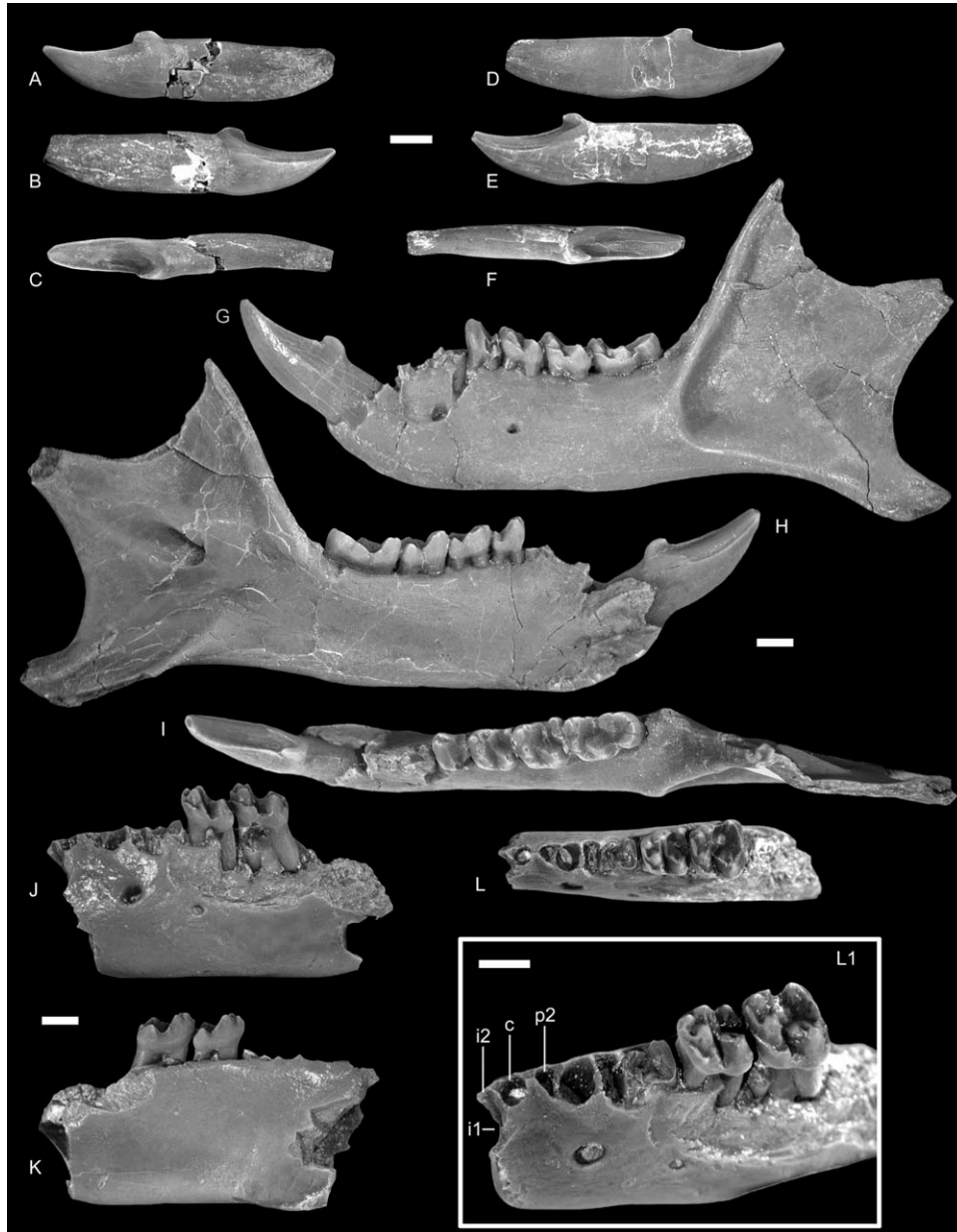


Fig. 5. *Prionothenectes gaoi* Fox from the early middle Tiffanian (Ti3) DW-2 (DW2) and Birchwood (BW) localities, Paskapoo Formation, Alberta. UALVP 46764 (DW2), left i1 in (A) lateral, (B) medial, and (C) occlusal view; UALVP 46765 (DW2), right i1 in (D) lateral, (E) medial, and (F) occlusal view; UALVP 39313 (BW), nearly complete left dentary with i1, p4, m1–3, and alveoli for i2, c, p2–3 in (G) labial, (H) lingual, and (I) occlusal view; UALVP 46762 (DW2), incomplete left dentary with m1–2, and alveoli for i1–2, c, p3–4, m3 in (J) labial, (K) lingual, and (L) occlusal view; box (L1) shows UALVP 46762 in oblique labial view at higher magnification; note the alveoli for i1–2, c, and p2. Scale bars = 2 mm.

P2. A complete P2 is preserved in two specimens of *Prionothenectes gaoi*, and its roots are preserved in a third; a short diastema separates the canine from P2 in each of these specimens (Figs. 3–4, and 9). P2 is two-rooted, with the posterior root larger and more nearly vertically oriented. The crown is triangular in profile and consists primarily of an inflated paracone. A weak preparacrista runs mesially from the apex of the paracone, where it joins a similarly weak mesial cingulum; the postparacrista is more sharply defined and extends distally to join the distal cingulum at the distolabial corner of the crown. An ectocingulum is absent.

Although a distinct protocone is not developed, the crown bulges distolingually, and the anterior and posterior cingula approach but do not unite with one another at the lingual margin of the crown. Neither the metacone nor conules are developed.

P3. See Supporting Information File 2 for description based on presently considered sample (Figs. 3–4, and 9).

DP4. The crown of DP4 is subrectangular in outline, with a slightly longer labial than lingual margin; a well-developed paracone, metacone, protocone, and conules enclose a deep trigon basin (Fig. 3R–T). The paracone is

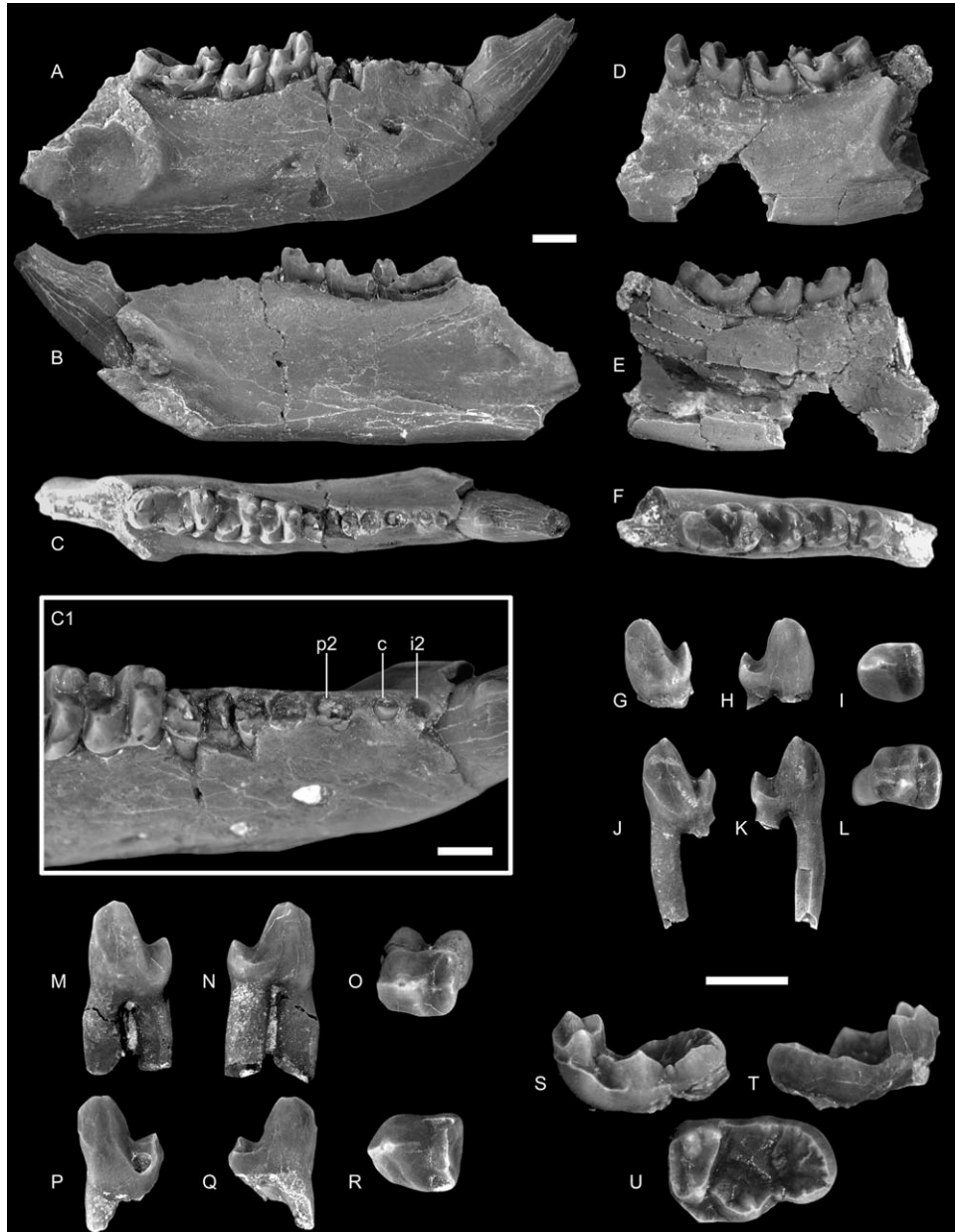


Fig. 6. *Pronothodectes gaoi* Fox from the early middle Tiffanian (Ti3) DW-2 (DW2) and Birchwood (BW) localities, Paskapoo Formation, Alberta. UALVP 46827 (BW), incomplete right dentary with i1, p4 (taloid), m1–3, and alveoli for i2, c, p2–3 in (A) labial, (B) lingual, and (C) occlusal view; box (C1) shows UALVP 46827 in oblique labial view at higher magnification; note the alveoli for i2, c, and p2; UALVP 46826 (BW), incomplete left dentary with p4, m1–3 in (D) labial, (E) lingual, and (F) occlusal view; UALVP 39335 (BW), left p3 in (G) labial, (H) lingual, and (I) occlusal view; UALVP 46776 (DW2), left p3 in (J) labial, (K) lingual, and (L) occlusal view; UALVP 39336 (BW), left p4 in (M) labial, (N) lingual, and (O) occlusal view; UALVP 46779 (DW2), left p4 in (P) labial, (Q) lingual, and (R) occlusal view; UALVP 39356 (BW), left m3 in (S) labial, (T) lingual, and (U) occlusal view. Scale bars = 2 mm.

the largest cusp on the crown, followed by the lower and less massive metacone; a sharp, deeply notched centrocrista connects the apices of the paracone and metacone. The styler shelf is narrow, and a small mesostyle is developed on the ectocingulum at the level of the centrocrista notch, although the centrocrista itself is not deflected labially and does not contact the mesostyle; a small metastylar cusp can be developed on the postmeta-crista. The conules are robust, subequal, and circular in cross-section. The paraconule is positioned slightly mesial to the level of the paracone, and a conspicuous preparaconular crista connects its apex to the mesial

cingulum; the postparaconular crista and metaconular cristae are undeveloped. The protocone is massive, its base occupying nearly half the width of the crown, and its apex is approximately the same height as that of the paracone and metacone; the lingual wall of the protocone is long and sloping, whereas its basin-facing side is steep and nearly flat. The protoconal cingula are wide and robust. The postprotocone fold is prominent and extends from the apex of the protocone to the distal cingulum; a faint swelling on the distal cingulum hints at an incipient hypocone, but a discrete cusp is not present on any of the specimens at hand.

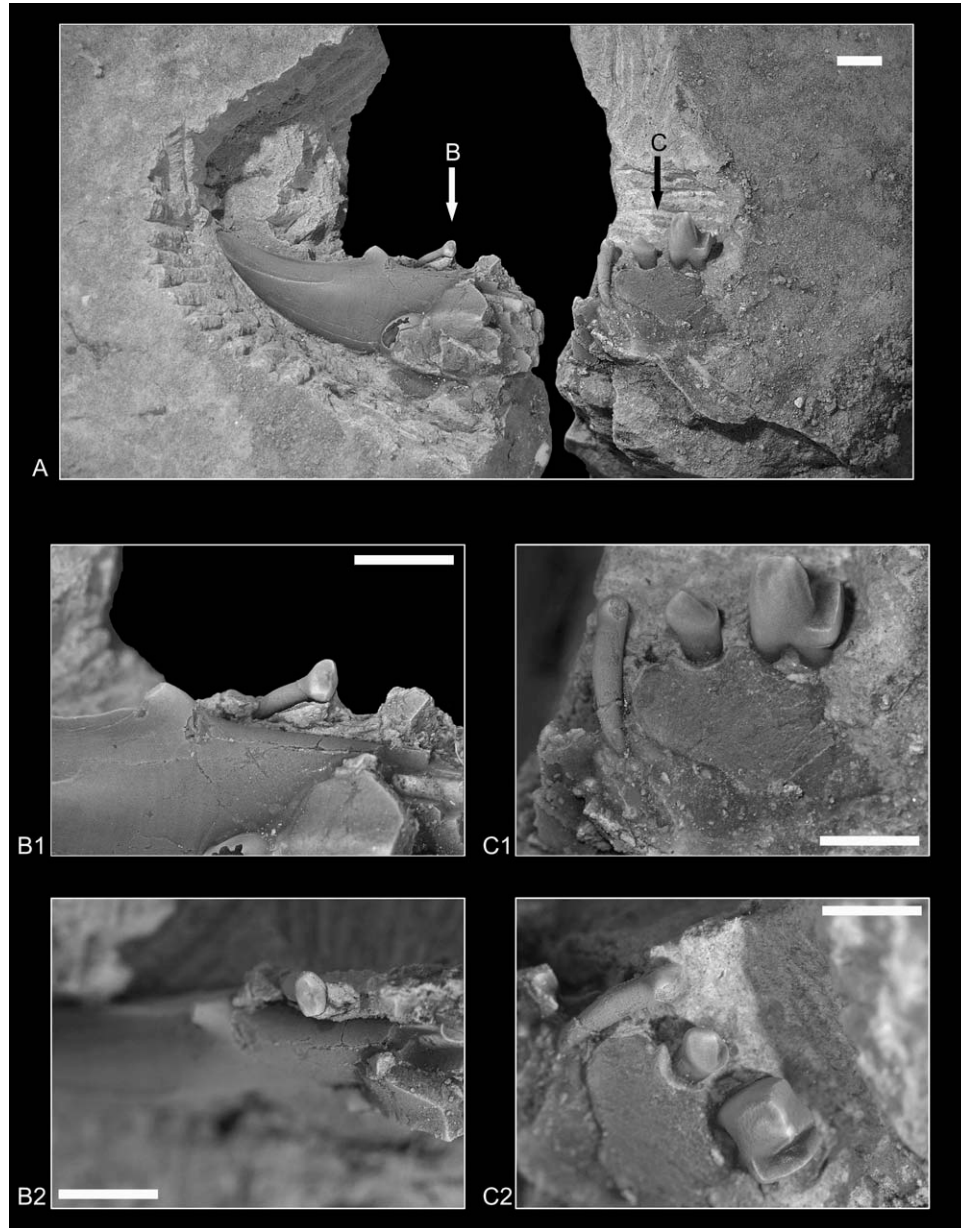


Fig. 7. *Pronothodectes gaoi* Fox from the early middle Tiffanian (Ti3) DW-2 locality, Paskapoo Formation, Alberta. UALVP 31536, incomplete right dentary with i1–2, canine, p2–3 in (A), medial view; (B1), (B2), higher magnification images of area denoted by arrow B; i2 in (B1) medial and (B2) occlusal view; (C1), (C2), higher magnification images of area denoted by arrow C; canine, p2–3 in (C1) lingual and (C2), occlusal view. Scale bars = 2 mm. Note the coronal structure of p2, otherwise known only in other species of *Pronothodectes*. The coronal structure of p2 in other plesiadapids is more like that of i2 and the lower canine of *Pronothodectes*.

P4. See Supporting Information File 2 for description based on presently considered sample (Figs. 3 and 9).

Lower dentition. The lower mesial dentition of *Pronothodectes gaoi* was described in detail by Fox (1990b). Since that publication, several additional specimens referable to *P. gaoi* have been recovered from the Blindman River localities (Scott, 2008), as well as from the middle Tiffanian Birchwood locality in central Alberta (Webb, 1996). The number and disposition of the mesial teeth of *P. gaoi* can now be documented for 12 specimens, all of which preserve alveoli for an enlarged, procumbent medial incisor (i1), a lower lateral incisor (i2), canine, and second lower premolar, although only UALVP 31536 pre-

serves the crowns of i2 and the lower canine (see Fox, 1990b: Fig. 5).

i1. The lower first incisor of *Pronothodectes gaoi* is enlarged and mediolaterally compressed, with the narrow tip directed mesiodorsally and slightly medially (Figs. 5A–I, 6A–C, and 7A). A margoconid is present on all specimens at hand, and the margoconid is sharply defined, extending mesially to the apex of the crown; a second crest defining the medial margin of the occlusal surface of the crown runs distomedially from the tip but fades away before reaching the margoconid. Although i1 varies in length and width, the crown is both shorter and shallower than that of i1 of *Plesiadapis anceps* and *Plesiadapis rex* (see Gingerich, 1976;

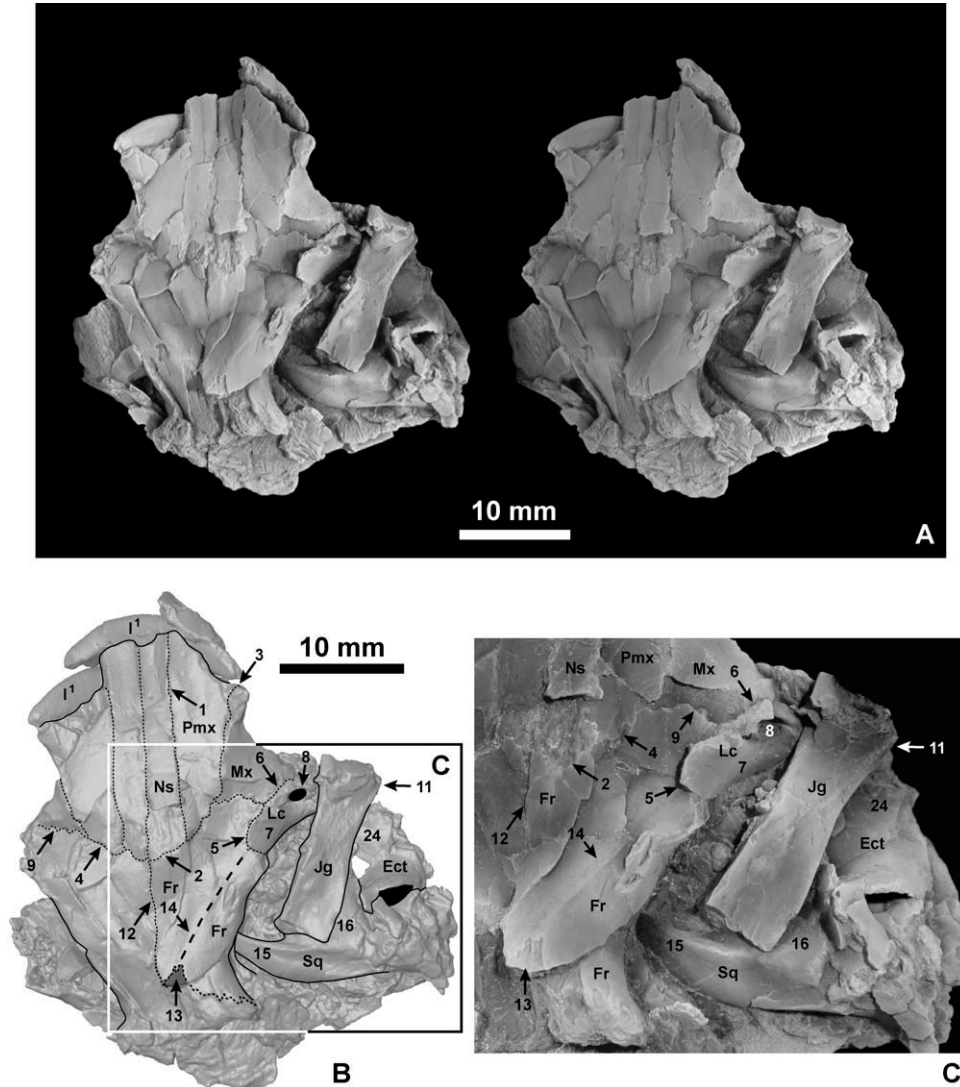


Fig. 8. *Pronothodectes gaoi* Fox from the middle Tiffanian (Ti3) DW-2 locality, Paskapoo Formation, Alberta. UALVP 46685, incomplete skull. **A**, stereophotograph of dorsal aspect. **B**, HRxCT image of dorsal aspect. Fine, black, dashed lines indicate sutures. Coarse, black, dashed line indicates position of temporal ridge of frontal. Solid lines indicate boundaries between major subdivisions of the specimen. **C**, inset of orbital region. **C'**, enlargement of **C**. Numbers and abbreviations: 1—nasal/premaxilla suture, 2—nasal/frontal suture, 3—premaxilla/maxilla suture, 4—premaxilla/frontal suture, 5—lacrimal/frontal suture, 6—lacrimal/maxilla suture, 7—orbital process of lacrimal, 8—lacrimal foramen, 9—maxilla/frontal suture, 11—level on jugal where width measurement was taken, 12—interfrontal suture, 13—frontal/parietal suture, 14—temporal ridge of frontal, 15—zygomatic process of squamosal, 16—glenoid fossa of squamosal, 24—remnants of tympanic bulla. Ect, ectotympanic; Fr, frontal; J, jugal; Lc, lacrimal; Mx, maxilla; Ns, nasal; Pmx, premaxilla; Sq, squamosal; Jg, jugal.

pls. 3B, 3C), and in these regards more closely approaches the proportions of *i1* of *Pronothodectes matthewi*.

***i2*.** The discovery of 12 additional mandibles of *Pronothodectes gaoi* from the Blindman River and Birchwood localities that preserve the mesial alveoli sheds light on the variation in development of this tooth (Figs. 5L1, 6C1, and 7B1–B2). Although none of the new specimens retain *i2*, its alveolus is invariably present, clearly indicating that *i2* is in fact a feature that characterizes *P. gaoi*, rather than being variably present as Gingerich (1991) maintained [and as is apparently the case, e.g., for *p2* in *Plesiadapis churchilli* (see Gingerich, 1976), or the lower canine in *Plesiadapis anceps* (see Watters and Krause, 1986) and now *Plesiadapis praecursor*, as documented here]. The alveolus for *i2* is best seen in UALVP

39372, 46827 (Fig. 6C1), 46762 (Fig. 5L1), and 39313 (Fig. 5G–I). The *i2* alveolus is only slightly smaller than that for the lower canine in UALVP 46827 and 46762, but is very small in UALVP 39313, and is slightly larger than the canine alveolus in UALVP 39372. Irrespective of its size, the aperture of the *i2* alveolus is circular and closely appressed to the alveolar rim of *i1* and is somewhat displaced toward the lateral margin of the dentary. The contours of the *i2* alveolus are best seen on UALVP 31238 (holotype), 31240, and 46762, where the anterior-most parts of the jaw have been broken away, essentially sectioning the *i2* alveolus in the transverse plane. The alveolus is slender throughout its depth (see, e.g., UALVP 46762, Fig. 5L1), in keeping with the thin *i2* root as described by Fox (1990b), and extends ventrally and slightly distally along the labial side of the jaw.

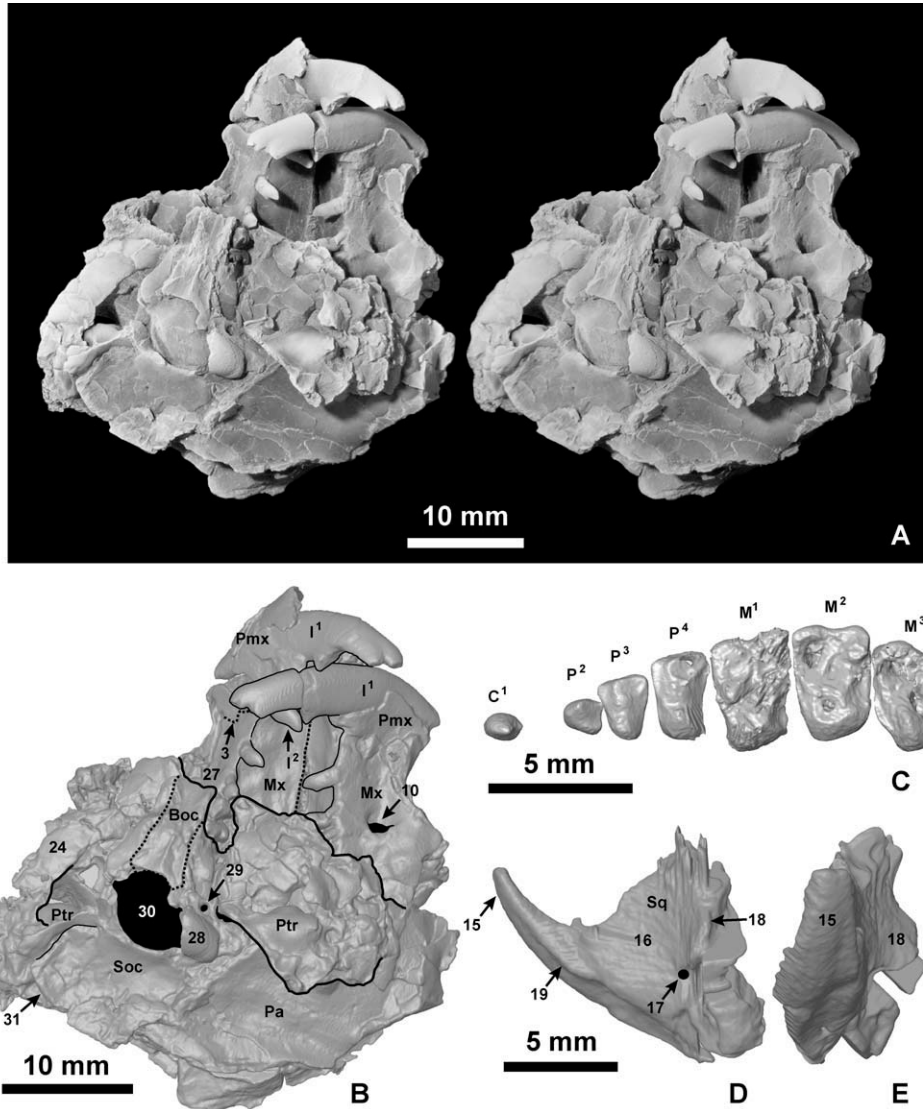


Fig. 9. *Pronothodectes gaoi* Fox from the middle Tiffanian (Ti3) DW-2 locality, Paskapoo Formation, Alberta. UALVP 46685, incomplete skull. **A**, stereophotograph of ventral aspect. **B**, HRxCT image of ventral aspect. **C**, HRxCT image of left C1, P2–3, M1–3 in occlusal view. **D**, close-up HRxCT image of right squamosal in ventral view. **E**, close-up HRxCT image of right squamosal in lateral view. Anterior to top for A, B, D, E. Fine dashed lines represent sutures; fine and heavy solid lines represent boundaries between major subdivisions of the specimen. Numbers and abbreviations: 3—premaxilla/maxilla suture, 10—infraorbital foramen, 15—zygomatic process of squamosal, 16—glenoid fossa of squamosal, 17—postglenoid foramen, 18—entoglenoid process, 19—level on zygomatic process of squamosal for measurement of width, 24—remnants of tympanic bulla, 27—anterior end of basioccipital, 28—occipital condyle, 29—hypoglossal foramen, 30—foramen magnum, 31—nuchal crest. Boc, basioccipital; Mx, maxilla; Pa, parietal; Pmx, premaxilla; Ptr, petrosal; Soc, supraoccipital; Sq, squamosal.

Although *i2* is not preserved in articulation with the jaw in any of the new specimens at hand, the orientation of its alveolus suggests that it was slightly procumbent, similar to *i2* in other species of *Pronothodectes* (Gingerich, 1976). The crown of *i2* is small and peg-like, somewhat elongate, with a low, flattened apex (Fig. 7B).

Lower canine. The lower canine of *Pronothodectes gaoi* is as yet known only from UALVP 31536, although its alveolus is present on 14 specimens preserving the anteriormost parts of the jaw (Figs. 5J–L, 6A–C, and 7C). The alveolar aperture is subequal in diameter to that of *p2* in UALVP 31536 but smaller in UALVP 46827 and 39372. Parts of the alveolar walls of the lower canine are exposed in UALVP 39373, and their contours indicate that the

canine was shallowly rooted, slender, and nearly vertically implanted in the jaw. A short diastema intervenes between the canine alveolus and *p2*, an observation made by Fox (1990b) for the hypodigm; the diastema varies slightly in length, and a small foramen is sometimes present on the alveolar surface of the diastema, occupying the position of the undeveloped *p1*. The crown of the lower canine in *P. gaoi* is slightly larger but otherwise resembles that of *i2* in being small and peg-like, with a low, blunt apex (Fig. 7C).

***p2*.** The single-rooted *p2* is preserved only in UALVP 31536 (Fig. 7A–C). The crown is premolariform, with a low, somewhat bulbous protoconid, and a weakly developed heel (Fig. 7C).

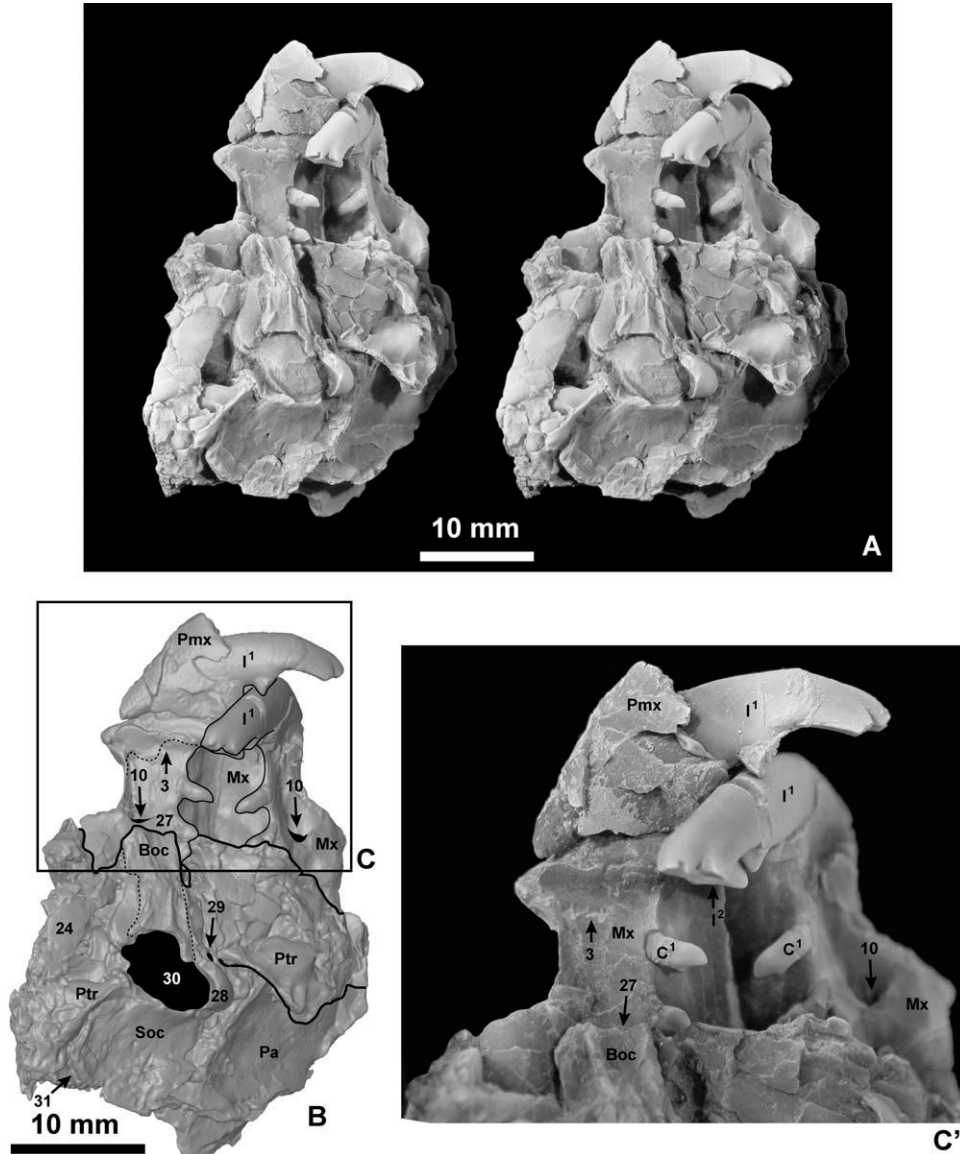


Fig. 10. *Pronothodectes gaoi* Fox from the middle Tiffanian (Ti3) DW-2 locality, Paskapoo Formation, Alberta. UALVP 46685, incomplete skull. **A**, stereophotograph of right lateral aspect. **B**, HRxCT image of right lateral aspect. **C**, inset of rostral region. **C'**, enlargement of **C**. Fine dashed lines represent sutures; fine and heavy solid lines represent boundaries between major subdivisions of the specimen. Numbers and abbreviations: 3—premaxilla/maxilla suture, 10—infraorbital foramen, 24—remnants of tympanic bulla, 27—anterior end of basioccipital, 28—occipital condyle, 29—hypoglossal foramen, 30—foramen magnum, 31—nuchal crest. Boc, basioccipital; Mx, maxilla; Pa, parietal; Pmx, premaxilla; Ptr, petrosal; Soc, supraoccipital; Sq, squamosal.

p3-4. See Supporting Information File 2 for description based on presently considered sample (Figs. 4-7).

m1-2. See Supporting Information File 2 for description based on presently considered sample (Figs. 4-6).

m3. The morphology of m3 has figured importantly in plesiadapid systematics (see, e.g., Gingerich, 1976), particularly the development of the hypoconulid lobe (Figs. 5G-I and 6A-F,S-U). Fox (1990b) briefly described the m3 in UALVP 31538, the only m3 referable to *Pronothodectes gaoi* at that time, whereas the current sample includes 22 m3s. The crown consists of a mesiodistally short trigonid and distally expanded talonid bearing a lobate hypoconulid. The protoconid and paraconid are subequal in stoutness and height and are transversely opposed to one another. The metaconid is variably devel-

oped: in most specimens (e.g., UALVP 39313, Fig. 5I), it is smaller than the paraconid and closely appressed to it, with the two cusps being connate for almost their entire height, while in other specimens (e.g., UALVP 39356, Fig. 6U), it is subequal to the paraconid and separated from it by a narrow notch. As on m1 and m2, the paracristid on m3 is low and curves mesiolingually from the protoconid to form a mesial shelf. The protocristid is long and concave dorsally, rather than being distinctly notched. The talonid is elongate, with a broad and shallow basin that is bounded by a tall, massively developed hypoconid, a poorly differentiated entoconid, and an enlarged and lobate hypoconulid. Although a few specimens have a more angular hypoconulid lobe (i.e., the posterior margin of the crown is labiolingually expanded and seems "squared off" in occlusal view, e.g., UALVP

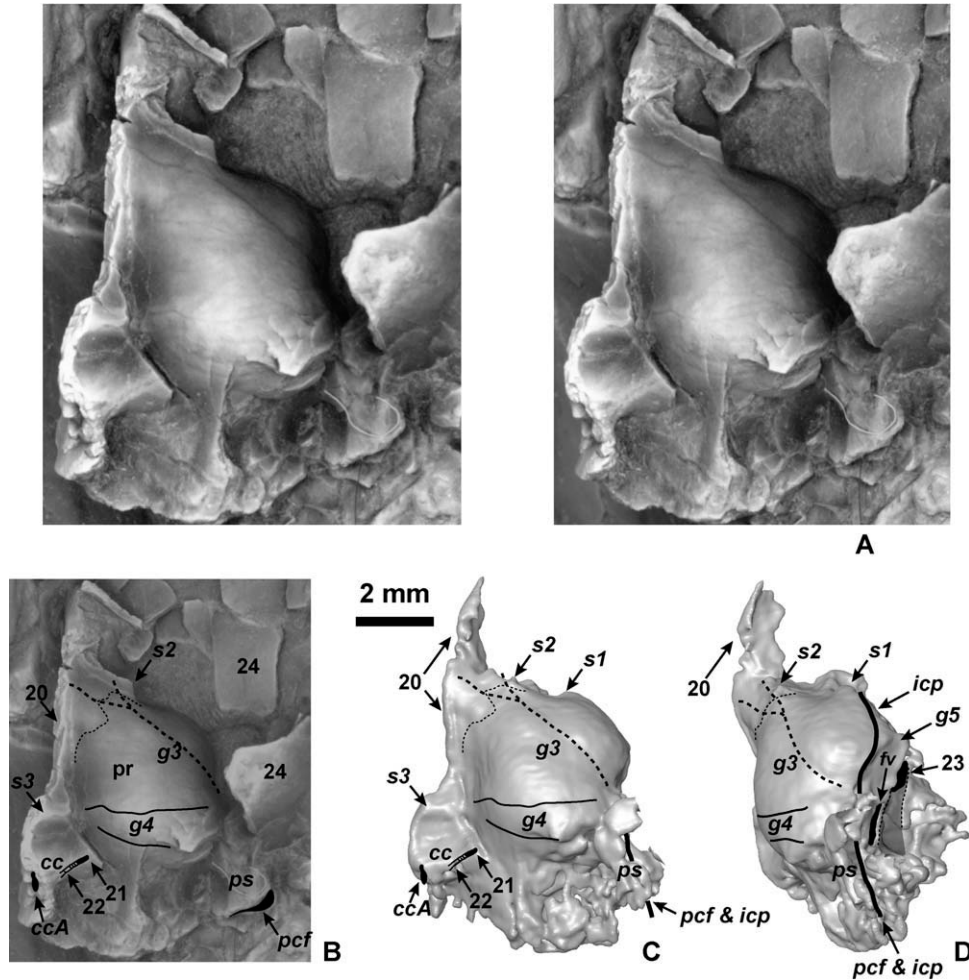


Fig. 11. *Pronothodectes gaoi* Fox from the middle Tiffanian (Ti3) DW-2 locality, Paskapoo Formation, Alberta. UALVP 46685, incomplete skull. **A**, stereophotograph of left promontorium in ventral aspect. **B**, left promontorium in ventral aspect—same image as in **A**—identifying key structures. **C**, HRxCT image of ventral view of left promontorium in ventral view. **D**, HRxCT image of left promontorium in ventrolateral view. Anterior to top in all figure parts. Fine dashed lines represent possible sutures; thick dashed line represents *g3* groove. Nerves reconstructed as thin black lines represent components of tympanic plexus. Neurovasculature reconstructed as thick black lines represent components of internal carotid plexus. 2 mm scale applies to **B**–**D**. Numbers and abbreviations: 20—rostral tympanic processes of petrosal, 21—Tympanic nerve foramen, 22—Tympanic nerve groove, 23—broken facial (for CN VII) canal, 24—remnants of tympanic bulla. cc, cochlear canaliculus; ccA, broken aperture of cochlear canaliculus; fv, fenestra vestibuli; *g3*, groove that leads to *s2* (for a small vein); *g4*, groove for tympanic plexus fibers to reach grooves *g1*–*3*; *g5*, groove that leads toward and then passes anterodorsal to epitympanic crest; icp, internal carotid plexus; pcf, posterior carotid foramen; ps, posterior septum (and internal carotid canal); pr, promontorium of petrosal; *s1*, first (anterior) septum; *s2*, second septum; *s3*, third septum.

46826, Fig. 6F), the majority of specimens have a more smoothly rounded lobe (e.g., UALVP 39313, 39356, Figs. 5I and 6U), similar to that in other species of *Pronothodectes* and stratigraphically earlier species of *Nannothodectes* (Gingerich, 1976). Incipient fissures can sometimes be developed on the hypoconulid lobe of some m3s at hand, superficially dividing the lobe into multiple parts (e.g., UALVP 39313, Fig. 5I), but deep distal and distolingual clefts are neither developed nor do the fissures extend into the talonid basin as they do in many species of *Plesiadapis*, including *Plesiadapis rex*. The cristid obliqua meets the postvallid wall in a low and labial position and occasionally can bear a mesoconid swelling close to its contact with the trigonid. The mesial cingulid is robust, extending distally past the hypoflexid to the hypoconid; the distal cingulid is represented only by a short shelf-like structure below the notch between the hypoconid and the hypoconulid lobe.

Description of new cranial material of *Pronothodectes gaoi*

UALVP 46685 is a highly deformed, incomplete skull of *Pronothodectes gaoi* that preserves right and left I1 right I2, right and left canine, P2–4, concealed left and right M1–3. Heavy wear on P4 and M1–3 (revealed with HRxCT imaging) demonstrates that this specimen is from an ontogenetically old individual. The alveolar processes of the maxillae have been rotated medially toward one another. The neurocranium has been rotated ventrally and folded anteriorly so that the right glenoid fossa faces dorsally (Fig. 8), whereas the basicranium has been translated anteriorly, ventral to the molar dentition, thereby concealing these teeth (Fig. 9A–B shows from ventral view that the basicranial region has been rotated and translated anteriorly to cover the maxillary dentition). Finally, the already distorted specimen was

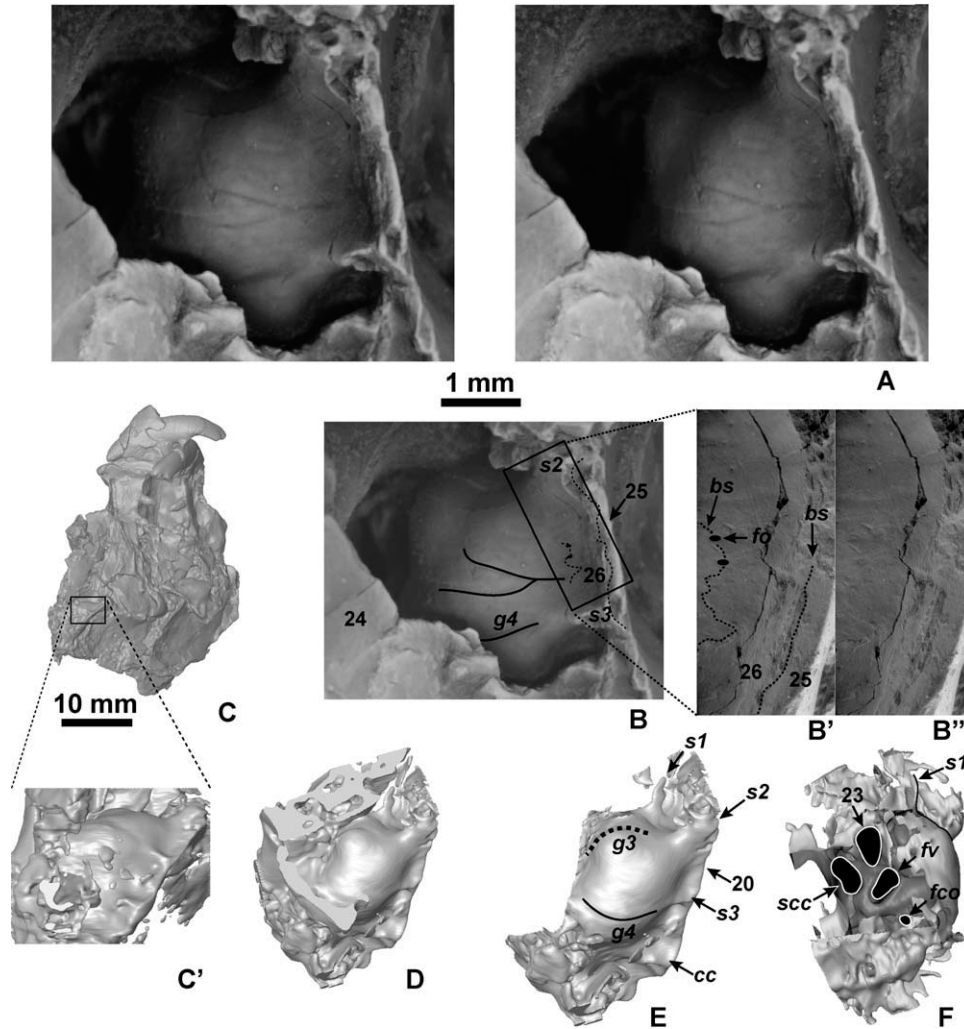


Fig. 12. *Pronothodectes gaoi* Fox from the middle Tiffanian (Ti3) DW-2 locality, Paskapoo Formation, Alberta. UALVP 46685, incomplete skull. **A**, stereophotograph of right promontorium in ventromedial aspect, with 1 mm scale below. **B**, same image as shown in **A** (right promontorium in ventromedial aspect) showing identification of major features. **B'**, medial tympanic process of right promontorium in ventromedial view showing identification of major features. **B''**, medial tympanic process of right promontorium in ventromedial view. **B'** and **B''** have been enlarged by 200% compared with **B**. **C**, HRxCT image of right lateral view of skull. **C'**, inset of promontorium in ventromedial view from **C**. **D**, image from **C'** rotated to ventral view. **C'**–**D** enlarged by 600% compared with **C**. **E**, labeled image from **D** with obscuring surfaces cropped away. **F**, labeled image from **E** rotated to lateral view, to reveal foramina and cross-sectioned canals. **E**–**F** enlarged by 121%, when compared with **C'**–**D**. Anterior to top in all images. Nerves reconstructed as thin black lines represent components of tympanic plexus. Thin black line associated with *s1* represents internal carotid plexus. Fine dashed lines represent sutures; thick dashed line represents *g3* groove. Numbers and abbreviations: 20—rostral tympanic process of petrosal, 23—broken facial (for CN VII) canal, 24—remnants of tympanic bulla, 25—dorsal (petrosal?) layer of bone on rostral process of petrosal, 26—ventral (nonpetrosal?) layer of bone on rostral process of petrosal; *bs*, bullar suture; *cc*, cochlear canaliculus; *fco*, fenestra cochleae; *fv*, fenestra vestibuli; *fo*, foramen (likely leads to canals that transmitted neurovasculature between tympanic cavity and jugular foramen); *g3*, groove that leads to *s2*; *g4*, groove for tympanic plexus fibers to reach grooves *g1*–*3*; *s1*, first (anterior) septum; *s2*, second septum; *s3*, third septum; *scc*, semicircular canal.

subsequently flattened dorsoventrally. Due to the deformation that UALVP 46685 has sustained, many sutures, foramina, and morphological details are obscured. Even so, the specimen provides the first substantial information about cranial morphology in *Pronothodectes*; this morphology can now be readily compared with that known for other plesiadapids, enabling a better assessment than before of the patterns of change that may have characterized the evolutionary history of this important family of early euprimate relatives.

Nasal. The nasal contacts its counterpart along the dorsal midline; it meets the premaxilla anteriorly (Fig. 8B: 1)

and the frontal posteriorly (Fig. 8C': 2). The nasal has distinct sutures with the premaxilla, but its contact with the frontal is more difficult to discern due to crushing and missing bone; the suture between the nasals at the midline, however, is exposed and is straight. The width of the nasal is fairly constant from anterior to posterior (average unilateral width = 2.6 mm). In length, the nasals seem to have extended posteriorly to a level above P3–4.

Premaxilla and premaxillary dentition. Both premaxillae are preserved, but the right element has suffered less damage than the left (Figs. 8, 9A–B, and 10). The sutures between the premaxilla and the nasal (Fig.

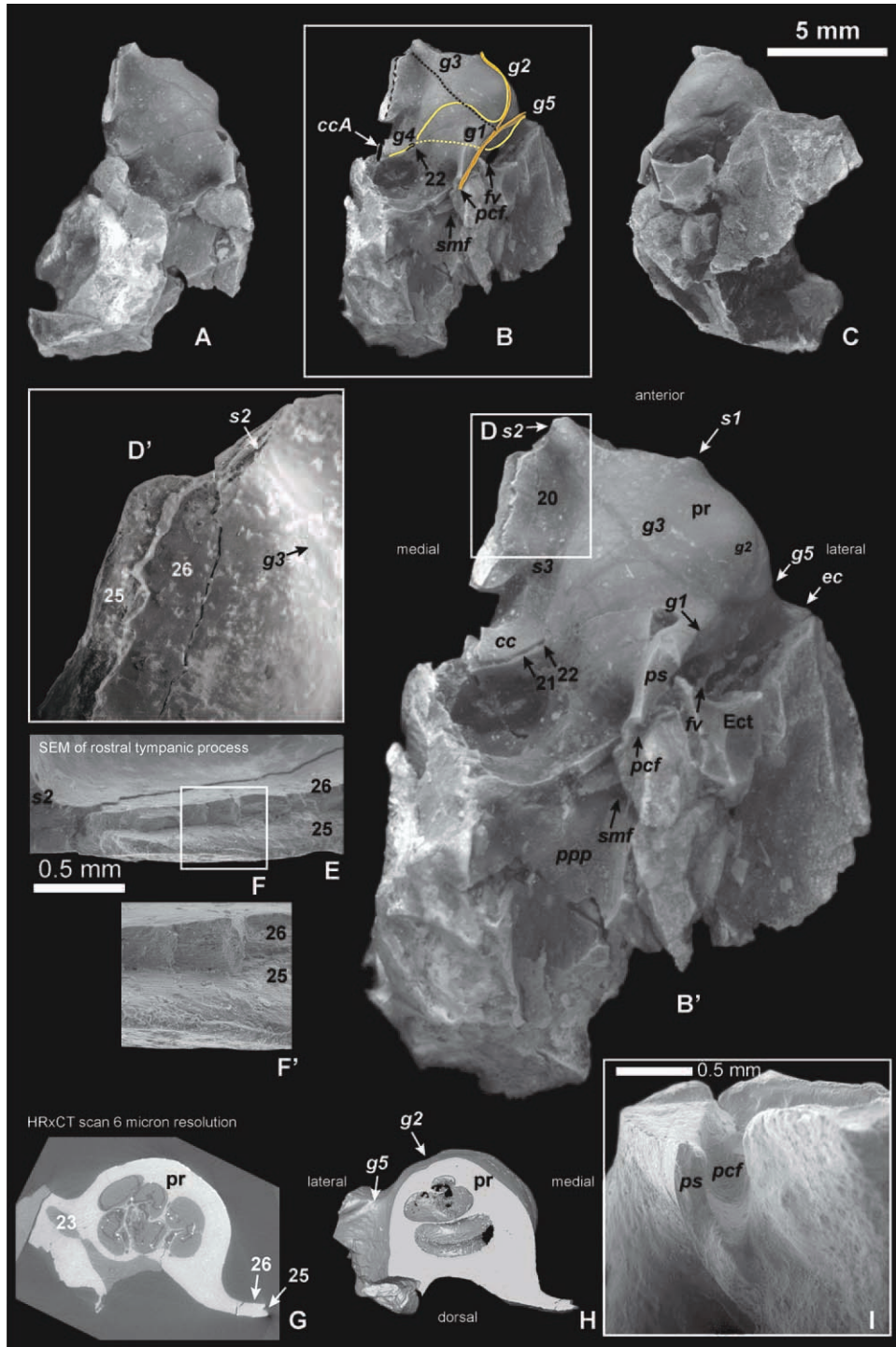


Fig. 13. *Pronothodectes gaoi* Fox from the middle Tiffanian (Ti3) Joffre Bridge locality, Paskapoo Formation, Alberta. UALVP 49105, basicranial fragment containing left petrosal. **A**, ventromedial view. **B**, ventral view. **B'**, enlargement of ventral view. **C**, lateral view. **D**, inset of medial tympanic process in ventral view. **D'**, enlargement of inset from **D**. **E**, Scanning Electron Microscopy (SEM) image, medial view of medial tympanic process. **F**, SEM inset of medial tympanic process in medial view. **F'**, enlargement of inset from **F**. **G**, HRxCT coronal cross-section through petrosal showing that the separation between the two laminae visible in **B** and **D-F** is not visible internally. **H**, HRxCT of petrosal. **I**, SEM of posterior view showing posterior carotid foramen with the ventral surface up. Anterior to top in **A-D'**. 5 mm scale applies to **A-C** (**B'** is enlarged by 215%, when compared with **B**). 0.5 mm scales apply to **E, F**, and **I** (**F'** is enlarged by 200%, when compared with **F**). Nerves reconstructed in yellow represent components of tympanic plexus. Neurovasculature reconstructed in brownish-orange represents components of internal carotid plexus. Coarse dashed line—boundary between laminae of medial tympanic process of petrosal (shown in **B** only), fine dashed line—*g3* groove. Numbers and abbreviations: 20—rostral tympanic processes of petrosal, 21—Tympanic nerve groove, 22—Tympanic nerve foramen, 25—dorsal (petrosal?) layer of bone on rostral process of petrosal, 26—ventral (nonpetrosal?) layer of bone on rostral process of petrosal. cc, cochlear canaliculus; ccA, broken open aperture of cochlear canaliculus; fv, fenestra vestibuli; *g1*, groove for internal carotid plexus; *g2*, groove for distal part of internal carotid plexus; *g3*, groove that leads to *s2* (for a small vein?); *g4*, groove for tympanic plexus fibers to reach routes *g1-3*; *g5*, groove that leads toward and then passes anterodorsal to epitympanic crest; ps – posterior septum; ec, epitympanic crest; Ect, ectotympanic; pcf, posterior carotid foramen; ppp, paroccipital process of petrosal; ptr, petrosal; *s1*, first (anterior) septum; *s2*, second septum; *s3*, third septum; smf, stylomastoid foramen (for CN VII).

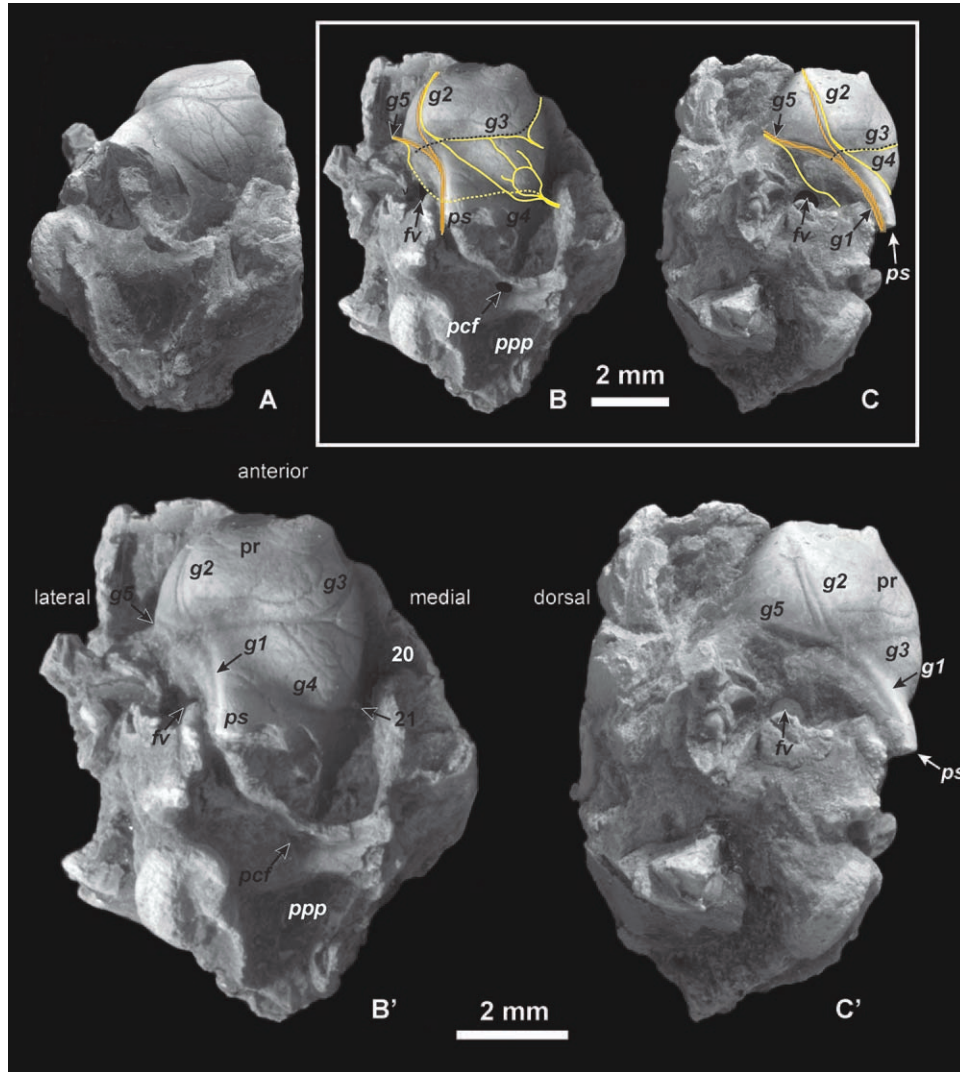


Fig. 14. *Pronothodectes gaoi* Fox from the middle Tiffanian (Ti3) DW-2 locality, Paskapoo Formation, Alberta. UALVP 46687, incomplete right petrosal. **A**, ventromedial view. **B**, ventral view, with major features identified. Note that unlabeled loop of nerves reconstructed here is not consistently evident in other specimens, but grooves labeled *g1*–*5* are present in each of them. Scale encircled by box around **B**–**C** applies to **A**–**C**. **B'** is enlarged by 150%, when compared with **B**. **C**, lateral view, with major features identified. **C'**, enlarged view of **C**. Nerves reconstructed in yellow represent components of tympanic plexus. Neurovasculature reconstructed in brownish-orange represents components of internal carotid plexus. Anterior is toward the top in all images. Fine dashed line—*g3* groove. Numbers and abbreviations: 20—rostral tympanic processes of petrosal, 21—Tympanic nerve foramen. *g1*, groove for internal carotid plexus; *g2*, groove for distal part of internal carotid plexus; *g3*, groove that leads to *s2* (for a small vein?); *g4*, groove for tympanic plexus fibers to reach routes *g1*–*3*; *g5*, groove that leads toward epitympanic crest; *fv*, fenestra vestibuli; *ps*, posterior septum; *pcf*, posterior carotid foramen; *ppp*, paroccipital process of petrosal; *pr*, promontorium of petrosal.

8B: 1), maxilla (Figs. 8B, 9B, and 10C–C': 3), and frontal (Fig. 8B–C: 4) are clearly visible. The suture with the nasal extends approximately anteroposteriorly; it is straight and simple (Fig. 8B: 1). The suture between the right premaxilla and maxilla is observable just posterior to I2 (Figs. 9B and 10C–C': 3); it is strongly sinuous and runs dorsoventrally for ~3 mm before meeting a conspicuous anteroposterior crack. Dorsal and posterior to the crack this suture is straighter, more like that with the nasal (Fig. 8B: 3). When the suture is followed farther posteriorly, it turns somewhat medially as the premaxilla narrows (Fig. 8). The premaxillary/maxillary suture intersects the frontal at a level slightly anterior to the junction between the premaxilla and the nasal. Thus, the premaxillary/frontal suture (Fig. 8B–C: 4) is oblique, from anterolateral to posteromedial. It is 4.36 mm long.

Whether the incisive foramen is contained completely within the premaxilla or in combination with the maxilla cannot be determined because of deformation in this region of the skull (Figs. 9A–B and 10A–C').

The premaxilla contains only two teeth, which we interpret to be I1–2 (Figs. 9A–B and 10A,C–C'). The structure and coronal dimensions of I1 (4.03 mm in mesiodistal length, 2.94 mm in mediolateral width) are characteristic of those referred to *Pronothodectes gaoi* as described above. I2 of this specimen is the only known tooth from this locus in the sample of *P. gaoi* at hand and has been described above.

Lacrimal. The dorsal half of the right lacrimal is exposed to view (Fig. 8: 7). Remnants of the left element, if present, have not been recognized. The suture of the

right lacrimal with the frontal (Fig. 8B–C: 5) and part of that between the right lacrimal and maxilla (Fig. 8B–C: 6) are clearly evident, although the anterior margin of the lacrimal is damaged such that the presence of a lacrimal tubercle cannot be determined. The lacrimal seem to have contributed extensively to the orbital mosaic (Fig. 8B–C: 7), and it also formed the anteromedial part of the orbital rim. The lacrimal does not, however, seem to have extended substantially outside of the orbit: there is no evidence of a large facial process. The right lacrimal foramen (Fig. 8B–C: 8) is relatively large ($\sim 1.53 \text{ mm} \times 1.61 \text{ mm}$), seems to be located on the orbital rim, and faces dorsolateroposteriorly (Fig. 8).

Maxilla and maxillary dentition. The right and left maxillae are present and each contains C, P2–4, M1–3 (Figs. 9 and 10), although all but C–P4 are concealed from external view by overlying bones. The rostral parts of the maxillae are well preserved (Figs. 9C and 10), but their more posterior parts were destroyed during preservation, and consequently the contribution of the maxilla to the orbital mosaic cannot be determined (Figs. 9A–B and 10).

The maxillae have been rotated medially through deformation so that the occlusal surfaces of the left and right tooth rows are at right angles to one another (Figs. 9A–B and 10). Canines, premolars, and molars contained in a skull of *Pronothodectes* have never been discovered previously. Although it is not possible to give detailed descriptions of P4–M3 in UALVP 46685, their dimensions and major structural features can be determined from the HRxCT image of the specimen (Fig. 9C).

The coronal structure of the canine and P2–4 of UALVP 46685 is consistent with that of other specimens referred to *Pronothodectes gaoi* as described above and have the following mesiodistal by buccolingual dimensions (mm): canine, 1.26×0.89 ; P2, 1.47×1.25 ; P3, 1.79×2.23 ; P4, 2.02×3.09 . The canine is separated from I2 by a diastema of 2.46 mm and from P2 by a diastema of 1.54 mm. No diastemata occur more distally in the tooth row. The canine and P2–4 exhibit substantial wear and some details of their coronal structure are difficult to discern as a result. HRxCT reconstructions of the concealed molars show that these teeth are also substantially worn. These teeth have the following mesiodistal by buccolingual dimensions (in millimeters): M1, 2.82×4.06 ; M2, 2.79×4.26 ; M3, 2.60×3.93 . The dimensions of the upper dentition of UALVP 46685 are in the middle of the range of the rest of the sample (Table 5), possibly suggesting that the skull represents an individual of average size. Repositioning of cropped scan images of the teeth in this specimen allows an estimate of the length of its tooth row from P2 to M3 at 13.47 mm.

The maxilla meets the frontal between the premaxilla (medially) and lacrimal (laterally), along a suture that is 3.77 mm long on the left side of the skull (Fig. 8B–C': 9). Contact between the palatal process of the maxilla with the palatine (along the transverse palatine suture) is concealed by bones displaced during the deformation that this specimen has sustained (Fig. 9). The osseous palate is, however, in view at a level anterior to P4, implying that the maxillary/palatine suture was located more posteriorly. The width of the palatal process of the right maxilla just posterior to I2 is 3.39 mm, while at the anterior margin of P2, it measures 5.45 mm. These dimensions thus reveal an anteriorly tapering snout. The length of the infraorbital canal cannot be determined due to crush-

ing of the posterior parts of the maxilla, but the diameters of the left infraorbital foramen are 2.12 mm (height) and 1.26 mm (width). The infraorbital foramen opens above P2–3 (Figs. 9A–B and 10A,C–C': 10).

Finally, at least three other maxillary specimens UALVP 46688 (Fig. 3C), UALVP 39359 (Fig. 3I), and UALVP 46686 (Fig. 4Q) provide information relevant to description of the maxilla. They exhibit an anteroposteriorly expanded zygomatic process which mirrors similar expansion of the ventral surface of the anterior end of the jugal of the skull, near its contact with the maxilla (Fig. 8: 11). From these specimens it can also be seen that the zygomatic process always arises lateral to M2.

Jugal. As indicated above, a fragment of the right jugal is preserved (Fig. 8), but it has been displaced from its articulations with the maxilla, and squamosal; consequently, its sutural relationships with these bones cannot be determined. The maximum dorsoventral depth of the jugal is $\sim 4 \text{ mm}$, while the mediolateral expansion of its ventral surface (for attachment of the masseter muscle) measures 1.29 mm (Fig. 8: 11).

Frontal. The frontal is exposed bilaterally on the dorsum of the skull and contacts the maxilla, premaxilla, nasal, and lacrimal (Fig. 8). Crushing, breakage, and distortion, however, make determination of contacts of the frontal with the palatine, orbitosphenoid, and alisphenoid impossible to assess. The only dimension of the frontal that can be meaningfully measured is the anteroposterior length of this element, 11.23 mm taken along the interfrontal (metopic) suture (Fig. 8: 12). The anteriormost extent of overlap of the frontal by the parietal is indicated by an impression along the posterior border of the frontal (Fig. 8: 13); the remainder of the frontal/parietal contact is not preserved. The unusual shape of this sutural margin indicates that in the undistorted specimen, viewed dorsally, its frontoparietal suture would have made an "M" shape, with the apex of the "M" pointing posteriorly along the midline. The right frontal displays a distinct ridge that runs from the anterolateral part of the bone, at its contact with the lacrimal, medially toward the interfrontal suture, meeting this suture at the posterior end of the bone, at its contact with the parietal (Fig. 8: 14). This ridge likely formed the margin of the temporalis muscle and is identified as the temporal ridge/line. With its counterpart on the opposite side, the temporal lines would have defined a distinct triangular area on the frontal. There is no evidence of a postorbital process having been developed on the frontal. HRxCT images reveal that the frontal is a thin plate of bone anteriorly, which then thickens posteriorly and is densely trabeculated. No diploic cavities have been recognized within the frontal nor are ethmoid foramina preserved.

Palatine. The palatines are completely obscured externally by overlapping bones and have been extensively crushed, to the degree that even HRxCT imaging has failed to reveal their structure.

Parietal. The parietals are only slightly better preserved than the palatines and are documented by a flat piece of bone exposed on the ventral side of the skull (Fig. 9A–B), but no more than this can be stated.

Squamosal. The right zygomatic process of the squamosal is exposed to view and seems to be undamaged (Figs. 8 and 9: 15). The glenoid fossa is intact as well (Figs. 8 and 9: 16),

although it is mostly obscured by other bones and by rock matrix. Neither the neurocranial part of the squamosal nor sutural contacts with other bones is preserved. The HRxCT image of the glenoid fossa and zygomatic process have been digitally extracted (Fig. 9D–E) and reveals that: 1) the postglenoid process is broken, but its base is clearly visible; 2) a postglenoid foramen is present and seems to have been medial (not posterior) to the postglenoid process (Fig. 9D–E: 17); and 3) a well-developed entoglenoid process arises medial to the postglenoid foramen (Fig. 9E: 18). In addition, the glenoid fossa seems to be almost flat and is antero-posteriorly longer (6.96 mm) than mediolaterally wide (5.38 mm), but its surface of articulation with the mandible has been deformed medially by compression from the crown of the right M1 or M2. The entoglenoid process is relatively large, projecting ventrally beyond the glenoid fossa by 1.79 mm. It is oriented parasagittally, at $\sim 90^\circ$ from the probable orientation of the postglenoid process and slopes medially. The width of the zygomatic process of the squamosal at its base, adjacent to the glenoid fossa, is 1.76 mm (Fig. 9E: 19). The length of the process is 4.95 mm, and its maximum depth is 3.77 mm.

Alisphenoid and basisphenoid. Neither of these elements has been identified in UALVP 46685.

Petrosal. The best-preserved structures in the basicranial region of UALVP 46685 are the promontoria of the petrosals (Figs. 9–12); two isolated petrosals, UALVP 46687 and 49105, also referable to *Pronothodectes gaoi*, provide additional information (Figs. 13 and 14). Tables A1 and A2 provide a summary of the structures exhibited by each specimen, as well as those exhibited by other plesiadapid petrosals for comparison.

Crushing and distortion of UALVP 46685 has obliterated most of the sutures between the petrosals and the bones of the skull that articulated with them in life (Fig. 9). The left petrosal is best exposed on the ventromedial aspect of the specimen (Figs. 9A–B and 11), where the promontorium of the pars cochlearis forms a fairly smooth but conspicuously swollen surface. This surface displays two major sets of grooves. One emerges from the posterolateral aspect of the promontorium, crosses its swollen surface, and disappears anteromedially. A groove following this particular course has been recognized in other plesiadapid specimens (see below) and is termed the “*g3*” groove in descriptions and discussions below (Table A1; Fig. 11A–B,E: *g3*). In other specimens, this groove begins anterolateral to the fenestra vestibuli, is often connected to another set of grooves (termed “*g4*” here—see below), and ultimately leads toward a consistently present anteromedial septum to which we refer as the second septum (*s2*) due to its location directly medial to the first septum¹ (Fig.

¹Russell numbers septa starting with the most medial and ending with the most lateral (see his Fig. 15A). However, his S3–4 seem related to the ectotympanic, while S5 seems to be equivalent to the epitympanic crest (MacPhee, 1981). Furthermore, he did not number additional more medial septa that we recognize here. Russell’s S2 seems equivalent to the anterior septum of MacPhee (1981) as defined by its relationship to the tubal canal, while S1 is most likely equivalent to the medial secondary septum of MacPhee (1981). Because of complications and potential confusion involved in partially adopting Russell’s scheme and then adding to it, we use a new scheme that numbers septa starting anterolaterally and moving posteromedially. We feel this is more easily relatable to the scheme of MacPhee and other authors’ (e.g., Wible, 2009, 2011), without implying strict homology to the structures these authors named for other taxa.

Strict Consensus:

90 topologies

Ti: 93

Ci: 65

Ri: 82

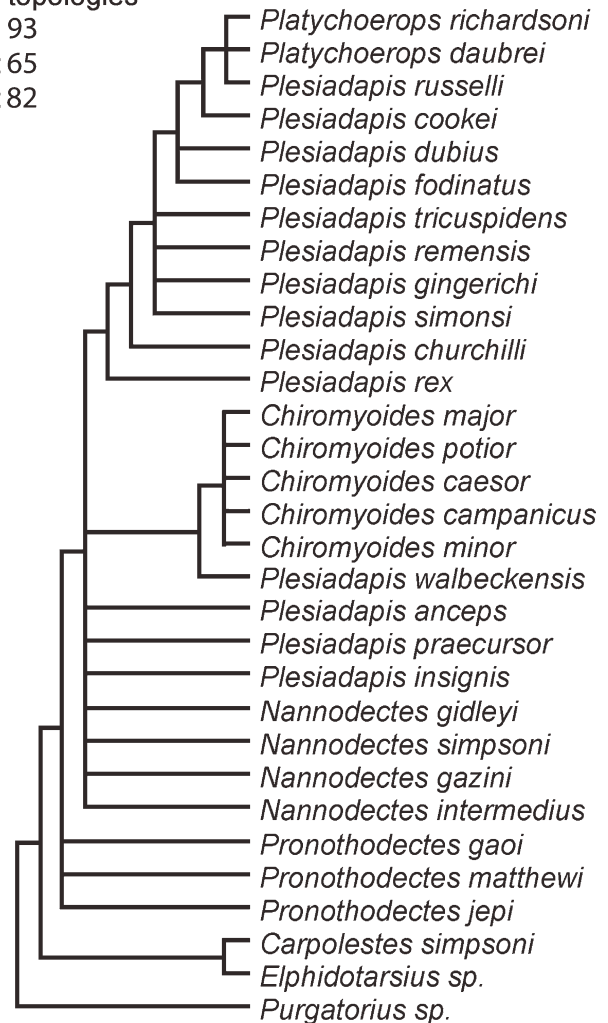


Fig. 15. Strict consensus tree of parsimony analyses of 66 morphological characters. See text for details on character and taxon sampling. Tables A6–A8 contain character codings.

11C–D: *s1*). The *s1* septum is obscured by matrix in this specimen (but visible with HRxCT). Note that the terminology we have used for these septa differs from that of Russell (1964; p. 94, Fig. 15), who termed our *s2* septum “S1” and our *s1*, “S2.”¹

One characteristic of the *g3* groove is that it leads to the ventral apex or to the medial side of *s2* (Fig. 11A–B,E). However, the ultimate target of the *g3* groove anteriorly and the pattern of its termination are unknown, because that part of its course is not preserved in UALVP 46685 nor in any other plesiadapid specimen that has been discovered so far.

The *g4* groove is more medially positioned on the promontorium (Fig. 11A–B,E: *g4*) and has a ventrolateral course that brings it into close proximity with the posterolateral origin of *g3*, although the two grooves do not seem to meet in this specimen. Many other plesiadapid specimens display sets of grooves with a similar pattern, differing only in that, the *g4* groove frequently directly intersects the *g3* groove posterolaterally.

The promontorium in UALVP 46685 is flanked on its medial side by a prominent rostral tympanic process (Fig. 11: **20**), which has been broken off at its base. Three ridge-like septa arise from this process and buttress the swollen promontorium. The most anterior of these is the *s2* (Fig. 11: *s2*).

A third septum (Fig. 11A–B, C'–E: *s3*) is located on the medial side of the promontorium opposite and slightly posterior to the level of *s1*. It is oriented mediolaterally and is the smallest of the three.

Still another septum, posterior to *s3*, houses the cochlear canaliculus (Fig. 11, Supporting Information Figs. 1–6: *cc*), a small canal that connects the scala tympani of the cochlea and the subarchnoid space, transmitting the perilymphatic duct (MacPhee, 1981). Note that our identification of this feature differs from Szalay et al. (1987) who identified similar morphology in *Plesiadapis tricuspidens* as the vestibular aqueduct (Szalay et al., 1987: Figs. 1 and 2). Our identification is supported by HRxCT imagery showing the canal within this septum to connect to the cochlea not the vestibule (Supporting Information Figs. 1–6). Furthermore, the arrangement of Szalay et al.'s (1987) reconstruction, in which the vestibular aqueduct is rostral to the cochlear canaliculus is problematic, given that the cochlea usually occupies a more rostral position than the vestibule. In more complete specimens of *P. gaoi* and other plesiadapids, the ventral surface of the septum of the cochlear canaliculus is often marked by a groove that, when present, often terminates laterally in a foramen. This feature is visible on the left side of UALVP 46685 (Fig. 11A–C: **21**, **22**), in which it appears as a groove on the septum of the cochlear canaliculus and ends laterally at a foramen on the promontorium. We infer based on similar, and more complete anatomy in other plesiadapid specimens (see Boyer, 2009: *Nannodectes gidleyi* AMNH 117388, Fig. 2.16) that the foramen on the promontorium leads to a shallow, laterally coursing intrapetrous canal. We suggest that this groove and foramen represent the course of the tympanic nerve after passing through the tympanic canaliculus, which is not itself preserved in any available specimens of *P. gaoi*. However, a structure that seems to be the tympanic canaliculus [based on 1) similarity to this structure in living taxa, as illustrated by MacPhee (1981) and 2) previous identifications of morphology relating to the tympanic plexus in plesiadapids (MacPhee et al., 1983)] is preserved in *P. tricuspidens* (MNHN CR 126; Supporting Information Fig. 7) as well as in *N. gidleyi* (Boyer, 2009: Fig. 2.16), and the more fragmentary morphology of *P. gaoi* can be related to it. Posterolateral to the septum of the cochlear canaliculus, the remnants of yet another septum are visible on the left side of UALVP 46685. This is the “blister-like” sheet of bone of Szalay et al. [1987 (identified in *P. tricuspidens* as a “homolog to the ventral shield in adapids and lemuroids” p. 85)]; also referred to as the “posterior septum” by MacPhee (1981; pp. 255–257, Table XXI: identified in “lemuriformes”) that often extends from the promontorium medial to the fenestra cochleae and arches laterally beneath it while also meeting the posterior wall of the auditory bulla. The most significant aspect of this feature is that its ventral margin often marks the canal and/or course of the internal carotid plexus in euprimates (MacPhee, 1981), *Plesiadapis* (Szalay et al., 1987), and paromomyids (Silcox, 2003). The plexus includes the internal carotid nerves and (often) the internal carotid artery (Fig. 11: *ps*). Its presence

and position demonstrate that the internal carotid plexus in *P. gaoi* had an intratympanic, transpromontorial course (Fig. 11) and that it entered the tympanic cavity from a position posterior and slightly lateral to the promontorium, instead of medial to it.

Digital extraction of the left petrosal allows visualization of the oval window or fenestra vestibuli (Fig. 11C–D: *fv*), which measures about 1.17 mm by 0.60 mm in its diameters. The fenestra vestibuli received the stapedial footplate and leads into the spiral cochlea, which measures 15.60 mm in maximum length, after completing two and a half turns. The round window or fenestra cochleae (*fco*), which supported the secondary tympanic membrane is not visible in this specimen. The facial canal for passage of CN VII into the tympanic cavity is visible dorsal to the fenestra vestibuli (Fig. 11D: **23**). The canal is labeled near where the cavum supracochleare (for the geniculate ganglion of CN VII) would have been located. Based on slice-by-slice examination of HRxCT data of this specimen (Supporting Information Fig. 3) and others (Supporting Information Figs. 1, 4, and 5), it seems that the canal remained enclosed in bone until some point caudal to the fenestra vestibuli, despite the appearance of an open canal in Figure 11 (which must represent breakage). The diameter of the facial canal where marked in Figure 11 measures 1.07 mm by 0.44 mm.

The right promontorium of UALVP 46685 is obscured everywhere except along its medial side. Its lateral, anterior, posterior, and ventral aspects are mostly covered by a flattened plate of what seems to be bulla-forming bone and remnants of the ectotympanic (Figs. 8–10 and 12: **24**). The *g4* groove, the *s2* and *s3* septa, and the cochlear canaliculus can be seen on the exposed medial surface (Fig. 12). Furthermore, the broken edge of the rostral tympanic process is in view and demonstrates that it was composed of two bony laminae (Fig. 12: **25**, **26**). This may indicate that more than one bone was involved in its construction and that, accordingly, the tympanic bulla may not have been entirely or even partly derived from the petrosal. This would be analogous to the conformation exhibited by *Sciurus* and *Tupaia*, in which a rostral tympanic process of petrosal (like **25**) is dorsal to an ectotympanic or entotympanic element, respectively (possibly like **26**) (see Boyer 2009; Figs. 2.32–2.33). The presence of two laminae only implies a nonpetrosal bulla if one assumes that the more dorsal lamina (**25**) has a more limited outgrowth than the more ventral lamina (**26**) as it does in the two taxa aforementioned. The presence of two distinct laminae comprising this process is evident in other specimens as well (see below). Unfortunately, the possibility that the bulla was formed from a bone other than petrosal cannot be presently determined, because the two laminae cannot be unequivocally differentiated by HRxCT data, meaning it is possible that they represent two outgrowths from a single ossification. HRxCT data concerning the right petrosal do, however, allow visualization of *s1* and the fenestra vestibuli (Table A2; Fig. 12F). The posterior septum is crushed mediolaterally, but it is nearly complete anteroposteriorly; the minimum length of the carotid canal (formed in the ventral margin of the posterior septum) is estimated at ~1.5 mm. The semicircular canals are well preserved (Supporting Information Fig. 2). Their dimensions are recorded in Silcox et al. (2009). Only the anterior and posterior canals were

measured by these authors. The anterior and posterior canals in UALVP 46685 have the same radius of curvature: 1.3 mm, which is small for an animal, the size of *P. gaoi* (~690 g; estimate from Boyer, 2009; Table 4.38A).

UALVP 49105 (Fig. 13) is another petrosal of *P. gaoi*. It was collected from the Joffre Bridge locality. This petrosal is excellently preserved, having been neither crushed nor distorted. It includes much of the pars cochlearis, pars canicularis, tympanic processes, and some of the ectotympanic bone. It was initially identified on the basis of its overall similarity in size and shape to the petrosals in UALVP 46685 but also from other features, including the posterior septum, that clearly identify it as belonging to a plesiadapiform. The cochlea in UALVP 49105 is about the same length as that of UALVP 46685, although the fenestra vestibuli is narrower, measuring only 1.03 mm in maximum diameter. The dimensions of the pars cochlearis are nearly identical to those in the skull, although the width is slightly greater. Clearly present is *g3*, identified by its relationship to *s2* and by its orientation and position on the promontorium (Fig. 13A–B',D–D'). However, *g3* in this specimen intersects another groove that approaches it from the medial side of the promontorium and connects it to the *g4* groove. The *g4* leads ventrolaterally from the vicinity of the foramen for the tympanic nerve (Fig. 13A–B': 22). The lateral side of this specimen is well preserved—unlike comparable parts of the petrosals in UALVP 46685—and contains the fenestra vestibuli, with the root of the posterior septum arising ventral to the fenestra. The dorsolateral aspect of the posterior septum is marked by a pair of parallel grooves (Fig. 13B–C: *g1*) that lead out from the posterior carotid foramen (Fig. 13A–B',I: *pcf*). These grooves lose definition at the contact between the posterior septum and the promontorium, but another groove becomes visible more anteriorly on the lateral aspect of the promontorium itself. This groove (*g2*) wraps ventromedially around the promontorium and approaches *s1* (Fig. 13B–C); *g2* (as defined by the relationships exhibited in UALVP 49105) is present in many plesiadapid specimens, but it is often developed as a pair of parallel grooves. A more dorsolaterally directed and more broadly excavated groove (Fig. 13B–C,H: *g5*) approaches the epitympanic crest, a ridge of bone that extends laterally from the promontorium, just anterior to the fenestra vestibuli (Fig. 13B–C,H: *ec*).

The remnants of *s1* and *s2* are preserved in UALVP 49105, as well as the *s3* septum, the cochlear canaliculus, and the posterior septum (Fig. 13). Furthermore, the posterior wall of the bulla is exposed at its contact with the posterior septum and contains a fragment of the internal carotid canal. Although the ventral margin of the canal is broken off, its mediolateral diameter is measurable and gives a value of 0.29 mm (Fig. 13A–B',I: *pcf*). The rostral tympanic process of UALVP 49105 is broken but clearly shows that it is composed of a dorsal and ventral lamina of bone (Fig. 13A–B',D–H: 25–26). Due to the interpretation by some authors (e.g., MacPhee and Cartmill, 1986) that the composition of the plesiadapid tympanic bulla includes an entotympanic element, it is tempting to conclude that these lamina represent two different bones. As with the skull, HRxCT imaging does not reveal differentiation between these two layers (Fig. 13B), even though this isolated specimen was scanned at a resolution five times higher than that

for the skull (8 μm vs. 40 μm). The semicircular canals of the pars canicularis surround a deeply excavated subarcuate fossa. These canals are well preserved but have not been measured at this time. Although a fragment of ectotympanic (Fig. 13B–C) is present in UALVP 49105, it is not extensively enough preserved to permit meaningful description.

Finally, a fourth petrosal, UALVP 46687 from the DW-2 locality, preserves most of the diagnostic structures seen in the other three specimens, plus some additional features not preserved in them (Tables A1 and A2; Fig. 14). The fenestra vestibuli and pars cochlearis are comparable in size to those in the other specimens referred to *P. gaoi*. Like UALVP 49105, UALVP 46687 preserves promontorial grooves *g1–5* and displays a groove that arises on the medial aspect of the promontorium to intersect *g3*. The groove *g1* is represented by two parallel grooves, like it is in UALVP 49105. Unlike *g2* of UALVP 49105, *g2* of UALVP 46687 is represented by a set of two parallel grooves, rather than by a single groove. UALVP 46687 preserves a foramen related to the tympanic canaliculus. Unfortunately, preservation of the septa in UALVP 46687 is not as complete as in the other petrosals at hand, and the septa *s1* and *s3* are not evident. Although the posterior septum is preserved toward its anterior margin, the posterior wall of the tympanic bulla is crushed dorsally into the roof of the tympanic cavity, with the posterior septum broken here and evidence of the internal carotid canal destroyed. The posterior carotid foramen is visible (although not measurable) on this fragment (Fig. 14A–B'). The anterior and posterior semicircular canals are preserved, and their measurements are reported in Silcox et al. (2009). UALVP 46687 has slightly smaller canals than UALVP 46685 (radius of curvature of anterior canal: 1.0; posterior canal: 1.1).

Ectotympanic. The external auditory meatus (eam) and what is most reasonably described as the base of the crista tympanica (the raised ridge that relates to the anchor point of the tympanic membrane) are preserved on the right side of UALVP 46685. They are both likely to have been formed from the ectotympanic, which is visible in the dorsal view of the skull (Fig. 8: Ect). The length of the external auditory meatus from its anterolateralmost extremity to the root of the crista tympanica is ~ 5.5 mm; its anteroposterior diameter is greater, at 5.75 mm. Thus, the ectotympanic is moderately expanded laterally but is neither “ring-like” nor “tubular.” Although the remains of the root of the crista tympanica can be recognized as a raised ridge on the internal surface of the ectotympanic, the ectotympanic does not preserve evidence of a distinct “annular component” with a “C”-shaped cross-section for attachment of the tympanic membrane as present in *Plesiadapis tricuspidens* (Gingerich, 1976), where the “root of the crista tympanica,” is more accurately described as the annular bridge (e.g., Bloch and Silcox, 2001). *Nannodectes intermedius* preserves evidence of an incipient annular bridge (Boyer, 2009; p. 123, Fig. 2.9 and p. 128, Fig. 2.12) because the root extends quite far from the auditory tube and is supported by bony struts/septae. It then curls laterally meaning that the crista tympanica, proper, is separated from its “root” or “incipient bridge” by the sulcus tympanicus (Wible, 2008). Whether the ectotympanic formed a substantial component of the walls and floor of the tympanic bulla in *P. gaoi* cannot be determined from available specimens.

Occipital. The basioccipital is preserved on the ventral surface of the skull between the two petrosals (Figs. 9A–B and 10A–B). It is 8.46 mm long; its anterior end, at its junction with the basisphenoid at the spheno-occipital synchondrosis, is 3.25 mm wide (Fig. 9A–B: 27); at its midpoint, the basioccipital is 2.96 mm wide and at its posterior end is 4.36 mm wide (Fig. 9A–B). HRxCT imaging reveals it to be a thin bone but that may only mean that any greater thickness of the bone had been eroded away after death and hence its apparent thinness is an artifact. The only clearly preserved remnants of the exoccipitals are the left occipital condyle (Fig. 9A–B: 28) and the corresponding hypoglossal foramen (Fig. 9A–B: 29). The condyle measures 3.87 mm dorsoventrally by 2.47 mm medio-laterally. The hypoglossal foramen, which is located a short distance anterior to the condyle, is 1.03 mm by 0.86 mm in its dimensions; the hypoglossal canal is subdivided internally by a septum. The root of the right occipital condyle is preserved, which is only informative inasmuch as it delineates part of the boundary of the foramen magnum (Figs. 9A–B and 10A–B: 30). The foramen magnum itself seems only slightly distorted and is about 7.4 mm wide, probably close to its width in life. The exoccipital and supraoccipital seem to be fused together because no suture marking their contact as separate elements is evident on the posterior aspect of the skull. The dorsoventral dimensions of the supraoccipital seem mostly intact, given that a remnant of the nuchal crest near the midline of the occiput is preserved (Figs. 9A–B and 10A–B: 31). The supraoccipital measures 8.30 mm dorsoventrally from the top of the foramen magnum to the dorsalmost part of this remnant. The external surface of the supraoccipital is concave in its dorsoventral profile, suggesting that the nuchal crest was prominent. Finally, the supraoccipital is marked by several small foramina, some of which open posterodorsally and others, directly posteriorly.

Comparisons of selected cranial elements

Nasal. In addition to its occurrence in *Pronothodectes gaoi*, the nasal is known in *Nannodectes intermedius* (USNM 309902), *Plesiadapis anceps* (YPM-PU 19642), *Plesiadapis tricuspidens* (MNHN CR 125 and the Pellouin skull), and *Plesiadapis cookei* (UM 89770). In proportions of the nasal, *P. gaoi* most closely resembles *N. intermedius*, *P. anceps*, and *P. cookei*, in which the anterior and posterior margins of the element are equal in width (Table A5, Nc/Nr and Nc/GM). In *P. tricuspidens*, the nasal is much narrower at its posterior margin, at its contact with the frontal, than anteriorly, whereas in *Carpolestes simpsoni* (Bloch and Silcox, 2006), the nasal maintains a fairly constant width throughout its length. *P. gaoi* is similar to all other plesiadapids, but unlike *C. simpsoni*, in that its nasal lacks an external contact with the maxilla.

Premaxilla. Other plesiadapids in which well-preserved premaxillae are known include the species cited above with regards to the nasals but also *Plesiadapis churchilli* from Wannagan Creek, North Dakota (SMM 74.24.168). Possibly, as a correlate of variation in nasal structure, the premaxilla of *Pronothodectes gaoi* most resembles that of *Nannodectes intermedius* and *Plesiadapis anceps* (that of *Plesiadapis cookei* is broken in some key areas) in having a relatively narrow (relative to the nasal) suture with the frontal (Table A5, Nc/Pmx and Pmx/GM). In *Plesiadapis tricuspidens*, this contact is much broader and positioned more posteriorly relative to the

extent of the nasals. *Carpolestes simpsoni* lacks a contact between the premaxilla and frontal altogether.

Lacrimal. Little is known of the lacrimal in Plesiadapidae. However, this element is preserved in all the specimens above that have been cited for the nasals, as well as in another specimen of *Plesiadapis tricuspidens* (MNHN CR 126), only the latter provides much useful information about the form and contacts of the lacrimal.

The lacrimal foramen seems to be of a similar relative size in *Pronothodectes gaoi* and *P. tricuspidens* (MNHN CR 126), and the facial process of the lacrimal seems to be similarly developed in both. Whether the lacrimal foramen in *P. gaoi* was located on the rostrum, just beyond the orbital rim as in *P. tricuspidens*, or in even a different position yet, cannot be determined due to poor preservation of UALVP 46685. Furthermore, it is not clear whether *P. gaoi* exhibited a lacrimal tubercle. In MNHN CR 126, the surface of the lacrimal is swollen medial and dorsal to the lacrimal foramen: this swelling seems to represent the lacrimal tubercle (contra Bloch and Silcox, 2006) but no comparable feature has been identified in UALVP 46685. Whether the lacrimal failed to contact an orbital wing of the palatine, as suggested by various authors for *P. tricuspidens* (e.g., Russell, 1964), is impossible to determine in the skull of *P. gaoi*. Moreover, examination of MNHN CR 126, the specimen that Russell (1964) cited as clearly lacking an orbital process of palatine that contacts the lacrimal is actually ambiguous on these points due to breakage and a complex pattern of suturing (Boyer, 2009). *Carpolestes simpsoni* exhibits a construction of the lacrimal which is similar to that in plesiadapids, in so far as can be determined from the fragmentary material available for the latter. In *C. simpsoni*, the lacrimal fails to contact the palatine (Bloch and Silcox, 2006).

Maxilla. Compared with other cranial bones of plesiadapids, the maxilla is unusually well represented in collections (e.g., see Gingerich, 1976). Many specimens preserve at least the zygomatic process, the alveolar process, and fragments of the palatal process, and some preserve sutural contacts with adjacent bones, as well (e.g., specimens of *Nannodectes intermedius*, *Nannodectes gidleyi*, *Plesiadapis anceps*, *Plesiadapis cookei*, and *Plesiadapis tricuspidens*).

The maxilla of *Pronothodectes gaoi* is similar to those known in other plesiadapids in contacting the frontal between the premaxilla and lacrimal on the dorsum of the skull and in contacting the palatine posterior to P4 in the palate. Although the position of the zygomatic process of the maxilla varies among plesiadapids, in most species it arises opposite M2, its position in *P. gaoi*. *Chiromyoides campanicus*, *Platychoerops richardsoni* (Gingerich, 1976), and *P. cookei* differ from other plesiadapids in which this feature is known (at present, it is not observable in other described species of *Chiromyoides*, *Plesiadapis russelli*, or *Platychoerops daubrei*), with the zygomatic process arising opposite M1. The degree of exposure of the molar roots in the dorsum of the maxilla also varies: as in *P. gaoi*, certain other plesiadapids display substantial dorsal exposure of these roots, including *N. intermedius* (e.g., USNM 309902) and *P. anceps* (CM 40564), whereas in *P. rex* (e.g., YPM-PU 21448), *Plesiadapis churchilli* (e.g., SMM 74.24.140), *P. tricuspidens* (e.g., MNHN CR 126), and *P. cookei* (UM 87990) only the distobuccal root of M3 is exposed. *Carpolestes simpsoni* resembles *P. gaoi* in the position of the zygomatic process of the maxilla, but it lacks exposure of

the roots of the molars in the dorsum of the alveolar process of the maxilla (Bloch and Silcox, 2006).

Jugal. Other plesiadapid species in which the jugal is known include *Nannodectes intermedius*, *Nannodectes gidleyi*, *Plesiadapis tricuspidens*, and *Plesiadapis cookei*; there are no discernible differences in the structure of the jugal among these species and *Pronothodectes gaoi*. Specimens of *P. tricuspidens* (MNHN CR 125–126) and *P. cookei* (UM 87990) show a contact between the jugal and lacrimal, which seems to differentiate at least these plesiadapids from *Carpolestes simpsoni* (Bloch and Silcox, 2006).

Frontal. The frontal in all plesiadapid specimens in which this bone is relatively well preserved is similar to that in *Pronothodectes gaoi*. For example, the frontals in *P. gaoi*, *Plesiadapis anceps*, *Plesiadapis tricuspidens*, and *Plesiadapis cookei* meet along a midline suture, exhibit a triangular area defined by temporal ridges, lack postorbital processes, and contact the nasal, premaxilla, maxilla, and parietal. Whether the frontal contacts the maxilla within the orbit in any plesiadapid is uncertain because of ambiguity regarding the development of an orbital process of the palatine. The maximum anteroposterior length of the frontal provides a useful dimension against which to standardize snout length in these animals. In *P. gaoi* and *P. anceps*, the nasal is longer relative to the frontal than in *P. tricuspidens* and *P. cookei* (Table A5: N/F). *C. simpsoni* resembles these plesiadapids in exhibiting an interfrontal suture, and a dorsal triangular area of the frontal defined by temporal ridges, and in lacking postorbital processes. We replicated Bloch and Silcox's (2006) measurement of the length of the internasal suture (equivalent to measurement 2 of Table A3 for plesiadapids) at 12.96 mm using a digital model of a scan of USNM 482354, *Carpolestes simpsoni*, and determined additionally that the frontal is 9.7 mm long in that specimen. Thus, in *C. simpsoni*, the nasal is much shorter relative to the frontal than in the plesiadapids cited above, and the snout of that carpolestid is proportionally shorter (N/F for *C. simpsoni* = 133, the lowest value for a plesiadapid is 148 for *P. tricuspidens*, whereas the highest is 169 for *P. anceps*, Table A5).

Squamosal. The aspects of the glenoid fossa, postglenoid process, postglenoid foramen, and entoglenoid process of *Pronothodectes gaoi* described above are also characteristic of other plesiadapids, including *Nannodectes intermedius*, *Nannodectes gidleyi*, *Plesiadapis tricuspidens*, and *Plesiadapis cookei*. In all, the glenoid is flat and slightly longer than wide, the postglenoid foramen is positioned medial to the postglenoid process, and the entoglenoid process is relatively wide. One trait that seems to differentiate *P. gaoi*, *N. intermedius*, and *P. cookei* from *N. gidleyi* and *P. tricuspidens* is the size of the glenoid relative to overall skull size (Table A5, Gld/GM): it is relatively larger in the latter taxa. In *Carpolestes simpsoni*, the postglenoid foramen occupies a medial position, like that in the plesiadapids above, but the glenoid fossa seems more concave in the carpolestid, at least in part owing to the greater ventral expansion of the entoglenoid process.

Petrosal and composition of the tympanic bulla. The petrosal, and especially the promontorium, is well represented in the plesiadapids that are available for comparison (see Tables A1 and A2 for a list of specimens). In *Pronothodectes gaoi* and most other plesiadapids

(Table A1), the promontorium is markedly swollen. *Nannodectes* and one isolated petrosal of *Plesiadapis tricuspidens* are exceptions with a measurably flatter promontorium. Furthermore, our measurements from the HRxCT dataset of USNM 482354, show that the promontorium of *Carpolestes simpsoni* is flatter as well, suggesting that the relatively flat promontorium in *Nannodectes intermedius* is a plesiomorphic feature for Plesiadapoidea.

The absolute values for the length of the fenestra vestibuli, the length of the cochlea, and the size of the promontorium (Tables A1 and A2) do not vary dramatically among the plesiadapids that we have included in this study, although there is a slight correlation of these values with overall size of the skull. However, note that the dimensions of these three structures of the petrosal are proportionally much lower in the large-bodied taxa, *P. tricuspidens* and *Plesiadapis cookei* (Table A5: Av/GM, Cl/GM, Pcsa/GM). Moreover, the cochlea of *C. simpsoni* is much shorter than that known for any plesiadapid. As in *P. gaoi*, the facial nerve in *N. intermedius*, *P. tricuspidens*, *P. cookei*, and *C. simpsoni* would have remained enclosed by bone until a point caudal to the fenestra vestibule. The stylomastoid foramen opens lateral to the posterior carotid foramen in all these taxa as well.

Features suggesting that the medial aspect of the promontorium and rostral tympanic process of the petrosal were comprised of multiple laminae of bone in *P. gaoi* are also present in specimens of *P. tricuspidens* and *P. cookei*. Although similar features have not as yet been observed in either of the species of *Nannodectes*, the fidelity of preservation in the available petrosals of those species is relatively poor.

Features equivalent to the *s1* and *s2* septa, and the septum of the cochlear canaliculus in *P. gaoi* are present in all the plesiadapids in this study in which the appropriate parts are preserved (Tables A1 and A2). Furthermore, only *Nannodectes gidleyi* may have lacked the posterior septum: it may either be broken away or naturally lacking in the available specimen, but the evidence is insufficient to determine which alternative is the case. The *s3* septum has been observed only in *P. gaoi* and in an isolated petrosal attributed to *P. tricuspidens* (Supporting Information Fig. 6). The petrosal of *C. simpsoni* exhibits a posterior septum, which was described as forming a "ventral shield" over the fenestra cochleae (Bloch and Silcox, 2006): the septum has a similar relationship in plesiadapids as well (e.g., Szalay et al., 1987). Otherwise, no other septa of the promontorium have been described in *C. simpsoni*, although our own examination of HRxCT data generated by Bloch and Silcox (2006) indicate that other septa are present around the petrosal of this species.

The *g1* groove, generally identified by its location on the lateral aspect of the posterior septum and ventral apex of the pars cochlearis, was observed in petrosals of all available plesiadapid species except *N. gidleyi*. In about half of the specimens, the *g1* groove is represented by two closely spaced, parallel grooves. If the *g1* groove represents the main branch of the internal carotid plexus (see Discussion section), then its position and structure differs from that in *C. simpsoni*, in which the groove is more medially and ventrally positioned on the promontorium and is of a much larger caliber (Bloch and Silcox, 2006).

The *g2* groove, defined as having a course that runs along the promontorium from the posterior septum to

the *s1* septum in *P. gaoi*, is present in at least some individuals among the comparative plesiadapid species (although neither of the most nearly complete *P. tricuspidens* skulls—MNHN CR 125 and the Pellouin skull—seem to exhibit it); the *g2* groove sometimes occurs as two parallel or subparallel grooves (in two specimens, see Table A1). If this groove represents the course of the promontorial part of the internal carotid plexus (see Discussion section), its lateral position differentiates it from that in *C. simpsoni*, in which the groove is more medially and ventrally placed on the promontorium and much larger (Bloch and Silcox, 2006).

The *g3* groove, defined as having a course that runs along the promontorium from a point just anteromedial to the fenestra vestibuli to the medial side of the *s2* septum in *P. gaoi*, is variably present in *P. tricuspidens* and *P. cookei*. It has not been identified in any *Nannodectes* specimens and was probably not developed in that taxon. The *P. tricuspidens* specimens that display markings on the promontorium in this position have a set of parallel grooves here. No comparable groove has been identified in *C. simpsoni* (Bloch and Silcox, 2006).

The *g4* groove, defined as having a course that runs from the canal and foramen for the tympanic canaliculus toward the root of the posterior septum in *P. gaoi* is present in specimens of all species, except *P. cookei*. No correlateable groove is evident on the promontoria of *C. simpsoni*.

The *g5* groove, defined as a trough-like groove located dorsolateral to *g2* and appearing as an anterior continuation of *g1* in *P. gaoi*, is observable in specimens of all species in the comparative sample of plesiadapids except those of *Nannodectes*.

In *P. gaoi*, the *g1* groove is associated with the posterior septum, which in turn is associated with the posterior carotid foramen. This latter association is also observable in the two most nearly complete specimens of *P. tricuspidens*. The posterior carotid foramen may be preserved in UM 87990, a skull of *P. cookei*, but it is severely damaged and distorted. Skulls of *C. simpsoni* preserve a posterior carotid foramen (Bloch and Silcox, 2006). These specimens show that the posterior carotid foramen and canal was not attached to the posterior septum in the way observed for plesiadapids. It was more medially and ventrally located. The diameter of this foramen does not seem to vary substantially among the specimens of plesiadapids that we have observed, e.g., the value of 0.28 mm for *P. gaoi* is only slightly less than values of 0.29 and 0.31 mm for *P. tricuspidens*. All these values are much lower than that measured in the absolutely smaller skull of *C. simpsoni*, which is 0.53 (Bloch and Silcox, 2006). In all plesiadapid taxa that we have examined, the posterior carotid foramen is positioned relatively laterally in the skull, in contrast with the condition in *C. simpsoni* in which it is positioned more medially (contra Bloch and Silcox, 2006).

Ectotympanic. Other plesiadapid species for which an ectotympanic is known include *Nannodectes intermedius*, *Plesiadapis tricuspidens*, and *Plesiadapis cookei*. In *N. intermedius*, the external auditory meatus is unexpanded, resembling that in *P. gaoi*, while in *P. tricuspidens* and *P. cookei* the external auditory meatus is elongate and tube-like (Table A5: EAM-S; Boyer et al., 2010). As described above, all exhibit at least an incipient annular bridge with development of septa, but only *P. tricuspidens* exhibits evidence of a strongly expanded annular component arising from the annular bridge. *Carpolestes simpsoni*

lacks the expanded external auditory meatus, but the available specimens are not well enough preserved to make further comparisons (Bloch and Silcox, 2006).

Occipital. The basioccipital is well preserved in specimens referred to *Nannodectes intermedius*, *Plesiadapis tricuspidens*, and *Plesiadapis cookei*, in addition to *Pronothodectes gaoi*. There are no substantial differences among these taxa nor *Carpolestes simpsoni* in the structure of this bone. Parts of the exoccipitals, but nothing else of the occipital-complex, are preserved in AMNH 17388, *Nannodectes gidleyi*.

The hypoglossal foramen is subdivided by a septum in all plesiadapids in which the appropriate parts are preserved, including *P. gaoi*, *P. tricuspidens*, and *P. cookei*. The jugular foramen (or posterior lacerate foramen) is observable in these same specimens: its form and position (medial to the posterior carotid foramen and lateral to the hypoglossal foramen) does not differ substantially among them. In *P. cookei* and possibly *N. intermedius*, the supraoccipital contributed to a prominent nuchal crest as in *P. gaoi*, whereas in the two skulls of *P. tricuspidens* the crest seems not to be as strongly developed. The exoccipitals and supraoccipitals in *C. simpsoni* differ little from those of *P. gaoi* in their major aspects. The jugular foramen in *C. simpsoni* was probably lateral to the posterior carotid foramen, but this seems more of a consequence of differences in petrosal morphology (see above).

Phylogenetic analysis

Cladistic analysis. Parsimony analysis of 66 morphological features yielded 90 most parsimonious trees with a length of 93 steps, a consistency index of 0.65, and a retention index of 0.82. *Pronothodectes gaoi* was recovered as basal to all other plesiadapids except other species of *Pronothodectes* in all trees (Fig. 15).

The strict consensus tree has the following features: Plesiadapidae are monophyletic in all trees. *P. gaoi* is resolved as basal to all plesiadapids except other species of *Pronothodectes*. Species of *Chiromyoides* form the only generic clade that is monophyletic in all trees. *Plesiadapis walbeckensis* is the sister taxon to the *Chiromyoides* clade. *Plesiadapis cookei* is always recovered as the sister taxon to a group including *Platycheorops* species and *Plesiadapis russelli*. *Plesiadapis fodinatus* and *Plesiadapis dubius* are always recovered as closer to the group including *P. cookei* than to any other plesiadapids. This latter grouping is always most closely linked with *Plesiadapis tricuspidens*, *Plesiadapis remensis*, *Plesiadapis gingerichi*, and *Plesiadapis simonsi*. The outgroup of this clade is always *Plesiadapis churchilli*. *Chiromyoides*, *Nannodectes*, and the remaining species of *Plesiadapis* are always more closely related to the clade including *P. churchilli* than any are to species of *Pronothodectes*. Thus, this analysis also shows the plesiadapid genus, *Plesiadapis*, to be paraphyletic and polyphyletic.

Character support for major, consistently recovered clades is as follows: Plesiadapidae are supported by the presence of a margoconid on *i1* (*ch2*) and loss of the *p4* paraconid (*ch17*). *P. gaoi* is recovered as a more basal taxon than any non-*Pronothodectes* species in all analyses; its basal position is constrained by its lack of derived features, such as loss of *i2* (it retains *i2*) (*ch4*), and the presence of a *p2* having a peg-like crown (its crown is premolariform with a distinctive talonid) (*ch15*), both of which support the more exclusive clade of non-*Pronothodectes* plesiadapids.

The clade *Chiromyoides* + *P. walbeckensis* is united by enlarged incisors relative to molars (*ch31*). *Chiromyoides* is united by two features, a central incisor having a short crown (*ch1*) and low-crowned molars (*ch32*).

The clade including *Platychoerops* and *P. russelli* is united by the presence of a molar-like paraconule on P4 (*ch24*). *P. cookei* is sister to this clade, a grouping supported by an elongated i1 crown (*ch1*), a reduced I1 laterocone and posterocone (*ch6-7*), lack of a mediocone on I1 (*ch8*), lack of an upper canine (*ch10*), presence of a trigonid on p4 (*ch19*), lack of a p4 (*ch21*), lack of premolar-type paraconules on P3-4 (*ch22-23*), absolutely large size (*ch27*), and a zygomatic process of the maxilla that arises lateral to M1 (*ch68*). *P. dubius* and *P. fodinatus* are sisters to the group including *P. cookei* based on the occasional to consistent presence of a paraconid on p4 (*ch17*), reduced premolar-type paraconules on P3-4 (*ch22-23*), and crestiform cheek teeth (*ch32*). *P. tricuspiciens*, *P. remensis*, *P. gingerichi*, and *P. simonsi* follow as supported by the presence of "curve-crested" entoconids (Gingerich, 1976) on the lower molars (*ch25*). *P. churchilli* is sister to this larger group (*Platychoerops*, *P. russelli*, *P. cookei*, *P. dubius*, *P. fodinatus*, *P. tricuspiciens*, *P. remensis*, *P. gingerichi*, and *P. simonsi*) as supported by the presence of well-developed mesostyles on M1-2 (*ch30*), and *P. rex* is the next sister, supported by the presence of a centroconule (which feature is eventually lost in the lineage leading to *Platychoerops*) (*ch9*) and a squared, fissured hypoconulid on m3 (*ch30*).

DISCUSSION AND CONCLUSIONS

New dental samples from the Paleocene of Alberta, Canada, corroborate the conclusion that *Pronothodectes gaoi* is a valid, morphologically distinct taxon (Fox, 1990b, 1991) and not a variant member of a more derived plesiadapid species, such as *Plesiadapis anceps* or *P. rex*, as (contra Gingerich 1991). Unlike species of more derived plesiadapids, *P. gaoi* lacks an I1 centroconule, consistently retains i2, possesses a premolariform p2, lacks upper molar mesostyles, and, in a majority of specimens, exhibits a primitive m3 talonid, all of which supports Fox's (1990b) original attribution of the species to *Pronothodectes*.

Our study of *P. gaoi* has additional implications. In particular, the cranial osteology of *P. gaoi* is of interest in being more primitive than that of *Plesiadapis tricuspiciens* or *Plesiadapis cookei* (Fig. 16), and in exhibiting similarities to that of *P. anceps*, *Nannodectes intermedius*, and even *Carpolestes*. Unlike the new dental evidence, however, this new cranial information does not yet bear on the issue of where *P. gaoi* fits within early plesiadapid evolution due to lack of cranial specimens representing other *Pronothodectes* species. Generally speaking, the infrequent representation of skull material among the many species included in our character matrix prevented cranial data from greatly influencing cladistic analysis results, despite apparently substantial interspecific variability. In fact, the only cranial character to form unambiguous support for any node was the position of the zygo-

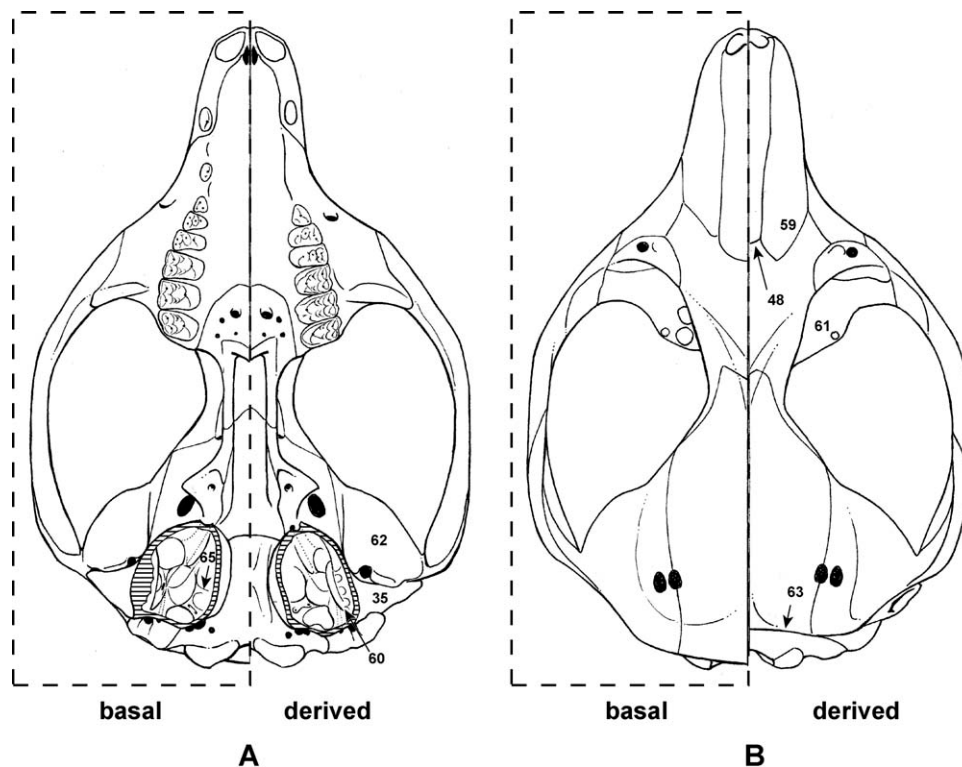


Fig. 16. Diagrams of plesiadapid skulls based on character state reconstructions. Comparison of the reconstructed skulls of basal (Based on measurements of *Pronothodectes gaoi* UALVP 46685 and optimization of character states in the cranium to the basal node for Plesiadapidae as per our phylogenetic analysis) and derived (based on *Plesiadapis tricuspiciens*) plesiadapids in **A**, ventral, and **B**, dorsal views. Numbers correspond to characters listed in Table A6. The derived composite was reconstructed using measurements from skulls of *P. tricuspiciens*, which are complete enough to reveal overall cranial proportions. Numbers correspond to features in which derived *P. tricuspiciens* (and in some cases *Plesiadapis cookei*) differs from primitive plesiadapids (Tables A6-A8).

matic process of the maxilla in *Platychoerops* and *Plesiadapis cookei*. Even taking a more informal approach, at this time we find no characters that clearly unite members of any one genus and distinguish them from others. However, when considered at the family level, the new information on plesiadapid crania has some notable implications. Our new observations help clarify several ambiguities in the understanding and interpretation of plesiadapid cranial anatomy, which we comment on in the sections that follow.

Presence and position of a posterior carotid foramen and canal

The evidence for an internal carotid plexus passing through the tympanic cavity in plesiadapids has recently been considered weak (MacPhee et al., 1983; Bloch and Silcox, 2001, 2006). However, all but one of the plesiadapid crania that were included in our study, and that are well enough preserved, show either a posterior carotid foramen and/or the remnants of its canal on the posterior septum, implying that the canal entered the tympanic cavity posterolaterally in plesiadapids. Although this interpretation differs from those expressed by several recent authors (MacPhee et al., 1983: absent; Silcox, 2001 and Bloch and Silcox, 2006: absent or medially positioned), it agrees with that of Wible (1993), who considered both plesiadapids and paromomyids to exhibit a “posterolateral” entrance of the internal carotid. Although we have not made a point of describing the comparison of plesiadapids to paromomyids in this article, it is worth noting that the carotid canal and grooves exhibited by plesiadapids are essentially identical to the condition in paromomyids. Silcox (2003) described a carotid canal in *Ignacius graybullianus*. Our inspection of her figures and a HRxCT scan of the specimen lead us to conclude that this canal is posterior to the pars cochlearis, in the same position as it is in plesiadapids described here. We find no evidence for a transpromontorial canal in *Ignacius* or any plesiadapid.

Although there is a great deal of similarity among basicrania of most plesiadapids considered here, the basicranium of AMNH 17388, as representative of *Nanodectes gidleyi*, is clearly different from that in other taxa in which this region is preserved (see above; see Boyer, 2009 for a discussion of the soft-anatomical significance of its structure) in that it may have lacked an intratympanic/transpromontorial carotid plexus.

Composition of the tympanic bulla and of the rostral tympanic process

The bony bulla of plesiadapids has been considered petrosally derived by some (Russell, 1964; Gingerich, 1976; Bloch and Silcox, 2006; Bloch et al., 2007) and nonpetrosal by others (MacPhee et al., 1983; MacPhee and Cartmill, 1986; Kay et al., 1992; Beard, 1993). A nonpetrosal bulla has been documented in paromomyid plesiadapiforms (Kay et al., 1992; Bloch and Silcox, 2001), but claims that the plesiadapid bulla is entotympanic (Kay et al., 1992) remain unsubstantiated. The hypothesis that plesiadapids have a nonpetrosal bulla predicts that a suture delimiting the presence of two different bones was present at some point during ontogeny. If the bulla was not petrosally derived, then it is possible that a suture, or some remnant thereof between the petrosal and the bulla, will eventually be observed in a plesiadapid specimen.

Our observations reveal evidence of multiple bony laminae comprising the rostral tympanic process of the petrosal in plesiadapids. This superficially suggests that the tympanic bulla in these animals is not derived from the petrosal. However, the laminae have not been recognized in the HRxCT data. Moreover, a similarly bilaminar rostral tympanic process has been observed in the extant lemur *Indri* (Boyer, 2009), in which the tympanic bulla is petrosal in origin. Furthermore, so-called “petroso-petrosal” sutures, i.e., sutures marking contact between different parts of the petrosal within the bulla, have been observed in *Tarsius*, probably as a consequence of relatively rapid growth of the tympanic processes (MacPhee and Cartmill, 1986). The hypothesis that plesiadapids exhibit a petrosally derived bulla is therefore not refuted by our observations but must be tested with additional comparative and fossil data.

Reconstruction of soft anatomy associated with promontorial grooves in plesiadapids

Previous studies have argued that the apparently variable expression of grooves on the plesiadapid promontorium reflect the course of randomly reticulating rami of a tympanic plexus (MacPhee et al., 1983). The corollary to this argument, that there were no grooves that occupy constant positions on the promontorium, was taken as evidence that the internal carotid plexus did not pass through the middle ear cavity (MacPhee et al., 1983). However, the descriptions and comparisons of plesiadapid crania presented in this study demonstrate that there are at least five sets of promontorial grooves, identifiable through their anatomical relationships to other structures on the pars cochlearis (Fig. 17). Not all these grooves are evident on each petrosal available to us for observation (Tables A1 and A2), but in most cases sporadic absence of grooves is demonstrably a product of variable expression of soft anatomical features on the bony surface of the promontorium among different individuals, rather than a variable presence and pattern of the neurovasculature.

In assessing the identity of the promontorial grooves, it is important that the identity of various septa in the plesiadapid tympanic cavity be established first because components of the neurovasculature in extant primates and treeshrews have specific relationships to these septa (MacPhee, 1981). We refrain from claiming strict homology between such septa due to the possibility that they were derived independently in plesiadapids, when compared with either treeshrews [in which similarly positioned septa are mostly entotympanic (Cartmill and MacPhee, 1980; MacPhee, 1981; Wible, 2009)], primates [in which these septa are petrosally derived (Cartmill and MacPhee, 1980; MacPhee, 1981)] or various other taxa including certain rodents like *Marmota* [in which they are mostly ectotympanic (e.g., Boyer, 2009)]. Most authors have interpreted differences in the bony construction of functionally similar septa to indicate independent derivation from a common ancestor lacking any such partitioning (e.g., Cartmill and MacPhee, 1980). Alternatively, at least one study has suggested the bony composition of a septum may change through evolution (Wible, 2009). If correct, dissimilar composition of such septa between two taxa would not be sufficient evidence for concluding a lack of septa in their common ancestor.

Whether or not these septa are homologous in different taxa that exhibit them, their presence can be used to aid in interpretation of soft-anatomical correlates of morpho-

separating septa from promontorium (see above) in plesiadapids (and paromomyids—Bloch and Silcox, 2001; Silcox, 2003) and 2) the likely closer phylogenetic relationship between at least the plesiadapiforms under consideration and euprimates, when compared with tree-shrews and euprimates (Bloch et al., 2007).

For the specimens of this study, the posterior septum and the septum of the cochlear canaliculus (Fig. 17) were identified initially by their relationship to the fenestra cochleae (MacPhee, 1981) and cochlear canaliculus (visible with HRxCT imagery), respectively. We propose that the *s1* of our study is functionally equivalent to the anterior septum of MacPhee (1981), in keeping with the observations that *s1* is 1) adjacent to the epitympanic crest as defined in other taxa (MacPhee, 1981) and 2) seems to be directly medial to the opening for the tubal canal (Fig. 17, and see also Russell, 1964). Most likely, it was also medially adjacent to the foramen lacerum (Fig. 17); however, this is not discernible in the available specimens. The anterior septum (*s1*) is present in various fossil euprimates (MacPhee and Cartmill, 1986), extant lemuroid and loroid primates, as well as in tree-shrews and elephant shrews (MacPhee, 1981; Wible, 2009). It has also been identified in the Paleogene paromomyid *Ignacius graybullianus* (Bloch and Silcox, 2001).

Either the *s2* or *s3* septum is equivalent to the medial secondary septum of MacPhee (1981), while the other of the pair cannot be analogized or homologized with any structure present in the sample of primates and tree-shrews studied by him. The hypothesis that *s2* is more nearly equivalent to the medial secondary septum is favored here because 1) *s3* is not retained in other plesiadapid species or any nonplesiadapid plesiadapiforms (Boyer, 2009) and 2) like the secondary septum of MacPhee (1981), which has a vein running inside of it, *s2* has a neurovascular groove associated with it, suggesting a more constant function than *s3*, which lacks such associated neurovascular evidence.

The *g1* groove is clearly related to the internal carotid plexus, as indicated by its position and anatomical relationships: it is located on the lateral aspect of the posterior septum and ventral apex of the pars cochlearis of the petrosal, and thus leads directly anterior from the internal carotid canal formed in the floor of the posterior septum. Furthermore, the fact that *g1* often appears as a pair of grooves is consistent with its association with the internal carotid plexus because the plexus commonly consists of two major, subparallel nerve bundles in various primates (MacPhee, 1981); tree-shrews (e.g., Wible, 2009); and other taxa such as domestic goats, *Capra hircus* (pers. obs. DMB).

The *g2* groove, which is usually present on the petrosal of the plesiadapids in this study, is also interpreted as having held contents of the internal carotid plexus. This groove begins where *g1* meets the promontorium and always approaches the lateral side of the *s1* (anterior septum). MacPhee (1981) and other authors (e.g., Conroy and Wible, 1978) demonstrated that the internal carotid plexus follows the anterior septum (and thus leads toward the tubal canal on its way to foramen lacerum) in various lemuroid euprimates, tree-shrews, and macroselideans. Observations made by one of us (DMB) reveal that the internal carotid plexus also leads toward the tubal canal in *Capra hircus*. These anatomical associations and the fact that *g2* is sometimes present as a pair of parallel grooves strongly suggest that it relates to the internal carotid plexus, as well.

The *g3* groove stems from an area on the promontorium that is slightly anteromedial to the fenestra vesti-

buli and leads to the medial side of the *s2* septum. Its course is thus more medially directed than that of the *g2* groove and provides no obvious route toward foramen lacerum. It therefore does not seem to be related to the internal carotid plexus. *g3* also seems unlikely to have held the lesser petrosal nerve, because of its position medial to the *g2* groove: the lesser petrosal nerve passes lateral to the route of the internal carotid plexus in euprimates, tree-shrews, and macroselideans (MacPhee, 1981). MacPhee (1981) determined that a small vein is within the medial secondary septum in lemuroids, loroids, and tree-shrews. While this is not identical to the situation of having a groove for a neurovascular structure, it at least shows that the medial secondary septum in extant euarchontans and the *s2* in *Pronothodectes gaoi* (unlike *s3*) both supported neurovasculature. We thus conclude that *s2* represents the functional equivalent of the medial secondary septum and that *g3* may have also held a small vein. However, grooves connecting *g3* and *g4* suggest that fibers of the tympanic plexus ran along the *g3* route, as well.

As described above, the *g4* groove in plesiadapids is often closely associated with the main groove and foramen for the tympanic nerve (Fig. 17), a relationship that is consistent with it representing branches of the tympanic nerve, as suggested by MacPhee et al. (1983) in AMNH 17388, *Nanodectes gidleyi*. The majority of these nerve fibers seems to have reached the lateral side of the pars cochlearis following either an intrapetrous route in some specimens or a subpetrous (intrabullar) route in others, as indicated by the asymmetrical morphology of AMNH 17388 (see Boyer, 2009 for further discussion and his Fig. 2.16).

The *g5* groove is a trough-like groove that sometimes appears as an anterior continuation of *g1* and is located dorso-lateral to *g2*. It is relatively broad and may represent the place of assembly of the main part of the tympanic plexus (MacPhee, 1981). The deep petrosal nerve likely stemmed from this point to meet the greater petrosal nerve.

As noted above, the pattern of some of the grooves that we have identified can differ from specimen to specimen of the same species: we have concluded that most of this variability does not necessarily reflect variability in the soft anatomical structures held by these grooves. The logic that we have followed in arriving at this conclusion can be illustrated by an example: in *Plesiadapis tricuspidens* (MNHN CR 125), the *g2* groove is absent, but the carotid canal and *g1* groove are present, so the internal carotid nerve, possibly accompanied by an arterial remnant, clearly gained entrance to the tympanic cavity. Hence, the absence of a *g2* groove along the usual course of the internal carotid plexus to the *s1* septum (MacPhee, 1981) is not sufficient evidence to conclude that the internal carotid plexus did not follow an intratympanic route. Given the absence of “alternative” grooves that could plausibly represent the internal carotid plexus in its crossing of the promontorium, the most conservative interpretation is that the internal carotid plexus had the same course as in other plesiadapids in which the groove is present. Variability in other structures, however, such as the *g3* groove, may actually reflect real variability in soft anatomy, partly because we cannot confidently infer the specific neurovascular structure it held.

Additional features

Our observations and analysis suggest different conclusions regarding morphological patterns characterizing the Plesiadapidae for two other features that have figured

in discussions of plesiadapid phylogeny. First, new data on the nasal bone morphology shows that, generally speaking, in neither plesiadapids nor carpolestids does this element narrow posteriorly, contrary to previous descriptions (Bloch and Silcox, 2006). The narrowing is present only in *Plesiadapis tricuspidens*. However, unlike paromomyids (for example) the nasal bone of other plesiadapids and *Carpolestes* does not become wider posteriorly either, it simply maintains roughly the same width along its entire anteroposterior length. A “constant-width” nasal may thus turn out to be a synapomorphy of a clade containing plesiadapids and carpolestids in future studies. Second, the presence of a nontubular external auditory meatus in both *P. gaoi* and *Nannodectes intermedius* makes them similar to carpolestids (among other taxa) and indicates that a tubular element in *P. tricuspidens* and *P. cookei* is derived within the clade; a tubular external auditory meatus is most likely not a synapomorphy for the Plesiadapidae as a whole, as previously thought (e.g., Bloch et al., 2007).

Phylogenetic analysis

Enough resolution was obtained in our phylogenetic analyses to allow for comment on many previous hypotheses concerning plesiadapid relationships. Considering geography and temporal distribution, our results suggest that cladogenetic events among *Pronothodectes*-like species took place before one lineage of these lost i2 and then gave rise to the *Nannodectes* and *Plesiadapis* lineages (contra Gingerich 1976). *Pronothodectes matthewi* is known from the Who Nose? locality in Alberta, which is thought to be middle Torrejonian in age (Scott, 2003). It may represent a basal member of a *Pronothodectes* lineage that separated from those in the Crazy Mountains and Clarks Fork Basins, eventually giving rise to *P. gaoi*. If *Pronothodectes gaoi* is descended from a more primitive *Pronothodectes* species, there should eventually be evidence for more species of this genus in early Tiffanian localities in this same region (e.g., Cochrane 1 and 2). Although *Plesiadapis praecursor*, *Nannodectes intermedius*, and *Pronothodectes* sp. have all been tentatively identified at Cochrane 2 (Youzwysyn, 1988; Fox, 1990b; Scott et al., 2002), only one specimen from Cochrane 2 preserves information on the anterior dentition (UALVP 24900), which is critical for confirming these taxonomic identifications. The dimensions of known parts of the dentition of this specimen fall within the ranges of both *P. praecursor* and *N. intermedius* (p4, 1.7×2.0 ; m1, 2.45×2.25 ; m2, 2.7×2.45 mm; m3, $4.5 \times ?$). UALVP 24900 seems to retain alveoli for at least a canine and possibly i2 (Fig. 18), suggesting that it pertains to *Pronothodectes*.

The linkage of *Plesiadapis walbeckensis* with *Chiro-myoides* also differs from Gingerich (1976) but was implied by Russell (1964, pg. 86, Fig. 12). This relationship seems plausible given the unusually proportionally large central incisors these taxa share (see Russell, 1964) and can be tested as additional remains of these currently poorly known animals are recovered from Europe and North America.

Finally, our results differ from the conception of plesiadapid phylogeny proposed by Gingerich (1976) in placing *Plesiadapis cookei*, *Plesiadapis russelli*, and *Platychoerops* species closer to *Plesiadapis fodinatus* and *Plesiadapis dubius* than to *Plesiadapis tricuspidens*, *Plesiadapis remensis*, *Plesiadapis gingerichi*, or *Plesiadapis simonsi*. On the other hand, Russell's (1964, p. 86, Fig. 12) depiction is consistent with ours in its placement of *P.*

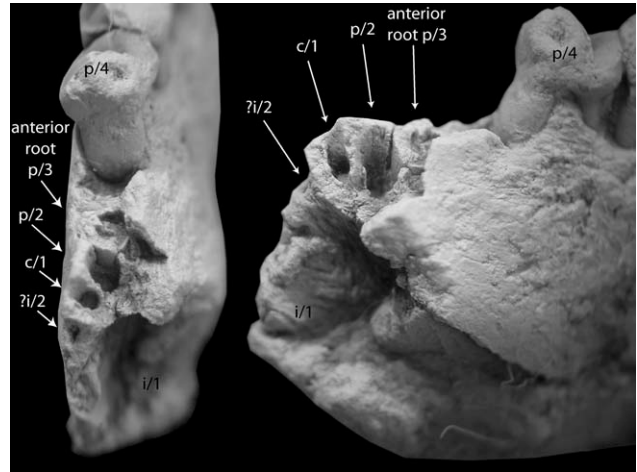


Fig. 18. UALVP 24900 from Cochrane 2 (early Tiffanian) (Fox, 1990a) showing alveoli for anterior dentition. Presence of i2 would allow consideration of this specimen as potentially ancestral to *Pronothodectes gaoi*.

cookei. Gingerich (1976) postulated that *P. churchilli* gave rise to a *P. fodinatus*-*P. dubius* lineage and a *P. simonsi* lineage, a phylogenetic pattern that is not contradicted by our results. We differ from Gingerich (1976), where he indicated that *P. simonsi* gave rise to both a *P. tricuspidens*-*Platychoerops* lineage and a separate *P. cookei* lineage. Our results suggest instead that *P. cookei* and *Platychoerops* are descended from *P. dubius*-like forms to the exclusion of *P. tricuspidens*. Although we feel that support for a close relationship between *P. cookei* and *Platychoerops* to the exclusion of *P. tricuspidens* is particularly strong, we stress that the potential discovery of new plesiadapids and of fossils better documenting presently known species will test these competing hypotheses.

ACKNOWLEDGMENTS

The authors thank J. Wible and one anonymous reviewer who read previous versions of this article twice: their reviews lead to significant improvements. A. Walker and T. Ryan provided HRxCT scans of UALVP 46685 and other petrosal specimens at the Center for Quantitative Imaging, Pennsylvania State University. M. Colbert and T. Rowe provided HRxCT scans of USNM 309902 at the High-Resolution X-ray CT Facility of the University of Texas at Austin. S. Judex and C. Rubin provided HRxCT scans at the Center for Biotechnology of the Department of Biomedical Engineering at Stony Brook University. M. Godinot, P. Tassy, and C. Sagne of MNHN and M. Pellouin provided access to important comparative specimens of *Plesiadapis tricuspidens*. R. Emry of the USNM granted access to and study of USNM 309902, *Nannodectes intermedius*. J. Meng of the AMNH granted access to and study of AMNH 17388, *Nannodectes gidleyi*. M. Coleman provided measurements of cochlea length in Tables A1 and A2. J. Scott of the University of Alberta, Department of Biological Sciences, helped acquire scanning electron microscope images of UALVP 46685, 46687, and 49105. N. Kley of Stony Brook University provided access to a digital microscope and copy stand for specimen imaging and measurement. J. Wible of the Carnegie Museum of Natural History assisted in interpreting soft anatomical cor-

APPENDIX

TABLE A1. Petrosal features of plesiadapid specimens

Taxon	Spec	ccl	fv	pd	pw	p-s	g1	g2	g3	g4	g5
<i>Pronothodectes gaoi</i>	UALVP 46685 R	nm	1.21	4.55	3.45	132	?	?	?	p	?
<i>Pronothodectes gaoi</i>	UALVP 46685 L	15.60	1.17	4.68	3.48	134	?	?	p	p	?
<i>Pronothodectes gaoi</i>	UALVP 46687 R	nm	1.20	4.29	3.73	115	pp	pp	p	p	p
<i>Pronothodectes gaoi</i>	UALVP 49105 L	15.30	1.03	4.61	3.84	120	pp	p	p	p	p
<i>N. intermedius</i>	USNM 309902 R	14.50	1.16	3.54	3.55	100	p	?	a	p	?
<i>N. intermedius</i>	USNM 309902 L	nm	1.19	~3.6	~3.8	95	p	n	a	?	a
<i>N. gidleyi</i>	AMNH 17388 R	nm	nm	nm	~3.5	nm	n	?	a	p	?
<i>N. gidleyi</i>	AMNH 17388 L	nm	nm	nm	~3.4	nm	n	?	a	p	?
<i>P. tricuspiciens</i>	MNHN CR 125 R	nm	1.53 ^a	nm	4.47	nm	p	a	a	p	p
<i>P. tricuspiciens</i>	MNHN CR 125 L	nm	nm	nm	nm	nm	?	a	a	p	p
<i>P. tricuspiciens</i>	Pellouin R	nm	nm	nm	nm	nm	?	a	pp	?	?
<i>P. tricuspiciens</i>	Pellouin L	nm	nm	nm	4.31	nm	p	a	pp	p	p
<i>P. tricuspiciens</i>	MNHN BR 1371	17.30	1.15	4.91	4.14	119	pp	p	pp	p	p
<i>P. tricuspiciens</i>	MNHN BR 17414	nm	nm	4.86	4.16	117	n	n	n	n	?
<i>P. tricuspiciens</i>	MNHN BR 17415	16.10	1.31	5.3	4.21	126	p	p	p	p	p
<i>P. tricuspiciens</i>	MNHN BR 17416	17.20	1.2	4.98	4.43	112	p	a	a	a	p
<i>P. tricuspiciens</i>	MNHN BR 17417	17.50	1.53	5.3	4.14	128	n	n	pp?	n	p
<i>P. tricuspiciens</i>	MNHN BR 17418	17.00	1.36	4.95	4.52	110	p	?	a	a	p
<i>P. tricuspiciens</i>	MNHN BR 17419	nm	nm	4.07	4.55	89	n	n	a	a	p
<i>Plesiadapis cookei</i>	UM 87990 R	21.03	1.32	~5.5	4.43	124	p	pp?	p	a	p
<i>C. simpsoni</i>	USNM 482354	8.64	nm	~2	~2.4	83	p	?	?	?	?
<i>I. graybullianus</i>	USNM 421608	nm	1.10**	3.28	3.04	108	p	n	n	n	?

Column headings: g1–5 – see main text Table 2; ccl, cochlear length (measurements courtesy of M. Coleman); fv, fenestra vestibuli maximum diameter (**stapes foot plate maximum diameter is used as a substitute in some cases); pd, petrosal depth: height of pars cochlearis measured perpendicular to the plane of the endocranial surface of the element; p-s, promontorium shape = (pd/pw); pw, petrosal width: mediolateral thickness of petrosal as taken perpendicular to previous measurement. Information in Tables A1 and A2 cells: a, morphology absent/different; n, morphology cannot be assessed because it is not preserved; nm, not measured or not measureable; p, morphology is present/preserved; pp, in the case of g1–4, indicates the presence of a set of parallel grooves are present in the appropriate position; ?, relevant anatomy for gauging the anatomical condition is preserved, but obscured by other bone or matrix, or just difficult to interpret for some reason.

^a Measured from illustration in Russell (1964, p. 95, figure 16).

TABLE A2. Petrosal features of plesiadapid specimens

Taxon	Spec	s1	s2	s3	tng	cc	ps	pcf	lam	bs
<i>Pronothodectes gaoi</i>	UALVP 46685 R	p	p	p	?	p	p	n	p	a
<i>Pronothodectes gaoi</i>	UALVP 46685 L	p	p	p	p	p	p	p/nm	a	p?
<i>Pronothodectes gaoi</i>	UALVP 46687 R	n	n	n	p	?	p	p/nm	a	a
<i>Pronothodectes gaoi</i>	UALVP 49105 L	p	p	p	p	p	p	p/0.28	p	a
<i>N. intermedius</i>	USNM 309902 R	?	p	n	n	p	n	n	?	?
<i>N. intermedius</i>	USNM 309902 L	p	p	a	?	?	n	n/0.29 ^a	?	a
<i>N. gidleyi</i>	AMNH 17388 R	?	p	a	p	p	?	n	?	a
<i>N. gidleyi</i>	AMNH 17388 L	?	p	a	p	p	?	n	?	a
<i>P. tricuspiciens</i>	MNHN CR 125 R	p	p	a	p	p	p	p/0.34	a	a
<i>P. tricuspiciens</i>	MNHN CR 125 L	p	p	a	p	p	p	n	a	a
<i>P. tricuspiciens</i>	Pellouin R	?	p	a	p	p	p	p/0.31	p	p?
<i>P. tricuspiciens</i>	Pellouin L	p	p	a	p	p	p	p/0.29	p	p?
<i>P. tricuspiciens</i>	MNHN BR 1371	p	p	a	n	p	n	n	n	n
<i>P. tricuspiciens</i>	MNHN BR 17414	n	?	n	n	p	n	n	n	n
<i>P. tricuspiciens</i>	MNHN BR 17415	p	p	a	?	p	n	n	p	a
<i>P. tricuspiciens</i>	MNHN BR 17416	p	p	a	n	p	n	n	p	a
<i>P. tricuspiciens</i>	MNHN BR 17417	n	p	?	n	p	n	n	p	a
<i>P. tricuspiciens</i>	MNHN BR 17418	p	p	p	?	p	n	n	p	a
<i>P. tricuspiciens</i>	MNHN BR 17419	p	p	n	?	p	n	n	p?	a
<i>Plesiadapis cookei</i>	UM 87990 R	p	p	a	p	p	n	n/0.40 ^a	n	p?
<i>C. simpsoni</i>	USNM 482354	?	?	?	?	?	p	p/0.53	?	?
<i>I. graybullianus</i>	USNM 421608	p	?	?	?	p	p	p/0.17	a	p?

Column headings: bs, cc, ps, pcf, s1–3, tca, see main text Table 2; lam, several specimens exhibit what appeared to be two laminae of bone comprising the remnant of the rostral tympanic process (the dorsolateral edge of the bulla). Information in Table A2 cells: see legend of Table A1.

^a In some cases, the posterior carotid foramen was not visible and had to be estimated from the width of the groove for the internal carotid plexus on the petrosal. If measureable, the value in millimeters is given after the condition symbol.

TABLE A3. Cranial measurements: basic measurements

Specimen	MNHN CR 125	Pellouin skull	MNHN CR 965	UM 87990	UALVP 46685	AMNH 17388	USNM 309902	YPM-PU 19642
Taxon	<i>P. tricuspidens</i>	<i>P. tricuspidens</i>	<i>P. tricuspidens</i>	<i>Plesiadapis</i>	<i>Pronothodectes</i>	<i>N. gidleyi</i>	<i>N. intermedius</i>	<i>P. anceps</i>
Element	Skull	Skull	Skull base	Skull	Skull	Skull	Skull	Rostrum
Locality	Berru	Berru	Berru	SC-117	DW-2	Mason Pocket	Bangtail	7-up Butte
Measures								
1	4.30	—	—	4.84	2.67	—	2.31	3.34
2	30.69	—	—	31.35	18.4	—	13.61	21.84
3	1.51	2	—	4.57	2.6	—	2.31	3.34
4	7.68	—	—	8.61	—	—	—	—
5	16.25	—	—	15.93	6.52	—	—	—
6	5.50	—	—	3.87	2.66	—	—	—
7	9.60	—	—	—	4.36	—	—	4.52
8	35.78	30.36	—	29.37	—	—	—	—
9	4.44	5.75	—	5.53	3.39	—	—	—
10	6.89	8.02	—	7.71	5.45	—	—	—
11	21.16	20.8	—	22.16	12.36	12.4	10.55	—
12	15.14	12.37	—	14.04	6.73	—	—	—
13	6.66	6.84	6.54	6.8	—	—	—	—
14	13.89	13.26	10.82	15.12	—	—	—	—
15	27.99	24.76	—	26.1	—	—	—	—
16	3.79	3.47	—	2.33	1.29	1.44	—	—
17	15.01	17.7	—	18.44	—	—	—	—
18	8.38	—	—	8.84	3.77	—	—	4.6
19	14.15	—	—	15.11	—	—	—	10.2
20	20.68	19.69	—	21.02	11.23	—	—	13.08
21	10.09	8.63	—	10.82	—	—	—	—
22	41.88	38.52	—	41	—	—	—	—
23	11.31	10.85	—	11.66	—	—	—	—
24	13.54	14.02	—	10.12	5.38	5.6	4.11	—
25	13.98	13.52	—	11.52	6.96	6.5	4.49	—
26	4.01	4.54	—	3.69	—	1.35	1.43	—
27	13.83	11.16	12.93	12.57	—	—	—	—
28	4.26	3.74	4.33	4.45	—	3.1	—	—
29	6.37	6.94	—	—	3.25	—	2.21	—
30	14.82	14.4	—	14.42	8.46	—	7.22	—
31	10.94	10.54	—	10.59	—	—	—	—
32	24.97	25	—	26	—	17.4	12.2	—
33	8.3	8.5	—	8.6	6.17	5.92	5.39	—
34	4.39	4.05	—	4.38	2.46	2.5	1.95	—
35	6.48	5.06	—	5.36	3.87	2.8	2.8	—
36	8.97	9.78	—	7.86	3.99	—	—	—
37	16.69	—	—	16.55	—	—	—	—
38	27.21	—	—	24	—	—	—	—
39	11.95	12.45	—	10.8	—	—	—	—
40	8.95	6.88	—	8.71	7.4	6.84	6.87	—
41	11.60	11.50	—	4.80	5.75	—	—	—
42	6.80	6.60	—	12.00	5.50	—	4.07	—
GM	10.6 (39)	10.28 (30)	—	10.71 (39)	4.91 (21)	4.45 (11)	4.32 (14)	—
% size of <i>Plesiadapis cookei</i> ^a	100.5 (39)	100.6 (30)	91 (4)	100 (39)	57 (21)	58 (11)	47 (14)	65 (6)
Length estimate ^b	106.3 mm	106.5 mm	96.5 mm	105.8 mm	61.2 mm	62.3 mm	50.4 mm	69.2 mm

(1–44: see Boyer et al., 2010 for illustrations (Fig. 1) and descriptions (Table A1).

^a Overall skull size of each specimen (one specimen per column) is here expressed as the antilogged average of a varying number of natural log ratios (the number in parentheses following the length estimate) of its cranial measurements to those of *Plesiadapis cookei*. In other words, each skull's measurements are expressed as an average of (n) direct comparisons to measurements on *Plesiadapis cookei*. The overall skull size of each specimen can then be given as a percentage of that of *Plesiadapis cookei*. Because different skulls preserve different numbers and combinations of measurements in common with *Plesiadapis cookei*, the values here do not necessarily correlate with the values of geometric means for the same skulls.

^b Cranial estimates based on multiplying number in “% size of *Plesiadapis cookei*” row by estimated length of 105.83 mm for *Plesiadapis cookei* UM 87990 (see Boyer et al. 2010), and then dividing by 100.

TABLE A4. Foramina and canal measurements (Table X)

Specimen	MNHN CR 125	Pellouin skull	MNHN CR 965	UM 87990	UALVP 46685	AMNH 17388	USNM 309902	YPM-PU 19642
Taxon	<i>P. tricuspidens</i>	<i>P. tricuspidens</i>	<i>P. tricuspidens</i>	<i>Plesiadapis cookei</i>	<i>Pronothodectes gaoi</i>	<i>N. gidleyi</i>	<i>N. intermedius</i>	<i>P. anceps</i>
Element	Skull	Skull	Skull base	Skull	Skull	Skull	Skull	Rostrum
Locality	Berru	Berru	Berru	SC-117	DW-2	Mason Pocket	Bangtail	7-up Butte
Foramina								
45	2.8	2.34	—	2.73	2.12	2.22	2.2	—
46	1.3	1.79	—	1.52	1.26	—	1.15	—
47	1.36	—	1.21	—	—	—	—	—
48	0.84	—	1.02	—	—	—	—	—
49	1.45	—	1.64	—	—	—	—	—
50	1.17	—	~1.4	—	—	—	—	—
51	4.08	—	—	—	—	—	—	—
52	—	—	2.08	~2	—	—	—	—
53	2.61	—	3.12	—	—	—	—	—
54	1.49	—	1.42	—	—	—	—	—
55	1.52	~1.7	—	1.75	1.03	—	—	—
56	1.05	~1.4	—	1.6	0.86	—	—	—
57	0.72	—	—	—	—	—	—	—
58	2.53	—	2.97	—	—	—	—	—
59	1.81	—	—	—	—	—	—	—
60	2.38	—	—	2.86	—	—	—	—
61	2.8	2.7	—	—	~1.6	—	—	—

(45) Infraorbital foramen major diameter, (46) Infraorbital foramen minor diameter, (47) Optic foramen major diameter, (48) Optic foramen minor diameter, (49) Suboptic foramen major diameter, (50) Suboptic foramen minor diameter, (51) Sphenorbital fissure major diameter, (52) Sphenorbital fissure minor diameter, (53) Foramen ovale major diameter, (54) Foramen ovale minor diameter, (55) Hypoglossal foramen major diameter, (56) Hypoglossal foramen minor diameter, (57) Major diameter of MNHN CR 125 foramen 93, (58) Postpalatine foramen major diameter, (59) Postpalatine foramen minor diameter, (60) Jugular foramen major diameter, (61) Length of internal carotid canal.

TABLE A5. Cranial shape variables

Specimen	MNHN CR 125	Pellouin skull	MNHN CR 965	UM 87990	UALVP 46685	AMNH 17388	USNM 309902	YPM-PU 19642
Taxon	<i>P. tricuspidens</i>	<i>P. tricuspidens</i>	<i>P. tricuspidens</i>	<i>Plesiadapis cookei</i>	<i>Pronothodectes gaoi</i>	<i>N. gidleyi</i>	<i>N. intermedius</i>	<i>P. anceps</i>
Element	Skull	Skull	Skull base	Skull	Skull	Skull	Skull	Rostrum
Locality	Berru	Berru	Berru	SC-117	DW-2	Mason Pocket	Bangtail	7-up Butte
Nc/Nr	35	—	—	94	97	—	100	100
Nc/GM	14	19	—	43	53	—	53	—
Nc/Pmx	16	—	—	—	60	—	—	74
Pmx/GM	91	—	—	—	89	—	—	—
N/F	148	—	—	149	164	—	—	167
Gld/GM	130	134	—	101	125	136	99	—
EAM-S	283	295	—	250	105	—	—	—
Cl/GM	161	—	—	196	318	—	336	—
Pcsa/GM	43	—	—	46	83	—	84	—
Av/GM	12	—	—	12	23	—	—	—

(Av/GM) Fenestra vestibuli relative length = [(Table A1: av)/GM]; (Cl/GM) Cochlea relative length = [(Table A1: ccl)/GM]; (EAM-S) External auditory meatus shape = (41/42); (Gld/GM) Glenoid relative size = $(\sqrt{24 \times 25})/GM$; (Nc/GM) Caudal nasal relative width = (3/GM); (Nc/Nr) Nasal caudal width relative to rostral width (3/1); (Nc/Pmx) Nasal width relative to Premaxilla width = (3/7); (N/F) Nasal length relative to frontal length = (2/20); (Pcsa/GM) Petrosal relative cross-sectional area = $[\sqrt{(\text{Table A1: } pd \times pw)/GM}]$; (Pmx/GM) Premaxilla relative width = (7/GM).

TABLE A6. Characters for species level analysis of Plesiadapidae

Dentition	
<i>Incisors</i>	
1	Incisor proportions: (0) occlusal height short compared with area in occlusal plane, (1) occlusal height intermediate, (2) occlusal height high.
<i>Lower incisors</i>	
2	(= character 4 of Bloch et al., 2001) Basal cusp on lingual cingulum of I ₁ : (0) absent, (1) present.
3	I ₁ : with squared tip: (0) absent, (1) present.
4	I ₂ : (0) present, (1) absent.
5	(= character 6 of Bloch et al., 2001) I ₃ : (0) present, (1) absent.
<i>Upper Incisors</i>	
6	I ¹ laterocone: (0) present, (1) reduced, (2) absent. Ordered.
7	I ¹ posterocone: (0) twinned (1) present, (2) reduced, (3) absent. Ordered.
8	I ¹ mediocone: (0) present, (1) reduced or absent.
9	I ¹ centroconule: (0) present, (1) reduced or absent.

TABLE A6. *continued*

Dentition	
<i>Canines</i>	
10	C ¹ : (0) present, (1) absent.
11	C ₁ : (0) present, (1) absent.
<i>Premolars</i>	
12	Diastemata between premolars and more anterior teeth: (0) absent, (1) present.
13	P ¹ or P ₁ : (0) present, (1) absent.
<i>Lower premolars</i>	
14	P ₂ : (0) large, (1) small, (2) absent. ordered
15	Form of P ₂ : (0) premolariform with talonid heel, (1) button shaped
16	(Modified from character 14 of Bloch et al., 2001) Metaconid on P ₄ : (0) absent, (1) present.
17	(d25 of Silcox, 2001) Paraconid on P ₄ : (0) present, (1) absent.
18	Entoconid on P ₄ : (0) present, (1) absent.
19	Trigonid of P ₄ : (0) present, (1) absent.
20	Proportions of P ₄ : (0) buccolingually broad relative to mesiodistal length, (1) narrow, (2) extremely narrow, relatively large and with multiple in-line apical cusps
<i>Upper premolars</i>	
21	P ² : (0) present, (1) absent.
22	P ³ paraconule: (0) present, (1) reduced, (2) absent. ordered
23	P ⁴ paraconule: (0) present, (1) reduced, (2) absent. ordered
24	P ⁴ molar-type paraconule: (0) absent, (1) present
<i>Lower molars</i>	
25	Entoconid of M ₁₋₂ : (0) squared and lacking crest (1) curved with crest
26	Length of M ₁ : (0) species sample mean less than 3.5 mm, (1) greater than or equal to 3.5 mm.
27	(= d80 of Silcox, 2001) Postvallid of M ₁ : (0) flush, (1) stepped
28	(modified from d75 of Silcox, 2001) Size of M ₃ hypoconulid: (0) small relative to talonid, (1) large
29	Shape of M ₃ hypoconulid: (0) rounded and unfissured, (1) squared and fissured
<i>Upper molars</i>	
30	M ¹⁻² mesostyles: (0) absent, (1) weakly present, (2) strong. ordered
31	Incisor size relative to molars: (0) slightly larger, (1) greatly enlarged (m1area / i1 area < 0.85).
32	Premolar and/or molar form: (0) cuspidate, (1) blunt, (2) crestiform, unordered.
Cranium ^a	
33	Structure of auditory bulla: membranous, or bony but nonpetrosal in origin (0), or no suture separating bulla from petrosal and/or no developmental evidence for additional elements (1). This character is modified from Beard and MacPhee (1994) and is designed to best employ the data that is available from fossils (i.e., under this definition microsopids can be coded despite the uncertainty about the composition of their bullae).
34	Relations of entotympanic: no entotympanic present (0), entotympanic contacts petrosal medially (1), entotympanic contacts basioccipital medially (2), or no medial contact (3). This character is modified from Kay et al. (1992), and was scored only in taxa for which an entotympanic could be positively identified.
35	Form of external auditory meatus: not expanded into bony tube (0), or expanded into bony tube (1). As defined here, this character does not differentiate between tubular external auditory meati that are formed from different bones. This reflects the difficulty of accurately reconstructing the contribution of all of the bones making up the auditory bulla in fossils.
36	Presence of subtympnic recess (between tympanic ring and bulla): subtympnic recess absent and ectotympanic does not include distinct ring-like element (0), or subtympnic recess present and ectotympanic includes ring-like element separated by annular bridge, membrane or gap between it and bulla (1). This character is modified from a character relating to the annular bridge employed by Beard and MacPhee (1994). See discussion in Silcox (2001). As configured here, this character allows the recognition of the basic similarity of a ring-like ectotympanic even if this is all that is preserved (i.e., as is the case for <i>Ignaciuss</i> ; Bloch and Silcox, 2001).
37	Presence of branches of internal carotid artery: grooves for at least promontorial branch, no tubes (0), tubes present for one or both arteries (1), or internal carotid artery absent (2).
38	Posterior carotid foramen position (or position of entry of internal carotid artery and/or nerves into middle ear): posteromedial (0), or posterolateral (1).
39	Subsquamosal foramen: present and large (0), or very small or absent (1). Note that this feature refers to a foramen located at the distal end of the zygomatic arch, making it equivalent to the opening called a suprameatal foramen by Kay et al. (1992; see discussion in Beard and MacPhee, 1994).
40	Width of central stem and relative size of hypotympanic sinus: broad with hypotympanic sinus restricted (0), or narrow with hypotympanic sinus expansive (1). Beard and MacPhee (1994; p. 79) define the central stem as "the midline keel of the posterior basicranium normally composed of the basisphenoid and basioccipital bones." Taxa with highly inflated bullae (i.e., an expansive hypotympanic sinus) also by necessity have a central stem, so the expanse of the hypotympanic sinus was not included as a separate character here (by contrast, it was employed as a character by MacPhee and Cartmill, 1986).
41	Snout: relatively long (0), or short (1). To code this character, the length of the snout was measured from the ventral base of the anterior extent of the zygomatic arch to the front of the premaxilla. This was then compared to total skull length, measured from the caudal-most point on the occiput to the front of the premaxilla. A least-squares regression was performed of snout length on cranial length using SPSS 10.05, with the constraint that it pass through the origin (Silcox, 2001). The resulting line had this equation: snout length = 0.039 × (cranial length). This line was a good fit to the data ($r^2 = 0.971$). Character state 1 was assigned to any taxon with a residual more negative than -5.0. This indicates that the snout is at least 5 mm shorter than would be predicted by the equation.

TABLE A6. *continued*

Cranium ^a	
42	Presence of postorbital bar: absent (0), postorbital process of frontal present but does not meet zygomatic (1), or complete postorbital bar present (2). Although it can be difficult to rule out absolutely the presence of a postorbital bar in damaged specimens, the absence of a process on either the zygomatic or the frontal can demonstrate that there was no complete bar.
43	Presence of mastoid process: no strong tubercle or inflation in mastoid region (0), or strong tubercle or inflation in mastoid region (1). This character was scored somewhat differently than in Kay et al. (1992) in that it was considered likely that an inflated mastoid region was on the same morphocline as a strong tubercle, rather than being most similar to the complete absence of any expansion of the mastoid.
44	Number of jugular (= posterior lacerate) foramina: single (0), or dual (1).
45	Position of caudal midsagittal margin of palate: near M ³ (0), well rostral to M ³ (1), or well caudal to M ³ (2). The states for this character differ somewhat from those used by Kay et al. (1992), who based the character on small variations in the position of the midsagittal margin of the palate.
46	Number of pterygoid plates: two (0), or one (1).
47	Supraorbital foramen: absent (0), or present (1).
48	Nasals: flare laterally at caudal extent with wide contact with frontal (0), or nasals do not flare laterally at caudal extent with narrow contact with frontal (1).
49	Diameter of infraorbital foramen: large (0), or small (1). For this analysis two measurements were taken from the infraorbital foramen, following Kay et al. (1992): the greatest diameter and the maximum length perpendicular to the first measurement. These two measurements were then multiplied together to give an approximation of the area of the foramen. A least squares regression analysis was performed of the infraorbital foramen area vs. the logarithm of M ¹ (calculated as buccal length × width). Taxa that fell outside the 99% confidence limit for this analysis were grouped together in the “small” category (Silcox, 2001).
50	Contact between lacrimal and palatine in orbit: present (0), obscured by maxillofrontal contact (1).
51	Lacrimal tubercle: absent (0), or present (1).
52	Size of optic foramen: small (0), moderate (1), or large (2). Coding for this character followed the ranges used by Kay et al. (1992).
53	Foramen rotundum: absent (0) or present (1).
54	Position of lacrimal foramen: on orbital rim (0), on face (1), or in orbit (2).
55	Cochlear window: not shielded (0), shielded by arterial tube (1), or shielded by bony septum (2).
56	Orientation of fenestra rotunda (= cochlear window): directed posterolaterally (0), or directed posteriorly (1). Although there is some slight variation in the orientation of the fenestra rotunda, the situation in dermopterans and chiropterans, where this opening points directly posteriorly, is particularly distinctive. The derived state of this character has been cited frequently as a volitantian synapomorphy (Novacek, 1986; Novacek and Wyss, 1986; Wible and Novacek, 1988).
57	Septae in middle ear cavity formed by entotympanic: absent (0), or present (1). The “present” state was only recognized in scandentians, in which the entotympanic forms a dorsal cover to petrosal structures on the roof of the middle ear cavity (MacPhee, 1981).
58	“Fattened” area on medial promontorium: absent (0), or present (1). This character was suggested by Szalay (1975). The “1” state represents a rounded, bulging promontorium, contrasting with the “deflated” appearance of taxa that exhibit the “0” state.
59	Expansiveness of premaxillary contact with frontal: absent (0), narrow (1), or broad (2).
60	Relative size of annular component of ectotympanic: small, not flaring greatly beyond bony struts by which it is connected to bullar part of ectotympanic (0), or large, flaring well beyond bony struts by which it is connected to bullar part of ectotympanic (1).
61	Exposure of maxillary tooth roots in orbit: present (0), reduced to only distobuccal root of M ³ or absent (1).
62	Glenoid fossa relative size: small (0), or large (1).
63	Nuchal crest length: projects posteriorly (0), or restricted (1).
64	Internal carotid artery functionality: functional (0), or nonfunctional (1).
65	Presence of s3 septum on promontorium: present (0), absent (1).
66	Position of zygomatic process of maxilla: lateral to M ² (0), lateral to M ¹ (1).

^a Cranial 33–58 correspond to characters used by Bloch et al. (2007), and numbered 83–108. Note that more extensive discussions of most of these characters are available in Bloch et al. (2007) and Silcox (2001). Sources for the characters in this dataset include Szalay (1975), Wible and Covert (1987), Kay et al. (1992), Wible (1993), Beard and MacPhee (1994), and Silcox (2001).

TABLE A7. Dental characters

Taxon	1	2	3	4	5	6	7	8	9	10	11	12	13	14	15	16	17	18	19	20	21	22	23	24	25	26	27	28	29	30	31	32			
<i>Purgatorius</i> sp.	1	0	0	0	0	0	1	0	1	?	0	0	0	1	0	0	0	0	1	0	0	1	1	0	0	0	0	0	0	0	0	0	0		
<i>Ephidotarsius</i> sp.	1	0	0	0	1	0	0	0	1	1	0	0	0	1	1	1	0	1	1	2	0	0	0	0	0	0	1	1	0	0	0	0	0		
<i>C. simpsoni</i>	1	0	0	0	1	0	0	1	1	0	0	0	1	2	?	1	0	1	1	2	0	0	0	0	0	0	1	1	0	0	0	0	0		
<i>Pronothodectes matthewi</i>	1	1	0	0	1	0	1	0	1	0	0	0	1	1	0	0	1	1	1	0	0	0	0	0	0	0	1	1	0	0	0	0	0		
<i>Pronothodectes jepi</i>	1	1	0	0	1	0	1	0	1	0	0	0	1	1	?	0	1	1	1	0	0	0	0	0	0	0	1	1	0	0	0	0	0	0	
<i>Pronothodectes gaoi</i>	1	1	0	0	1	0	1	0	1	0	0	0	1	1	0	0	1	1	1	0	0	0	0	0	0	0	1	1	0	0	0	0	0	0	
<i>Plesiadapis praecursor</i>	1	1	0	1	1	0	1	0	1	0	0	1	1	1	?	0	1	1	1	0	0	0	0	0	0	0	1	1	0	0	0	0	0	0	
<i>Plesiadapis insignis</i>	1	1	0	1	1	0	1	0	1	0	1	1	1	0	?	?	1	1	1	0	0	?	?	0	0	0	1	1	0	0	0	0	0	0	
<i>P. anceps</i>	1	1	0	1	1	0	1	0	1	0	0	1	1	1	?	0	1	1	1	0	0	0	0	0	0	0	1	1	0	0	0	0	0	0	
<i>Plesiadapis walbeckensis</i>	1	1	0	1	1	0	1	0	1	0	1	1	1	1	?	0	1	1	1	0	0	0	0	0	0	0	1	1	0	1	0	0	0	0	
<i>Plesiadapis rex</i>	1	1	0	1	1	0	1	0	0	0	1	1	1	1	?	0	1	1	1	0	0	0	0	0	0	0	1	1	1	0	0	0	0	0	
<i>N. intermedius</i>	1	1	0	1	1	0	1	0	1	0	0	0	1	1	?	0	1	1	1	1	0	0	0	0	0	0	1	1	0	0	0	0	0	0	0
<i>Nannodectes gazini</i>	1	1	0	1	1	0	1	0	1	0	0	0	1	1	?	0	1	1	1	1	0	1	0	0	0	0	1	1	0	0	0	0	0	0	0
<i>Nannodectes simpsoni</i>	1	1	0	1	1	?	?	?	?	?	?	1	1	1	?	0	1	1	1	1	0	2	0	0	0	0	1	1	0	1	0	0	0	0	0
<i>N. gidleyi</i>	1	1	0	1	1	0	1	?	1	0	1	1	1	1	?	0	1	1	1	1	0	0	0	0	0	0	1	1	0	1	0	0	0	0	0
<i>Chiromyoides minor</i>	0	1	0	1	1	0	1	0	1	?	1	0	?	2	?	?	?	?	?	?	?	?	?	?	?	?	?	?	?	?	?	?	?	?	?
<i>Chiromyoides campanicus</i>	0	1	0	1	1	0	1	0	1	?	1	0	1	2	?	?	?	?	?	?	?	?	?	?	?	?	?	?	?	?	?	?	?	?	?
<i>Chiromyoides caesor</i>	0	?	?	?	?	?	?	?	?	?	?	?	?	?	?	?	?	?	?	?	?	?	?	?	?	?	?	?	?	?	?	?	?	?	?
<i>Chiromyoides potior</i>	0	1	1	1	1	0	1	0	1	?	1	1	?	2	?	?	?	?	?	?	?	?	?	?	?	?	?	?	?	?	?	?	?	?	?
<i>Chiromyoides major</i>	0	1	1	1	1	0	1	0	1	?	1	1	?	2	?	?	?	?	?	?	?	?	?	?	?	?	?	?	?	?	?	?	?	?	?
<i>Plesiadapis churchilli</i>	1	1	0	1	1	0	1	0	0	1	1	1	1	1	?	0	1	0	1	0	0	0	0	0	0	0	1	1	2	0	0	0	0	0	
<i>Plesiadapis gingrichi</i>	1	?	?	?	?	?	?	?	?	?	1	1	1	2	?	?	?	?	?	?	?	?	?	?	?	?	?	?	?	?	?	?	?	?	?
<i>Plesiadapis simonsi</i>	?	?	?	?	?	?	?	?	?	?	?	?	?	?	?	?	?	?	?	?	?	?	?	?	?	?	?	?	?	?	?	?	?	?	?
<i>Plesiadapis remensis</i>	1	1	0	1	1	0	1	0	0	?	1	1	1	2	?	?	?	?	?	?	?	?	?	?	?	?	?	?	?	?	?	?	?	?	?
<i>P. tricuspidens</i>	1	0	0	1	1	0	1	0	0	1	1	1	1	2	?	1	1	1	1	0	0	0	0	0	0	1	1	1	1	1	1	1	1	1	1
<i>Plesiadapis fodinatus</i>	1	1	0	1	1	0	1	0	0	1	1	1	1	2	?	1	0	0	1	0	0	1	1	1	0	1	0	1	1	2	0	0	2	0	2
<i>Plesiadapis dubius</i>	1	1	0	1	1	0	1	0	1	0	1	1	1	2	?	?	?	?	?	?	?	?	?	?	?	?	?	?	?	?	?	?	?	?	?
<i>Plesiadapis cookei</i>	2	0	0	1	1	1	2	1	1	1	1	1	1	2	?	0	0	0	0	0	1	2	2	0	1	1	1	1	2	0	0	2	0	2	
<i>Plesiadapis russelli</i>	2	?	?	1	1	1	2	1	1	1	1	?	1	2	?	?	?	?	?	?	?	?	?	?	?	?	?	?	?	?	?	?	?	?	?
<i>Platychoerops daubrei</i>	2	0	0	1	1	2	3	1	1	1	1	1	1	2	?	1	0	0	0	0	?	?	?	?	?	?	?	?	?	?	?	?	?	?	?
<i>Platychoerops richardsoni</i>	?	?	?	?	?	?	?	?	?	?	?	?	?	?	?	?	?	?	?	?	?	?	?	?	?	?	?	?	?	?	?	?	?	?	?

TABLE A8. Cranial characters

Taxon	33	34	35	36	37	38	39	40	41	42	43	44	45	46	47	48	49	50	51	52	53	54	55	56	57	58	59	60	61	62	63	64	65	66		
<i>Purgatorius</i> sp.	?	?	?	?	?	?	?	?	?	?	?	?	?	?	?	?	?	?	?	?	?	?	?	?	?	?	?	?	?	?	?	?	?	?	?	
<i>Elphidotarsius</i> sp.	?	?	?	?	?	?	?	?	?	?	?	?	?	?	?	?	?	?	?	?	?	?	?	?	?	?	?	?	?	?	?	?	?	?	?	
<i>C. simpsoni</i>	1	?	0	?	?	0	1	1	0	0	0	0	0	0	1	1	1	1	0	0	1	2	0	?	?	1	0	0	0	0	0	1	0	1	0	0
<i>P. matthewi</i>	?	?	?	?	?	?	?	?	?	?	?	?	?	?	?	?	?	?	?	?	?	?	?	?	?	?	?	?	?	?	?	?	?	?	?	?
<i>P. jepi</i>	?	?	?	?	?	?	?	?	?	?	?	?	?	?	?	?	?	?	?	?	?	?	?	?	?	?	?	?	?	?	?	?	?	?	?	?
<i>Pronothodectes gaoi</i>	1	0	0	1	0	1	?	1	0	0	1	0	?	?	0	0	?	?	?	?	?	1	0	?	?	1	0	0	0	0	0	0	0	0	0	0
<i>P. praecursor</i>	?	?	?	?	?	?	?	?	?	?	?	?	?	?	?	?	?	?	?	?	?	?	?	?	?	?	?	?	?	?	?	?	?	?	?	?
<i>P. insignis</i>	?	?	?	?	?	?	?	?	?	?	?	?	?	?	?	?	?	?	?	?	?	?	?	?	?	?	?	?	?	?	?	?	?	?	?	?
<i>P. anceps</i>	?	?	?	?	?	?	?	?	?	?	?	?	?	?	?	?	?	?	?	?	?	?	?	?	?	?	?	?	?	?	?	?	?	?	?	?
<i>P. walbeckensis</i>	?	?	?	?	?	?	?	?	?	?	?	?	?	?	?	?	?	?	?	?	?	?	?	?	?	?	?	?	?	?	?	?	?	?	?	?
<i>P. rex</i>	?	?	?	?	?	?	?	?	?	?	?	?	?	?	?	?	?	?	?	?	?	?	?	?	?	?	?	?	?	?	?	?	?	?	?	?
<i>N. intermedius</i>	1	0	0	1	0	1	?	1	0	0	1	0	?	?	0	0	?	?	?	?	?	?	0	?	?	1	0	0	0	0	0	0	1	0	0	0
<i>N. gazini</i>	?	?	?	?	?	?	?	?	?	?	?	?	?	?	?	?	?	?	?	?	?	?	?	?	?	?	?	?	?	?	?	?	?	?	?	?
<i>N. simpsoni</i>	?	?	?	?	?	?	?	?	?	?	?	?	?	?	?	?	?	?	?	?	?	?	?	?	?	?	?	?	?	?	?	?	?	?	?	?
<i>N. gidleyi</i>	1	0	?	?	?	?	?	1	0	?	1	?	0	1	?	?	0	?	?	?	?	?	0	?	?	?	?	?	?	?	?	?	?	?	?	?
<i>C. minor</i>	?	?	?	?	?	?	?	?	?	?	?	?	?	?	?	?	?	?	?	?	?	?	?	?	?	?	?	?	?	?	?	?	?	?	?	?
<i>C. caesor</i>	?	?	?	?	?	?	?	?	?	?	?	?	?	?	?	?	?	?	?	?	?	?	?	?	?	?	?	?	?	?	?	?	?	?	?	?
<i>C. potior</i>	?	?	?	?	?	?	?	?	?	?	?	?	?	?	?	?	?	?	?	?	?	?	?	?	?	?	?	?	?	?	?	?	?	?	?	?
<i>C. major</i>	?	?	?	?	?	?	?	?	?	?	?	?	?	?	?	?	?	?	?	?	?	?	?	?	?	?	?	?	?	?	?	?	?	?	?	?
<i>P. churchilli</i>	?	?	?	?	?	?	?	?	?	?	?	?	?	?	?	?	?	?	?	?	?	?	?	?	?	?	?	?	?	?	?	?	?	?	?	?
<i>P. gingerichi</i>	?	?	?	?	?	?	?	?	?	?	?	?	?	?	?	?	?	?	?	?	?	?	?	?	?	?	?	?	?	?	?	?	?	?	?	?
<i>P. simonsi</i>	?	?	?	?	?	?	?	?	?	?	?	?	?	?	?	?	?	?	?	?	?	?	?	?	?	?	?	?	?	?	?	?	?	?	?	?
<i>P. remensis</i>	?	?	?	?	?	?	?	?	?	?	?	?	?	?	?	?	?	?	?	?	?	?	?	?	?	?	?	?	?	?	?	?	?	?	?	?
<i>P. tricuspidens</i>	1	0	1	1	0	1	1	1	0	0	1	0	0	1	0	1	0	?	?	?	?	?	?	?	?	?	?	?	?	?	?	?	?	?	?	?
<i>P. fodinatus</i>	?	?	?	?	?	?	?	?	?	?	?	?	?	?	?	?	?	?	?	?	?	?	?	?	?	?	?	?	?	?	?	?	?	?	?	?
<i>P. dubius</i>	?	?	?	?	?	?	?	?	?	?	?	?	?	?	?	?	?	?	?	?	?	?	?	?	?	?	?	?	?	?	?	?	?	?	?	?
<i>Plesiadapis cookei</i>	1	0	1	1	0	1	?	1	0	0	1	0	?	?	?	0	?	?	?	?	?	?	?	?	?	?	?	?	?	?	?	?	?	?	?	
<i>P. russelli</i>	?	?	?	?	?	?	?	?	?	?	?	?	?	?	?	?	?	?	?	?	?	?	?	?	?	?	?	?	?	?	?	?	?	?	?	?
<i>P. daubrei</i>	?	?	?	?	?	?	?	?	?	?	?	?	?	?	?	?	?	?	?	?	?	?	?	?	?	?	?	?	?	?	?	?	?	?	?	?
<i>P. richardsoni</i>	?	?	?	?	?	?	?	?	?	?	?	?	?	?	?	?	?	?	?	?	?	?	?	?	?	?	?	?	?	?	?	?	?	?	?	?

TABLE A9. Specimens scanned

Taxon	Specimen	kV	μ A	x-y res	z spacing	Slices	Wedge	Facility
<i>Pronothodectes gaoi</i>	UALVP 46685	150	325	43.9	49.1	861	rice	CQI PSU
<i>Pronothodectes gaoi</i>	UALVP 46687	150	325	40	49.1	123	rice	CQI PSU
<i>Pronothodectes gaoi</i>	UALVP 49105	150	325	40	49.1	246	rice	CQI PSU
<i>Pronothodectes gaoi</i>	UALVP 49105	55	145	6	6	207 (3)	air	SBU CBT
<i>N. intermedius</i>	USNM 309902	150	325	40	49.1	246	rice	CQI PSU
<i>N. intermedius</i>	USNM 309902	180	133	35.8	38.4	405	air	HRxCT UT
<i>P. tricuspiciens</i>	MNHN BR 1371	150	200	50	58.11	205	air	CQI PSU
<i>P. tricuspiciens</i>	MNHN BR 17414	150	200	50	58.11	205	air	CQI PSU
<i>P. tricuspiciens</i>	MNHN BR 17415	150	200	50	58.11	205	air	CQI PSU
<i>P. tricuspiciens</i>	MNHN BR 17416	150	200	50	58.11	205	air	CQI PSU
<i>P. tricuspiciens</i>	MNHN BR 17417	150	200	50	58.11	205	air	CQI PSU
<i>P. tricuspiciens</i>	MNHN BR 17418	150	200	50	58.11	205	air	CQI PSU
<i>P. tricuspiciens</i>	MNHN BR 17419	150	200	50	58.11	205	air	CQI PSU
<i>Plesiadapis cookei</i>	UM 87990	150	325	52.7	61.4	1435	water	CQI PSU
<i>I. graybullianus</i>	USNM 482353	55	145	6	6	418 (1)	air	SBU CBT
<i>Acidomomys hebeticus</i>	UM 108207	55	145	6	6	426 (1)	water	SBU CBT
<i>Sciurus caroliniensis</i>	SBU MRd-12	55	145	8	8	213 (1)	air	SBU CBT
<i>L. maximus</i>	AMNH 41527	70	114	8	8	213 (1)	air	SBU CBT

CQI PSU, Center for Quantitative Imaging, Pennsylvania State University; HRxCT UT, High-Resolution X-ray CT Facility of the University of Texas at Austin; SBU CBT, Stony Brook University Center for Biotechnology.

relates of the osteology of the tympanic region. This research was further enhanced by discussions with J. Bloch, P. Gingerich, M. Godinot, J. Perry, M. Silcox, and many other researchers.

LITERATURE CITED

- Beard KC. 1993. Phylogenetic systematics of the Primatomorpha, with special reference to Dermoptera. In: Szalay FS, McKenna MC, Novacek MJ, editors. Mammal phylogeny: placentals. New York: Springer-Verlag. p 129–150.
- Bloch JI, Fisher DC, Rose KD, Gingerich PD. 2001. Stratocladistic analysis of Paleocene Carpolestidae (Mammalia, Plesiadapiformes) with description of a new late Tiffanian genus. *J Vert Paleont* 21:119–131.
- Bloch JI, Gingerich PD. 1998. *Carpolestes simpsoni*, new species (Mammalia, Proprimates) from the late Paleocene of the Clarks Fork Basin, Wyoming. *Contribs Mus Paleont U Michigan* 30:131–162.
- Bloch JI, Silcox MT. 2001. New basicrania of Paleocene-Eocene *Ignacius*: re-evaluation of the plesiadapiform-dermopteran link. *Am J Phys Anthropol* 116:184–198.
- Bloch JI, Silcox MT. 2006. Cranial anatomy of the Paleocene plesiadapiform *Carpolestes simpsoni* (Mammalia, Primates) using ultra high-resolution X-ray computed tomography, and the relationships of plesiadapiforms to Euprimates. *J Hum Evol* 50:1–35.
- Bloch JI, Silcox MT, Boyer DM, Sargis EJ. 2007. New Paleocene skeletons and the relationship of plesiadapiforms to crown-clade primates. *Proc Natl Acad Sci USA* 104:1159–1164.
- Boyer DM. 2009. New cranial and postcranial remains of late Paleocene Plesiadapidae (“Plesiadapiformes,” Mammalia) from North America and Europe: description and evolutionary implications, Ph.D. dissertation, Stony Brook, New York: Stony Brook University.
- Boyer DM, Evans AR, Jernvall J. 2010. Evidence of dietary differentiation among late Paleocene-early Eocene plesiadapids (Mammalia, Primates). *Am J Phys Anthropol*. 142:194–210.
- Cartmill M, MacPhee RDE. 1980. Tupaiid affinities: the evidence of the carotid arteries and cranial skeleton. In: Luckett WP, editor. Comparative biology and evolutionary relationships of tree shrews. New York: Plenum. p 95–132.
- Clemens WA. 2004. *Purgatorius* (Plesiadapiformes, Primates?, Mammalia), a Paleocene immigrant into northeastern Montana: stratigraphic occurrences and incisor proportions. *Bull Carnegie Mus Nat Hist* 36:3–13.
- Clemens WA Jr. 1966. Fossil mammals of the type Lance Formation Wyoming. Part II. Marsupialia. *Univ Calif Publ Geol Sci* 62:1–122.
- Conroy GC, Wible JR. 1978. Middle ear morphology of *Lemur variegatus*: some implications for primate paleontology. *Folia Primatol* 29:81–85.
- Evans HE. 1993. Miller's anatomy of the dog, 3rd ed. Philadelphia: W. B. Saunders.
- Fox RC. 1984. A new species of the Paleocene primate *Elphidotarsius* Gidley: its stratigraphic position and evolutionary relationships. *Can J Earth Sci* 21:1268–1277.
- Fox RC. 1990a. The succession of Paleocene mammals in western Canada. In: Bown TM, Rose KD, editors. Dawn of the age of mammals in the northern part of the Rocky Mountain Interior, North America. *Geol Soc Am, Boulder: Colorado. Spec Paper* 243. p 51–70.
- Fox RC. 1990b. *Pronothodectes gaoi* n. sp. from the late Paleocene of Alberta, Canada, and the early evolution of the Plesiadapidae (Mammalia, Primates). *J Paleontol* 64:637–647.
- Fox RC. 1991. Systematic position of *Pronothodectes gaoi* Fox from the Paleocene of Alberta: reply. *J Paleontol* 65:700–701.
- Fu J-F, Wang J-W, Tong Y-S. 2002. The new discovery of the Plesiadapiformes from the early Eocene of Wutu Basin, Shandong Province. *Vert PalAs* 40:219–227.
- Gidley JW. 1923. Paleocene primates of the Fort Union, with discussion of relationships of Eocene primates. *Proc US Natl Mus* 63:1–38.
- Gingerich PD. 1971. Cranium of *Plesiadapis*. *Nature* 232:566.
- Gingerich PD. 1973. First record of the Paleocene primate *Chiroomyoides* from North America. *Nature* 244:517–518;245:226.
- Gingerich PD. 1975a. Systematic position of *Plesiadapis*. *Nature* 253:111–113.
- Gingerich PD. 1975b. New North American Plesiadapidae (Mammalia, Primates) and a biostratigraphic zonation of the middle and upper Paleocene. *Contr Mus Paleontol Univ Michigan* 24:135–148.
- Gingerich PD. 1976. Cranial anatomy and evolution of Early Tertiary Plesiadapidae (Mammalia, Primates). *Univ Michigan Papers Paleontol* 15:1–141.
- Gingerich PD. 1991. Systematic position of *Pronothodectes gaoi* Fox from the Paleocene of Alberta. *J Paleontol* 65:699.
- Gingerich PD, Gunnell GF. 2005. Brain of *Plesiadapis cookei* (Mammalia, Proprimates): surface morphology and encephalization compared to those of Primates and Dermoptera. *Contr Mus Paleontol Univ Michigan* 31:185–195.
- Gingerich PD, Houde P, Krause DW. 1983. A new earliest Tiffanian (late Paleocene) mammalian fauna from Bangtail Plateau, western Crazy Mountain Basin, Montana. *J Paleontol* 57:957–970.

- Goloboff PA. 1999. NONA ver. 2. Tucumàn, Argentina. Published by the author.
- Gradstein FM, Ogg JG, Smith AG. 2004. A geologic time scale 2004. Cambridge, UK: Cambridge University Press.
- Gunnell GF, Gingerich PD. 1987. Skull and partial skeleton of *Plesiadapis cookei* from the Clarks Fork Basin, Wyoming [abstract]. *Am J Phys Anthropol* 72:206.
- Hoffstetter R. 1977. Phylogénie des primates. Confrontation des résultats obtenus par les diverses voies d'approche du problème. *Bulletins and Mémoires Société d'Anthropologie de Paris* t.4, série XIII:327–346.
- Kay RF, Thewissen JGM, Yoder AD. 1992. Cranial anatomy of *Ignaciuss graybullianus* and the affinities of the Plesiadapiformes. *Am J Phys Anthropol* 89:477–498.
- Linnaeus C. 1758. Tomus 1. *Systema naturae per regna tria naturae, secundum classes, ordines, genera, species, cum characteribus, differentiis, synonymis, locis*. Editio decima, reformata. Stockholm: Laurentii Salvii.
- Lofgren DL, Lillegraven JA, Clemens WA, Gingerich PD, Williamson TE. 2004. Paleocene biochronology: the Puercan through Clarkforkian land mammal ages. In: Woodburne MO, editor. *Late Cretaceous and Cenozoic mammals of North America: biostratigraphy and geochronology*. Berkeley: University of California Press. p 43–105.
- MacPhee RDE. 1981. Auditory regions of primates and eutherian insectivores, morphology, ontogeny, and character analysis. *Contribs Primatol* 18:1–282.
- MacPhee RDE, Cartmill M. 1986. Basicranial structures and primate systematics. In: Swindler D, Erwin J, editors. *Comparative primate biology, Volume 1: systematics, evolution, and anatomy*. New York: Alan R. Liss, Inc. p 219–275.
- MacPhee RDE, Cartmill M, Gingerich PD. 1983. New Palaeogene primate basicrania and the definition of the order Primates. *Nature* 301:509–511.
- Nixon KC. 1999–2002. WinClada ver. 1.0000 Published by the author, Ithaca, NY, USA.
- Nomina Anatomica, 5th ed. 1983. Baltimore: Williams & Wilkins.
- Nomina Anatomica Veterinaria, 5th ed. 2005. Hanover, Columbia, Gent, Sapporo: World Association of Veterinary Anatomists Editorial Committee.
- Russell DE. 1959. Le crâne de *Plesiadapis*. *Bull Soc Géol France* (7th ser) 1:312–314.
- Russell DE. 1964. Les mammifères paléocènes d'Europe. *Mémoires du Muséum National d'Histoire Naturelle (Paris)*, Série C, Sciences de la Terre 13:1–324.
- Scott CS. 2003. Late Torrejonian (middle Paleocene) mammals from south central Alberta, Canada. *J Paleontol* 77:745–768.
- Scott CS. 2008. Late Paleocene mammals from near Red Deer, Alberta, and a phylogenetic analysis of the earliest Lipotyphla (Mammalia, Insectivora), Ph.D. dissertation, Edmonton: University of Alberta.
- Scott CS, Fox RC, Youzwyshyn GP. 2002. New earliest Tiffanian (late Paleocene) mammals from Cochrane 2, southwestern Alberta, Canada. *Acta Palaeontol Polonica* 47:691–704.
- Secord R. 2008. The Tiffanian land-mammal age (middle and late Paleocene) in the northern Bighorn Basin, Wyoming. *Univ Michigan Papers Paleontol* 35:1–192.
- Silcox MT. 2001. A phylogenetic analysis of Plesiadapiformes and their relationship to euprimates and other archontans, Ph.D. dissertation, Baltimore: The Johns Hopkins University.
- Silcox MT. 2003. New discoveries on the middle ear anatomy of *Ignaciuss graybullianus* (Paromomyidae, Primates) from ultra high resolution X-ray computed tomography. *J Hum Evol* 44:73–86.
- Silcox MT, Gunnell GF. 2008. Plesiadapiformes. In: Janis CM, Gunnell GF, Uhen MD, editors. *Evolution of tertiary mammals of North America, Volume 2: small mammals, xenarthrans, and marine mammals*. Cambridge: Cambridge University Press. p 207–238.
- Silcox MT, Krause DW, Maas MC, Fox RC. 2001. New specimens of *Elphidotarsius russelli* (Mammalia, Primates, Carpolestidae) and a revision of plesiadapoid relationships. *J Vert Paleontol* 21:132–152.
- Silcox MT, Bloch JI, Boyer DM, Godinot M, Ryan TM, Spoor F, Walker A. 2009. Semicircular canal system in early primates. *J Hum Evol* 56:315–327.
- Simons EL. 1960. New fossil primates: a review of the past decade. *Am Sci* 48:179–192.
- Simons EL. 1964. The early relatives of man. *Sci Am* 211:50–62.
- Simons EL. 1967. Fossil primates and the evolution of some primate locomotor systems. *Am J Phys Anthropol* 26:241–253.
- Simons EL. 1972. *Primate evolution, an introduction to man's place in nature*. New York: Macmillan.
- Simpson GG. 1927. Mammalian fauna and correlation of the Paskapoo Formation of Alberta. *Am Mus Novitates* 268:1–10.
- Simpson GG. 1935. The Tiffany fauna, Upper Paleocene. II.—Structure and relationships of *Plesiadapis*. *Am Mus Novitates* 816:1–30.
- Szalay FS. 1971. Cranium of the late Palaeocene primate *Plesiadapis tricuspidens*. *Nature* 230:324–325.
- Szalay FS. 1972. Cranial morphology of the early Tertiary *Phenacolemur* and its bearing on primate phylogeny. *Am J Phys Anthropol* 36:59–75.
- Szalay FS, Delson E. 1979. *Evolutionary history of the primates*. New York: Academic Press.
- Szalay FS, Rosenberger AL, Dagosto M. 1987. Diagnosis and differentiation of the Order Primates. *Yrbk Phys Anthropol* 30:75–105.
- Thewissen JGM, Williams EM, Hussain ST. 2001. Eocene mammal faunas from northern Indo-Pakistan. *J Vert Paleontol* 21:347–366.
- Trouessart EL. 1897. *Catalogue des mammalium tam viventium quam fossilium*. Berlin: R. Friedländer und Sohn.
- Van Valen LM. 1994. The origin of the plesiadapid primates and the nature of *Purgatorius*. *Evol Monogr* 15:1–79.
- Watters JP, Krause DW. 1986. Plesiadapid primates and biostratigraphy of the North American late Paleocene [abstract]. *Am J Phys Anthropol* 69:277.
- Webb MW. 1996. Late Paleocene mammals from near Drayton Valley, Alberta. M.Sc. thesis, Edmonton: University of Alberta.
- Wible JR. 1993. Cranial circulation and relationships of the colugo *Cynocephalus* (Dermoptera, Mammalia). *Am Mus Novit* 3072:1–27.
- Wible JR, Gaudin TJ. 2004. On the cranial anatomy of the yellow armadillo *Euphractus sexcinctus* (Dasypodidae, Xenarthra, Placentalia). *Ann Carnegie Mus* 73:117–196.
- Wible JR. 2008. On the cranial osteology of the Hispaniolan solenodon, *Solenodon paradoxus* Brandt, 1833 (Mammalia, Lipotyphla, Solenodontidae). *Ann Carnegie Mus* 77:321–402.
- Wible JR. 2009. The ear region of the pen-tailed treeshrew, *Ptilocercus lowii* Gray, 1848 (Placentalia, Scandentia, Ptilocercidae). *J Mam Evol* 16:199–234.
- Wible JR. 2011. On the treeshrew skull (Mammalia, Placentalia, Scandentia). *Ann Carnegie Mus* 79:149–230.
- Witmer LM. 1995. The extant phylogenetic bracket and the importance of reconstructing soft tissues in fossils. In: Thomason J, editor. *Functional morphology in vertebrate paleontology*. Cambridge: Cambridge University Press. p 19–33.
- Youzwyshyn GP. 1988. Paleocene mammals from near Cochrane, Alberta, M.Sc. thesis, Edmonton: University of Alberta.